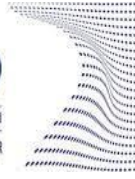




**ScuDo**  
Scuola di Dottorato - Doctoral School  
WHAT YOU ARE, TAKES YOU FAR



Doctoral Dissertation  
Doctoral Program in Metrology (33rd cycle)

# **Acoustic Thermometry Based on Accurate Measurements of Speed of Sound in Air**

**Srijith Bangaru Thirumalai Raj**

\* \* \* \* \*

**Supervisor**  
Dr Marco Pisani

Doctoral Examination Committee:

Dr. Sergio Bobbo, CNR-ITC  
Dr. Cécile GUIANVARC'H, CNAM-LNE

Politecnico di Torino  
October 04, 2021

This thesis is licensed under a Creative Commons License, Attribution - Noncommercial - NoDerivative Works 4.0 International: see [www.creativecommons.org](http://www.creativecommons.org). The text may be reproduced for non-commercial purposes, provided that credit is given to the original author.

I hereby declare that the contents and organisation of this dissertation constitute my own original work and does not compromise in any way the rights of third parties, including those relating to the security of personal data.



.....  
Srijith Bangaru Thirumalai Raj  
Turin, October 04, 2021

## Summary

Accurate measurements at large distances in air are carried out using laser interferometers. The air-refractive index of the medium in which the measurement is carried out is the limiting factor for the measurement accuracy. In turn, air temperature is the key measurement to be performed. In order to achieve an uncertainty of  $10^{-7}$  in large distance measurements, the uncertainty of temperature measurements over the whole optical path shouldn't exceed 0.1 °C. This level of accuracy is required in the field of manufacturing processes of large structures in particular aerospace industries and windmill blades.

To achieve this level of accurate temperature measurements an acoustic thermometer experimental set-up is presented in the first part of the thesis. The thermometer has demonstrated a resolution of the order of 0.1 °C, over a distance of 11 m. The temperature is inferred from the measurement of the speed of sound through the inversion of the Cramer formula which allows to calculate the speed of sound from temperature. The intrinsic accuracy of this formula is 300 ppm and this is the main limit to the accuracy of the thermometer.

In the second part of the thesis, an experiment to measure the speed of sound in a selected set of environment conditions has been carried out. The uncertainty of the results is within 100 ppm allowing to improve the knowledge of the speed of sound with respect to the Cramer equation by a factor three.

## **Acknowledgement**

I would like to thank Dr Marco Pisani for the guidance and support that he constantly gave me during my doctoral studies in Politecnico di Torino and INRiM. He gave me the opportunity to get experience with metrology research during this period and proceed with research related to ring laser gyroscope, acoustic thermometer and speed of sound experiments. His expertise and experience in the field of metrology was precious and helped me in completing this experiment successfully. I would also like to thank Dr Milena Astrua for giving me support during my doctoral studies. I thank Dr Roberto Gavioso for reviewing my thesis and giving comments which were very useful in improving the quality of the thesis.

I would like to thank all colleagues in INRiM and Professors in Politecnico di Torino for supporting my doctoral studies at various points.

Finally, I would like to thank my parents for always believing in me.

## Table of Contents

<b>List of Figures .....</b>	<b>viii</b>
<b>List of Tables .....</b>	<b>xi</b>
<b>1. Introduction.....</b>	<b>1</b>
<b>2. Speed of Sound Theory.....</b>	<b>5</b>
2.1. Thermodynamic definition of Speed of Sound.....	5
2.2. Speed of Sound in air dependence on Pressure .....	6
2.3. Speed of Sound in air dependence on Frequency .....	7
2.4. Composition of Atmospheric air .....	8
2.5. Speed of Sound in air dependence on Temperature .....	9
2.6. Speed of Sound in air dependence on Relative Humidity.....	10
2.7. Speed of Sound in air dependence on Carbon dioxide content .....	12
2.8. Uncertainties in Speed of Sound.....	14
2.9. Cramer Equation for calculating Speed of sound in air based on Environmental Parameters .....	14
<b>3. A review of calculating methods of Speed of Sound in air.....</b>	<b>16</b>
3.1. Basic theory of Acoustic Thermometer .....	16
3.2. Overview about acoustic thermometer .....	17
3.3. History related to Speed of Sound in air by various researchers.....	19
3.4. Review on speed of sound in air calculating methods.....	20
3.5. Estimation of Speed of sound in air through time-of flight method.....	21
<b>4. Acoustic Thermometer: Experiment and Results .....</b>	<b>24</b>
4.1. Working Principle of acoustic thermometer .....	25
4.2. Choice of Operating Frequency.....	27
4.3. Experimental Set-up.....	29
4.4. Results and Discussion .....	33
4.4.1. Speed of Sound comparison at 8.2 m.....	34
4.4.2. Speed of Sound comparison at 11 m.....	36
4.4.3. Comparison of temperature values: Acoustic Thermometer vs Classical Temperature Sensor .....	37
<b>5. Speed of Sound in air: Experiment and Results.....</b>	<b>39</b>
5.1. Working Principle .....	39
5.2. Experimental Set-Up .....	41
5.3. Results and Discussion .....	46
5.4. Calibration of moving rail and experimental set-up.....	47
5.5. Results at different temperature ranges .....	49
5.6. Temperature Gradients.....	55

<b>5.7.</b>	<b>Temperature dispersion .....</b>	<b>57</b>
<b>5.8.</b>	<b>Effect of frequency.....</b>	<b>58</b>
<b>5.9.</b>	<b>Relative alignment of Microphone and Loudspeaker.....</b>	<b>62</b>
<b>5.10.</b>	<b>Effect of reflections on the floor .....</b>	<b>64</b>
<b>5.11.</b>	<b>Uncertainty Budget.....</b>	<b>66</b>
5.11.1.	Uncertainty in Speed of Sound in air calculated from Experiment .....	66
5.11.2.	Uncertainty in speed of sound in air calculated from Cramer equation .....	67
<b>5.12.</b>	<b>Comparison of Speed of Sound in air measurements from Acoustic     Thermometer Experiment &amp; Spherical Resonator .....</b>	<b>70</b>
	<b><i>Conclusions .....</i></b>	<b><i>72</i></b>
	<b><i>Bibliography.....</i></b>	<b><i>74</i></b>
	<b><i>Appendix.....</i></b>	<b><i>79</i></b>

# List of Figures

FIGURE 1-SPEED OF SOUND IN AIR AT STD ATMOSPHERE (1 ATM) VS VARIOUS TEMPERATURE AND VARIOUS RELATIVE HUMIDITY .....	11
FIGURE 2-MEAN ANNUAL MOLE FRACTION OF CARBON DIOXIDE IN DRY AIR FROM 1958 TO 1999[41] .....	13
FIGURE 3-VARIOUS TECHNIQUES FOR ACOUSTIC MEASUREMENT UTILIZED (A)UNIDIRECTIONAL TECHNIQUE (B)UNIDIRECTIONAL WITH MIRROR (C)BI-DIRECTIONAL (D)BI-DIRECTIONAL WITH REFLECTOR [26].....	17
FIGURE 4-ALONG THE OPTICAL PATH OF AN INTERFEROMETRIC MEASUREMENT THE TEMPERATURE CAN VARY CONSIDERABLY, AND FOR A CORRECT ESTIMATION, A LARGE NUMBER OF THERMOMETERS SHOULD BE USED. ON THE OTHER HAND, HUMIDITY AND PRESSURE ARE QUITE UNIFORM IN SPACE AND CAN BE SAMPLED LOCALLY. THE ACOUSTIC MEASUREMENT ALLOWS TO MEASURE THE AVERAGE TEMPERATURE ALONG THE SAME PATH TRAVELLED BY LIGHT. ....	24
FIGURE 5-WORKING PRINCIPLE OF ACOUSTIC THERMOMETER EXPERIMENT. A CONTINUOUS ACOUSTIC WAVE IS GENERATED BY THE LOUDSPEAKER DRIVEN BY A SYNTHESIZER AT THE LEFT OF THE PICTURE. AFTER HAVING RUN THE DISTANCE D, THE WAVE REACHES THE MICROPHONE AT THE RIGHT. A PHASE-METER IS USED TO MEASURE THE PHASE DELAY BETWEEN THE GENERATED WAVE AND THE RECEIVED WAVE THAT IS PROPORTIONAL TO THE DISTANCE AND INVERSELY PROPORTIONAL TO THE SPEED OF SOUND. ....	25
FIGURE 6- EFFECTIVE DISTANCE MEASUREMENT BETWEEN LOUDSPEAKER AND MICROPHONE. THE EFFECTIVE DISTANCE IS THE VALUE D IN EQ 4.1. THIS DISTANCE IS NOT EASILY DEFINABLE FROM THE PHYSICAL CONSTRUCTION OF THE DEVICES AND MUST BE FOUND THROUGH EQ. 4.2 BY THE SEEPING METHOD.....	27
FIGURE 7-ATTENUATION OF ACOUSTIC WAVES VS FREQUENCY AND HUMIDITY [73] .....	28
FIGURE 8-ATTENUATION OF ACOUSTIC WAVES VS FREQUENCY AND INTENSITY: COMPARING THE 100 HZ WITH THE 20 KHZ FREQUENCY, IT CAN BE SEEN THAT THE MUCH HIGHER ATTENUATION AT HIGH FREQUENCY CAN BE PARTIALLY COMPENSATED BY THE FACT THAT THE SAME CAN BE MADE HIGHLY DIRECTIONAL (ORANGE CURVE) COMPARED TO THE 1/D BEHAVIOR OF THE LOW FREQUENCY (BLUE CURVE). ....	28
FIGURE 9- SOME OF THE MICROPHONES AND LOUDSPEAKERS USED IN THE PRELIMINARY STUDY FOR THE EXPERIMENT. ABOVE: A HORN LOUDSPEAKER AND A LOUDSPEAKER PLACED IN THE FOCUS	

OF A PARABOLIC REFLECTOR. BELOW: AN INTERFERENCE SUPER-CARDIOID MICROPHONE AND AN OMNI-DIRECTIONAL MICROPHONE PLACED IN THE FOCUS OF A PARABOLA. ....	30
FIGURE 10- THE LOUDSPEAKER AND THE MICROPHONE USED IN THE FINAL VERSION OF THE EXPERIMENTS RELATED TO THE RESULTS REPORTED HERE. THE LOUDSPEAKER (LEFT) IS A DYNAMIC TWEETER LOADED WITH AN EXPANSION HORN MODEL HERTZ S25 NEO. THE MICROPHONE IS A SUPER CARDIOID INTERFERENCE CONDENSER MODEL BOYA-PVM1000. ....	31
FIGURE 11- THE LOUDSPEAKER AND THE MICROPHONE USED IN THE FINAL VERSION OF THE EXPERIMENTS RELATED TO THE RESULTS REPORTED HERE. THE LOUDSPEAKER (LEFT) IS A DYNAMIC TWEETER LOADED WITH AN EXPANSION HORN MODEL HERTZ S25 NEO. THE MICROPHONE IS A SUPER CARDIOID INTERFERENCE CONDENSER MODEL BOYA-PVM1000. ....	32
FIGURE 12- PRELIMINARY EXPERIMENTS WITH DIFFERENT LOUDSPEAKER AND MICROPHONES. ....	33
FIGURE 13- PICTURE OF THE EXPERIMENT CARRIED OUT AT 8.2 M. ....	34
FIGURE 14- SPEED OF SOUND (EXP & CRAMER) VS TIME ALONG WITH DIFFERENCES @8.2 M. RED CURVE: SPEED OF SOUND MEASURED THROUGH THE ACOUSTIC SET-UP. BLUE CURVE: SPEED OF SOUND ESTIMATED WITH THE CRAMER EQUATION FROM THE MEASURED ENVIRONMENTAL PARAMETERS. GREEN CURVE: DIFFERENCE BETWEEN MEASURED AND ESTIMATED SPEED OF SOUND (RIGHT SCALE IN M/S). ....	35
FIGURE 15- SPEED OF SOUND (EXPERIMENT & CRAMER) VS TIME ALONG WITH DIFFERENCES @11M. ....	36
FIGURE 16- TEMPERATURE VALUES (EXPERIMENT AND SENSOR) VS TIME ALONG WITH DIFFERENCE. ....	38
FIGURE 17- EXPERIMENTAL SET-UP FOR SPEED OF SOUND IN AIR. THE KEY OF THE EXPERIMENT IS THE ACCURATE MEASUREMENT OF THE CHANGE OF THE DISTANCE BETWEEN LOUDSPEAKER AND THE MICROPHONE. THE LOUDSPEAKER IS MOUNTED ON A CARRIAGE HAVING THE CAPABILITY OF 1 M DISPLACEMENT WHILE AN INTERFEROMETER ACCURATELY MEASURES THE SAME DISPLACEMENT. ....	41
FIGURE 18- INTERFEROMETER SET-UP USED TO MEASURE THE DISPLACEMENT OF THE CARRIAGE CARRYING THE LOUDSPEAKER. IT IS BASED ON A HP INTERFEROMETER AND ON PROPRIETARY ACQUISITION SYSTEM. ....	42
FIGURE 19- DATA ACQUISITION LABVIEW USER INTERFACE. ....	43
FIGURE 20- TYPICAL DATA ACQUISITION FOR THE 6 TEMPERATURE VALUES. THE TEMPERATURE UNIFORMITY IN THE MEASUREMENT VOLUME CAN BE APPRECIATED. ....	44

FIGURE 21-SPHERICAL RESONATOR USED FOR THE ACCURATE MEASUREMENT OF THE SPEED OF SOUND WITH A COMPLEMENTARY METHOD. THE SPHERICAL RESONATOR METHOD HAS AN INTRINSIC UNCERTAINTY OF FEW PPM. ....	45
FIGURE 22-ULTRASOUND ANEMOMETER SET-UP FOR WIND SPEED MEASUREMENT.....	45
FIGURE 23-EXPERIMENTAL SET-UP FOR THE MEASUREMENT OF THE SPEED OF SOUND. AT THE BACKGROUND/LEFT IS VISIBLE THE CARRIAGE CARRYING THE LOUDSPEAKER. AT THE FOREGROUND ON THE RIGHT IS VISIBLE THE MICROPHONE ON THE TRIPOD. AT THE LEFT THE ARRAY OF RESISTANCE THERMOMETERS. TOP RIGHT THE EXPERIMENT WITH THE SPHERICAL RESONATOR. ON THE FLOOR FOAM ABSORBERS FOR REDUCING ACOUSTIC REFLECTIONS .....	46
FIGURE 24- ERRORS OF THE MOVING RAIL VS TEMPERATURE OVER 1 M STROKE DUE TO THERMAL EXPANSION OF THE SCREW (CALIBRATION OF MOVING RAIL WITH INTERFEROMETER SET-UP)47	
FIGURE 25-PRELIMINARY MOVING RAIL CALIBRATION.....	48
FIGURE 26-ON THE LEFT THE HYGROMETER HEAD, ON THE RIGHT THE PT100 THERMAL SENSORS...48	
FIGURE 27-SPEED OF SOUND (EXPERIMENT VS CRAMER) AT 6 °C TO 20 °C .....	50
FIGURE 28-TEMPERATURE VS DIFFERENCE IN SPEED OF SOUND (EXP & CRAMER) AT 6 °C TO 20 °C...50	
FIGURE 29-SPEED OF SOUND (EXPERIMENT VS CRAMER) AT 18.9 °C TO 19.3 °C.....	51
FIGURE 30-TEMPERATURE VS DIFFERENCE IN SPEED OF SOUND (EXP & CRAMER) AT 18.9 °C TO 19.3 °C.....	51
FIGURE 31-SPEED OF SOUND (EXPERIMENT VS CRAMER) AT 20 °C TO 28 °C.....	52
FIGURE 32-TEMPERATURE VS DIFFERENCE IN SPEED OF SOUND (EXP & CRAMER) AT 20 °C TO 28 °C.52	
FIGURE 33- SCATTER PLOT OF SPEED OF SOUND DIFFERENCE VALUES AT TEMPERATURE RANGE OF 7 °C TO 28 °C. THE VERTICAL AXIS IS THE DIFFERENCE BETWEEN THE SPEED OF SOUND MEASURED WITH THE ACOUSTIC METHOD AND THE SPEED OF SOUND CALCULATED FROM THE ENVIRONMENTAL PARAMETERS THROUGH THE CRAMER FORMULA. THE DIFFERENT COLORS REPRESENT THE DIFFERENT MEASUREMENT RUNS. ....	53
FIGURE 34- SCATTER PLOT OF SPEED OF SOUND DIFFERENCE VALUES AT TEMPERATURE RANGE OF 7 °C TO 28 °C WITH AVERAGE AND STANDARD DEVIATION VALUES (RESPECTIVELY SOLID AND DASHED RED LINES). THE BLACK DASHED LINE IS THE LINEAR TENDENCY CURVE INCLUDING ALL DATA.....	54
FIGURE 35-TYPICAL TEMPERATURE HORIZONTAL GRADIENT OF THE MEASUREMENT VOLUME.....	55
FIGURE 36-TEMPERATURE VERTICAL GRADIENT OF 6 PT-100 SENSORS (T1-T6).....	56
FIGURE 37-THERMAL DISPERSION VALUES AMONG 6 PT-100 SENSORS(T1-T6) .....	57
FIGURE 38-SPEED OF SOUND MEASUREMENT AT DIFFERENT FREQUENCIES BASED ON ZUCKERWAR EQUATION WITH SPEED OF SOUND VALUES BASED ON EXPERIMENT AT 20 KHZ .....	58

FIGURE 39-SPEED OF SOUND DIFFERENCE VALUES (EXPERIMENT & CRAMER) @ 16 KHZ .....59

FIGURE 40-SPEED OF SOUND DIFFERENCE VALUES (EXPERIMENT & CRAMER) @ 18 KHZ .....59

FIGURE 41-SPEED OF SOUND DIFFERENCE VALUES(EXPERIMENT & CRAMER) @ 20 KHZ .....60

FIGURE 42-SPEED OF SOUND DIFFERENCE VALUES (EXPERIMENT & CRAMER) @ 22 KHZ .....60

FIGURE 43-SCATTER PLOT OF SPEED OF SOUND DIFFERENCE VALUES AT 16 TO 22 KHZ.....61

FIGURE 44-SPEED OF SOUND VS FREQUENCY.....61

FIGURE 45-HORIZONTAL ALIGNMENT BETWEEN LOUDSPEAKER AND MICROPHONE VS SPEED OF SOUND DIFFERENCE (EXPERIMENT) .....62

FIGURE 46-VERTICAL ALIGNMENT BETWEEN LOUDSPEAKER AND MICROPHONE VS SPEED OF SOUND DIFFERENCE (EXPERIMENT) .....63

FIGURE 47-ANGULAR ALIGNMENT BETWEEN LOUDSPEAKER AND MICROPHONE VS SPEED OF SOUND DIFFERENCE (EXPERIMENT) .....63

FIGURE 48-FOAMS BETWEEN LOUDSPEAKER AND MICROPHONE AT ORIGINAL POSITION.....64

FIGURE 49- FOAMS BETWEEN LOUDSPEAKER AND MICROPHONE AT RE-ARRANGED POSITION.....64

FIGURE 50-SPEED OF SOUND DIFFERENCES (EXPERIMENT & CRAMER) VS ACOUSTIC INTERFERENCES AT DIFFERENT POSITIONS OF FOAMS .....65

FIGURE 51-GRAPH OF SPEED OF SOUND FROM EXPERIMENT AT 20 °C WITH RESPECTIVE UNCERTAINTY LIMITS.....69

FIGURE 52-SPEED OF SOUND VALUES AT 20°C (EXPERIMENT & CRAMER) WITH UNCERTAINTY LIMITS .....69

FIGURE 53-COMPARISON OF EXPERIMENTAL SPEED OF SOUND IN AIR MEASUREMENTS WITH AN ACOUSTIC INTERFEROMETER AND A SPHERICAL RESONATOR THE INTERFEROMETER OPERATES AT 20 KHZ; SEVERAL RADIAL (0, N) RESONATOR MODES SPAN THE FREQUENCY RANGE BETWEEN 2 KHZ AND 20 KHZ EXPERIMENTAL RESULTS ARE COMPARED TO THE THEORETICAL PREDICTION OF ZUCKERWAR AT 3 KHZ AND 20KH THE TEMPERATURE OF AIR RISES IN TWO HOURS FROM 293.44 K TO 293.48 K, AT 99.95 KPA, HR = 55 %, XCO2 =540 PPM..... 70

FIGURE 54-COMPARISON OF THEORETICAL SPEED OF SOUND IN HUMID AIR AT ZERO FREQUENCY AS PREDICTED BY CRAMER (CR) AND ZUCKERWAR (ZU) FOR A SAMPLE OF AIR UNDERGOING A TEMPERATURE RISE BETWEEN 293.44 K AND 293.48 K, AT 99.95KPA,HR=55%, XCO2 = 540 PPM ..... 71

FIGURE 55-PROPOSED PORTABLE ACOUSTIC THERMOMETER SET-UP FOR OUTDOOR MEASUREMENT .....73

# List of Tables

<i>TABLE 1- EFFECTS OF ENVIRONMENTAL PARAMETERS ON THE ACCURACY OF AIR-REFRACTIVE INDEX</i>	<i>2</i>
<i>TABLE 2-STANDARD CONSTITUENTS OF AIR</i>	<i>9</i>
<i>TABLE 3-DRY CARBON DI OXIDE FREE AIR AND DRY 1999 AIR CONSTITUENT'S MOLE FRACTION [41]</i>	<i>12</i>
<i>TABLE 4-SPEED OF SOUND AT 0 °C FOUND BY SOME INVESTIGATORS SINCE 1919 [72]</i>	<i>22</i>
<i>TABLE 5-CHOICE OF OPERATING FREQUENCY. ULTRASOUND FREQUENCIES HAS THE HIGH DRAWBACK OF SUFFERING FROM STRONG ATTENUATION IN ATMOSPHERE. ON THE OTHER HAND, THE ADVANTAGES OF ULTRASOUNDS ARE EVIDENT. IN RED WE HAVE HIGHLIGHTED THE DISADVANTAGES, IN GREEN THE ADVANTAGES WITH RESPECT TO OTHER FREQUENCY RANGES. AT LEAST OVER MEDIUM DISTANCES (TENS OF METERS), THE ULTRASOUND RANGE IS THE PREFERRED ONE.</i>	<i>29</i>
<i>TABLE 6-UNCERTAINTY BUDGET FOR ALIGNMENT BETWEEN MICROPHONE AND LOUDSPEAKER</i>	<i>66</i>
<i>TABLE 7-UNCERTAINTY BUDGET FOR SPEED OF SOUND (EXPERIMENT)</i>	<i>67</i>
<i>TABLE 8-UNCERTAINTY BUDGET RELATED TO TEMPERATURE (CRAMER)</i>	<i>68</i>
<i>TABLE 9- UNCERTAINTY BUDGET FOR SPEED OF SOUND (CRAMER)</i>	<i>68</i>

# Chapter 1

## Introduction

Accurate measurements of long distances (tens of meters or more) rely on laser interferometry. These accurate measurements are needed in manufacturing processes of large structures such as the aerospace industry and wind turbines. In the large distance accurate measurements, the interferometer technique employs the wavelength as a measuring scale. The distance between two points can be measured based on the count of wavelength propagated between the start and endpoint in case of vacuum condition. Real measurements are not made in an ideal vacuum situation, but carried out in a natural environment that is composed of air. So, the air refractive index ( $n_{\text{air}}$ ) is considered as a correction value to determine the wavelength of a laser in air. Hence, it becomes very important to have accurate knowledge of the value of air refractive index for accurate large distance measurements. The refractive index of air depends on environmental parameters such as temperature, pressure, relative humidity and CO<sub>2</sub> content. Amongst these parameters the one having the larger influence is air temperature. In order to achieve a relative accuracy of  $10^{-7}$  on large distance measurements, a knowledge of air temperature along the interferometer path of 0.1 °C is needed [1]–[4].

The air-refractive index estimation based on the environmental parameters can be carried out with the help of several models like the Edlen's formula [5]–[7]. There are also some alternatively proposed models from Ciddor or by Potulski and Bonschi [2]–[4], by which the refractive index of air can be calculated based on measured parameters from the environment. In summary from these models, an uncertainty of temperature values around 0.1 °C results in an uncertainty of about  $10^{-7}$  in the refractive index of air subsequently. In terms of length measurement, using their values can result in an uncertainty of 1µm over 10 m. It is also important to consider other parameters like relative humidity and pressure adding up to uncertainties in the refractive index measurement.

The review of [5], [8]–[15] discusses methods to compensate for the accurate refractive index of air in laser interferometry to measure distances. It describes achieving an uncertainty of  $10^{-8}$  under standard conditions in the distance measurement by using the empirical dispersion equation. The following table reports the effect of the parameters on the refractive index values under the standard conditions of temperature at 20 °C, Pressure at 101350 Pa, Humidity at 40 % and CO<sub>2</sub> content of 500 ppm [16].

Table 1- Effects of environmental parameters on the accuracy of air-refractive index

Environmental Parameters	Refractive index of air (Edlen)
$\Delta T = \pm 1 \text{ }^\circ\text{C}$	$\pm 9.4 \times 10^{-7}$
$\Delta P = \pm 100 \text{ Pa}$	$\pm 2.7 \times 10^{-7}$
$\Delta H = \pm 1 \text{ \%}$	$\pm 9.0 \times 10^{-9}$
$\Delta \text{CO}_2 = \pm 5 \text{ ppm}$	$\pm 1.0 \times 10^{-9}$

Based on the values from Table 1 it can be clearly seen that the temperature values have a greater impact on the refractive index of air measurement over other parameters [17]. Although there is no significant change of values with both methods, the Elden equation is used for measurements carried around 20 °C and the Ciddor equation is employed at outdoor and extreme conditions.

An alternative experimental method to determine the air-refractive index value is carried out with refractometers. The refractometer can be considered as an interferometer in which a vacuum cell is connected in addition. The distance is measured by transmitting a laser beam inside a vacuum cell and also through a cell containing ambient air. The refractive index of air is based on the ratio between optical path length in air and optical path length along the vacuum cell assuming the vacuum cell built zero refractive index. Important challenge in this method is to maintain the rigidity of the vacuum cell from deforming due to the pressure difference in the ambient conditions. It is primarily important to maintain the exact physical length to exist between the points along the vacuum cell and air conditions for the laser beam to transmit. The commonly used refractometer is Fabry-Perot refractometer which, with the help of a tunable laser, provides much more accurate values of air-refractive index. The limit of the refractometer, although, is to provide a local measurement, not suited for long distances.

A solution proposed for accurate estimation of air-refractive index in real-time is explained in the research paper [18] and is based on the principle of two-color method. In this method, two different laser wavelengths are transmitted simultaneously over the same distance. The geometrical interferometric distance is determined based on the optical path length of two frequencies transmitted. The method of compensating for air-refractive index in real time using the two-color method is first formulated in 1989. The research carried out at the Japan Metrology Institute demonstrates about attaining the accuracy of  $2 \times 10^{-7}$  m in length measurement using an optical instrument. This method is capable of producing such accuracy for length measurements carried out at the range of 0.5 to 1 m. After this successful attempt, many further researches were carried out in order to estimate air-refractive index at very high precision. Over the long-distance interferometric distance measurement, the research was carried out to present a method to measure distance of up to 30 m at an uncertainty of about  $1.2 \times 10^{-7}$  m. This measurement system provides better uncertainty over refractors and Ciddor, Edlen equations. But, the system with two different wavelength method makes the measurement system more complicated, expensive and makes it tougher to employ in the portable mode. Another advancement in this two-color method in recent

days is the estimation of air-refractive index through femto-second lasers. These methods of researches are mainly in development stages and showed its ability to measure distance of up to 2.5 m at an uncertainty level of  $10^{-8}$  m. The feasibility of using this method measuring larger distance are yet to be developed under ambient conditions. Based on these literature study carried out with various research paper, it becomes important to develop an alternate method for developing high precision technique to estimate air-refractive index [19], [20].

In order to attain the relative uncertainty of  $10^{-7}$  in large distance measurements, it is important to have measurement knowledge of relative humidity with an uncertainty of 12% (@20 °C) and the ambient pressure with an uncertainty of 40 Pa. The rate at which water vapor pressure and ambient pressure changes over time is very slow and these two values remain rather uniform over space. Whereas the temperature of air can undergo rapid changes with space and time. It is practically impossible to have a number of thermometers over the larger distance measurements. With this high uncertainty on temperature values, it becomes challenging for attaining a target accuracy in the range of  $10^{-7}$  on large distances interferometric measurements. Based on these reasons, it becomes important to propose a better model to determine the temperature values.

The review paper presented by J. Fischer and B. Fellmuth emphasizes the role of temperature measurements in industries and manufacturing processes [21]. Various temperature reading techniques using gas thermometers, noise thermometers, magnetic thermometers, total radiation thermometers, spectral radiation thermometers are discussed. Many researches were carried out regarding acoustic thermometry in the past. Using this technique, the transmit time of sound waves which is dependent on the temperature is used to measure accurate temperature. The medium of transmission can be solid, liquid or gas. Since the purpose of this research work is to measure temperature for air-refractive index in air thereby contributing for accurate laser interferometry measurements, we concentrate on acoustic gas thermometry. The paper [22], describes the challenges dealt with temperature measurement regarding precision metrology. This paper recommends the employment of acoustic techniques for measuring the air temperature and its future potential in dimensional metrology.

The research carried out at NPL, U.K., exploited the possibility of non-contact temperature measurements in meteorological perspective for detailed assessment of saturation or super-saturation in stratosphere conditions. This experiment is carried out with a frame built with loudspeaker, microphone and parabolic reflector and the carbon fiber tubes are used to link the framework. This research work has proved its ability to operate at atmospheric conditions and its ability to produce a couple of thermal measurements per second. The researchers proposed an expected uncertainty of 0.1 °C based on preliminary results and recommended a possible increase in uncertainty with higher temperatures [23]. Also, this method gives a local measurement, thus is not suitable for long distance measurements.

To fulfil the above-mentioned level of accuracy in temperature measurements, the experimental set-up based on acoustic thermometer to measure the temperature along the path of interferometric signals will be presented in this thesis.

Various acoustic methods have been used in the past to measure the speed of sound. One of the most common of those methods is based on “time-of-flight” measurement, where the average of speed of sound in medium is measured by transducers separated by a known distance, where the sound speed is found by dividing the distance between transducers by the time it takes for a *sound pulse* to travel across the distance. The method proposed in this thesis is based on measuring the phase delay of a *continuous acoustic wave*. The experiments are carried out in a controllable condition in an acoustic laboratory by placing a number of thermometers along the path run by the moving receiver. Environmental parameters like temperature, humidity and pressure are recorded continuously while measuring the speed of sound in order to correlate the results. Different combinations of sound source and receiver microphones are employed to achieve higher efficient results.

The thesis is structured as follows. In chapter two, the theory related to speed of sound in air is presented. In chapter three, the various speed of sound calculating methods carried out in the past by various researchers and the uncertainty calculating methods related to it are presented for better understanding. With all these in consideration, in chapter four the working principle and the experimental set-up of a practical acoustic thermometer are discussed in detail. A first set of results are presented in the form of comparing the speed of sound calculated from Cramer equation and experimental set-up and their differences are presented at a distance of 8.2 m. In the second experiment, exploiting the maximum length permissible in anechoic chamber (11 m) the temperature values are calculated from the Cramer equation and compared with the values obtained with the help of a set of thermometers placed along the path of acoustic waves. In both cases, the temperature values are calculated based on the Cramer equation which comes with an uncertainty value of about 300 ppm. In order to reduce this uncertainty, as described in chapter five, an experimental set-up was built to perform accurate measurements of the speed of sound in a controlled environment to improve the knowledge of the dependence of the speed of sound from environmental parameters to reduce the uncertainty to less than 100 ppm. The experimental set-up is based on measuring the phase delay of a continuous acoustic wave while changing the distance between the source and the receiver under the control of an interferometer.

## Chapter-2

# Speed of Sound Theory

### 2.1. Thermodynamic definition of Speed of Sound

The speed of sound can be defined as the distance travelled per time unit by the sound waves as it passes through an elastic medium. The speed of sound in air is influenced by many factors like specific heat, virial B- and C-coefficients, relaxation time, and relaxation strength. The uncertainties in calculating the speed of sound in air is based on quantities like relative humidity, temperature, pressure and sound frequency. Various designations of air can be considered while calculating the speed of sound in air such as CO<sub>2</sub> free air, standard air and atmospheric air. As the name suggests CO<sub>2</sub> free air is carbon dioxide removed from the standard air. Standard air is generally considered as dry air at sea level consisting of several gas species with relative concentrations. The addition of water vapor in standard air makes the atmospheric air conditions.

For calculating the speed of sound, it is far more important to have the clear study of speed of sound in theoretical aspects. Speed of sound can be represented using Laplace's adiabatic assumption for an ideal gas as follows,

$$U = \left( \gamma \frac{P}{\rho} \right)^{\frac{1}{2}} \quad (\text{eq3.1})$$

where  $P$ ,  $\rho$  and  $\gamma$  are the pressure, density of the medium and specific heat ratio respectively.

Based on Boyle's law ideal gas equation can be modified as follows,

$$U = \left( \frac{RT\gamma}{M} \right)^{\frac{1}{2}} \quad (\text{eq3.2})$$

Where  $R$  is the Universal Gas constant,  $T$  is absolute temperature and  $M$  is the molar mass.

The speed of sound can be expressed as follows based on the consideration of temperature and pressure as independent variables.

$$U^2 = \left[ \frac{1}{(\partial\rho/\partial p)T - (T/\rho^2 c_p)(\partial\rho/\partial T)^2 p} \right] \quad (\text{eq3.3})$$

Based on the consideration of temperature and density as the independent variables, the speed of sound values can be expressed as follows.

$$U^2 = [(\partial\rho/\partial p)T + (T/\rho^2 c_v)(\partial\rho/\partial T)^2 p] \quad (\text{eq3.4})$$

Where  $\rho$  is the mass density,  $p$  is the pressure,  $c_p$  is the isobaric specific heat capacity,  $c_v$  is the isochoric specific heat capacity.

In the consideration of all gases becoming perfect gases at a sufficiently low pressure, the equation (3.1) becomes as follows to represent the speed of sound in terms of the function of temperatures [35].  $A_0, A_1, A_2$  are the coefficients of the functions of temperature values.

$$U^2 = A_0 T + A_1 T p + A_2 T p^2 + \dots \quad (\text{eq3.5})$$

The virial state equation is presented below, which is important in the consideration of the pressure dependance on the speed of sound in air.

$$\frac{P}{RT} = \rho + B\rho^2 + C\rho^3 + \dots \quad (\text{eq3.6})$$

Where B is the second virial co-efficient and C is the third virial co-efficient etc,

## 2.2. Speed of Sound in air dependence on Pressure

The pressure values related to the speed of sound in air can be represented based on the virial coefficient of dry air and water vapor combined based on the mixing rules. The second virial coefficient is considered as it varies based on the interaction between molecular particles. The virial-B coefficient can be represented based on the second virial coefficient of dry air ( $B_{dd}$ ), water vapor ( $B_{hh}$ ), interaction coefficient ( $B_{dh}$ ) and mole fraction of water vapor ( $x_h$ ).

$$B = B_{dd}(1 - x_h)^2 + 2B_{dh}(1 - x_h)x_h + B_{hh}x_h^2 \quad (\text{eq3.7})$$

The second order virial co-efficient of dry air and water vapor can be presented as follows,

$$B_{dd} = a_d - b_d \exp\left(\frac{\gamma_d}{T}\right) \quad (\text{eq3.8})$$

$$B_{hh} = a_h - b_h \exp\left(\frac{\gamma_h}{T}\right) \quad (\text{eq3.9})$$

From the Table [4], it can be seen that at early stages of speed of sound calculating methods didn't take into account the pressure values or mention it in their paper explicitly during their calculation techniques. The pressure values are greatly influenced by acceleration due to gravity and it varies according to its geographical location. For example, it varies about 865 ppm when values from Paris and Washington are compared [36]. The authors in this paper [37], [38] however taken this into account and calculated pressure values based on their latitude locations. The authors from [39] [40] carried out the sound speed calculation in room temperature and stated about the change of its value at 0.001 m/s for change in every kilopascal. From these research works, the dependence of speed of sound in air on pressure is studied. As mentioned before, the interferometer accuracy at  $10^{-7}$  can be achieved with pressure values of uncertainty of 40 Pa. The pressure values of this uncertainty can be achieved by some of the best barometers available in the market.

### 2.3. Speed of Sound in air dependence on Frequency

Another factor to be considered while determining the speed of sound in air is the frequency of acoustic waves employed. The effect of frequency can be studied based on the relaxation in the medium of experiment. Atmospheric air is considered in our experiment, the main four constituents contributing to the relaxation are oxygen, nitrogen, carbon-di-oxide and water vapour. But, the combination of oxygen and nitrogen alone makes about 99% of the atmospheric air composition. So, it contributes to the most absorption of sound waves caused by the medium. The relaxation frequency values about 9 Hz for nitrogen at the pressure of 1 atm and zero humidity [41].

In order to study about the dependence of speed of sound in air on frequency, the experiment carried out by D.H. Smith and R.G. Harlow is studied [42]. The experiment was carried out inside a cylindrical resonator, in which the dry and Carbon-di-oxide free air is passed from outside after the treatment. The pressure values are maintained at 1 atm and temperature is kept around 303.15 K. In this experiment, the range of frequencies utilized are 93.5-1505.2 Hz. The authors claimed an uncertainty of 0.0028 % for their speed of sound values. With the temperature of 303.15 K, 1 atm and frequency of 93.3 Hz, the speed of sound values to be 349.32 m/s. At the frequency of 1024.53 Hz, it values to be around 349.23 m/s and at 1505.2 Hz it values to be 349.19 m/s. In theory based on the Cramer equation, the frequency of sound waves doesn't have an effect on speed of sound. The method developed by Owen Cramer to determine the speed of sound in air didn't have any frequency dependence. But the equations proposed by Zuckerwar [54] got very little dependence on frequency and it is valued as only few parts per million. So, in order to study this detail, the speed of sound values calculated by our experiment are carried out in different frequencies and the speed of sound values from environmental parameters are also presented at different frequencies based on Zuckerwar in addition to Cramer equation.

## 2.4. Composition of Atmospheric air

The speed of sound value accuracy is also based on the accurate determination of atmospheric-air composition. During early stages except for a few investigators, most of them did not give a clear picture about composition of air in their research method. Researcher Hebb performed his experiments indoors and came up with the air composition as follows: Nitrogen and Oxygen makes 97.2 % with 1.85 % for water vapor and 0.95% of argon. But he failed to give methodology used by him for finalizing these values [43].

Many investigators noted that the difference in oxygen and nitrogen composition alone can cause an uncertainty level up to  $\pm 150$  ppm for their measured speed of sound value. Some investigators decided on using pure air by removing the  $\text{CO}_2$  from their experimental conditions. Also reduced 0.018m/s from the sound speed values for the correction of  $\text{CO}_2$  absence [44].

The geography, altitude from sea level and geography makes a huge impact on the composition of air which influences the speed of sound in air. The major variation in variability is caused by the amount of water vapor and carbon dioxide presence.

$x_i$  can be considered as mole fraction in multi-constituent mixture of the  $i^{\text{th}}$  constituent can be defined as follows

$$x_i = \frac{n_i}{n} \quad (i = 1, 2, \dots) \quad (\text{eq3.10})$$

where,

$n_i$  is the molar density per unit volume of  $i^{\text{th}}$  constituent

$n$  is the molar density of the total composition.

$$\sum x_i = 1 \quad (\text{eq3.11})$$

The research work presented in [45] to measure the speed of sound was carried out in tubes and the air composition was not discussed in detail. Also, researchers presented the medium as pure air instead of carbon dioxide free air resulting in a correction of 0.032 m/s to compensate for the missing carbon-di-oxide content. The composition of air is mainly influenced by the geographical location and altitude from the sea level and resulting in the influence on the speed of sound in air. As a result of geographical factors, the major variability in speed of sound in air is caused by the amount of water vapor and carbon-di-oxide content.

The standard constituents of air near sea level based on ISO 25333-1975 [43] is presented below in the table (2).

Table 2-Standard constituents of air

Constituent	Molar mass (g/mol)	Mole fraction	Mass contribution (g/mol)
Nitrogen	28.01348	0.78084	21.874046
Oxygen	31.9988	0.209476	6.7029806
Argon	39.948	0.00934	0.3731143
CO <sub>2</sub>	44.0095	0.000314	0.013819
Neon	20.1797	1.818*10 <sup>-5</sup>	0.0003669
Helium	4.002602	5.24*10 <sup>-6</sup>	2.097*10 <sup>-5</sup>
Krypton	83.8	1.14*10 <sup>-6</sup>	9.553*10 <sup>-5</sup>
Methane	16.04246	2.0*10 <sup>-6</sup>	3.208*10 <sup>-5</sup>
Hydrogen	2.01588	5.0*10 <sup>-7</sup>	1.008*10 <sup>-6</sup>
Xenon	131.29	8.7*10 <sup>-8</sup>	1.142*10 <sup>-5</sup>
Nitrous Oxide	44.01288	2.7*10 <sup>-7</sup>	1.188*10 <sup>-5</sup>
Carbon monoxide	28.011	1.9*10 <sup>-7</sup>	5.322*10 <sup>-6</sup>
Total			28.9645

## 2.5. Speed of Sound in air dependence on Temperature

The absolute temperature plays an important role in determining the accurate value of speed of sound in air. Around 180 ppm of uncertainty value could be caused by the speed of sound values as a result of 0.1 °C of uncertainty [46]. More than any other environmental parameters, the role of temperature in determining the speed of sound in is important. In the acoustic thermometer, the thermal sensitivity of acoustic waves is utilized to determine the accurate temperature values.

When the speed of sound in air is calculated, the individual gas of composition is considered and ratio of specific heat to universal gas constant is presented below,

$$\frac{\gamma_0}{R} = a_0 + a_1T + a_2T^2 + a_3T^3 \quad (\text{eq3.12})$$

Where  $\gamma_0$  is the specific heat of the respective gas and  $a_0, a_1, a_2, a_3$  are the co-efficient and have their respective values for dry and water vapor respectively. As atmospheric air is the medium of experiment, the specific heat of the humid air can be represented as follows,

$$\gamma = \gamma_a x_a + \gamma_h x_h \quad (\text{eq3.13})$$

Where  $x_d$  and  $x_h$  is the mole fraction of dry air and water vapor respectively.

Most of the research work carried out [37], [38], [47]–[51] to determine the speed of sound in air presented their temperature values around 0.1 °C of uncertainty. The research work carried out by Owen Cramer [52] also presents about the dependance of speed of sound in air on various environmental parameters particularly on temperature is discussed before. Also, [53] presents about the speed of sound in air as the function of temperature based on the time delay experiment carried out by them.

## 2.6. Speed of Sound in air dependence on Relative Humidity

The water vapor content has the ability to vary with short intervals in relative to the atmospheric conditions and it becomes important to take care about the readings of the same while performing the speed of sound in air experiments. Usually, the relative humidity is measured in percentage with help of a hygrometer which represents the ratio of partial pressure of water vapor present in the air to the equilibrium water vapor pressure. The relative humidity depends on the temperature of the atmospheric conditions as well.

The relative humidity can be defined as the ratio between the water vapor mole fraction to mole fraction of water vapor at saturation.

$$h = \frac{x_i}{x_{sat}} \quad (eq3.14)$$

There are many other researches carried out in the past to discuss the effect of humidity effect on the speed of sound in air. In particular [54] describes about the speed of sound in air's dependence on the frequency of sound waves and relative humidity combined. The research work carried out by Cyril.M. Harris [55] performed experimental work to determine the speed of sound in air at 20 °C with varying range of relative humidity. The authors [56], [57] published a paper stating the variation and dependence of the sound speed in air based on humidity along with the temperature values. This paper's author proposes their experimental work to be capable of yielding speed of sound in air with uncertainties of  $\pm 400$  ppm. These values of uncertainties for speed of sound in air proves to be valid for the temperature range of 0 to 30 °C [47]. Some research to determine the speed of sound in air is done from humid air and some on dry air. From the following equation, the ratio of speed of sound values from dry and humid air is presented as follows,

$$\frac{u_h}{u_0} = 1 + h(9.66 * 10^{-4} + 7.2 * 10^{-5}t + 1.8 * 10^{-6}t^2 + 7.2 * 10^{-8}t^3 + 6.5 * 10^{-11}t^4) \quad (eq3.15)$$

where,  
 $u_h$  is the speed of sound in humid air  
 $u_o$  is the speed of sound in dry air  
 $h$  is the humidity and  
 $t$  is the temperature

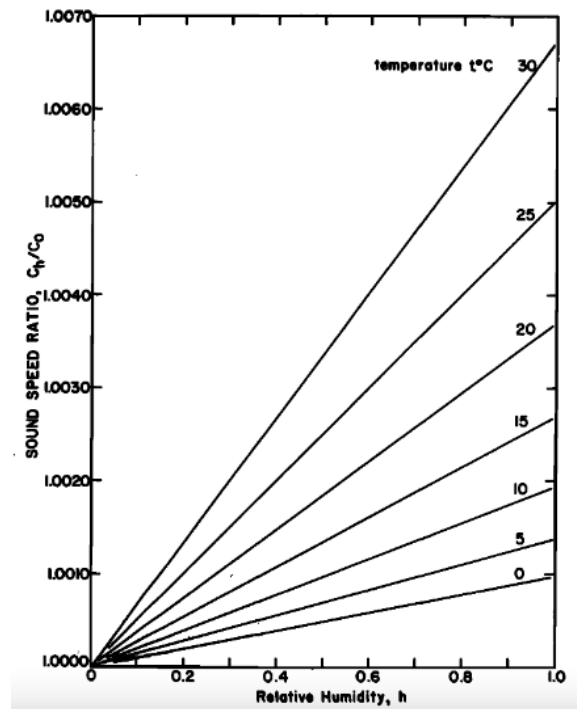


Figure 1-speed of sound in air at Std atmosphere (1 atm) vs Various temperature and various relative humidity

[41]

The above fig-1 represents the speed of sound in air variation based [55] on the different humidity and temperature values at standard atmospheric pressure of 101.325 kPa (1 atm). The recent experiment [58] carried out in Universidad de Salamanca, Spain demonstrated the temperature dependence of speed of sound in air through simple classroom method. They demonstrated the speed of sound in air value changes depending on specific heat and temperature over a span of an hour at  $0.6 \pm 0.06$  m/s per °C of temperature change in air.

## 2.7. Speed of Sound in air dependence on Carbon dioxide content

As mentioned in previous sections, the carbon dioxide content changes drastically with geographic locations and it becomes important to study about their variations in detail. The following table represents the composition of various constituents in atmospheric air and CO<sub>2</sub> free air.

*Table 3-Dry carbon di oxide free air and dry 1999 air constituent's mole fraction [41]*

Constituent	Mole fraction in CO <sub>2</sub> free air	Mole fraction in 1999 air
Nitrogen	0.78109	0.78080
Oxygen	0.20954	0.20946
Argon	0.009343	0.009339
CO <sub>2</sub>	0	0.000368
Neon	$1.819 \cdot 10^{-5}$	$1.818 \cdot 10^{-5}$
Helium	$5.242 \cdot 10^{-6}$	$5.240 \cdot 10^{-6}$
Krypton	$1.14 \cdot 10^{-6}$	$1.140 \cdot 10^{-6}$
Methane	$2.001 \cdot 10^{-6}$	$2.000 \cdot 10^{-6}$
Hydrogen	$5.002 \cdot 10^{-7}$	$5.000 \cdot 10^{-7}$
Xenon	$8.703 \cdot 10^{-8}$	$8.700 \cdot 10^{-8}$
Nitrous Oxide	$2.701 \cdot 10^{-7}$	$2.700 \cdot 10^{-7}$
Carbon monoxide	$1.901 \cdot 10^{-7}$	$1.900 \cdot 10^{-7}$

The figure-2 was presented below to show the carbon dioxide content increases in the atmospheric air over the period of 4 decades. The CO<sub>2</sub> mole fraction was only about 314 ppm during the year of 1958 and by the end of 1999 it increased up to 368 ppm. With the more utilization of fossil fuels, there is no signs of CO<sub>2</sub> content reducing drastically in the near future. It gives an idea about the dependency of air composition on CO<sub>2</sub> content and its importance about considering it while carrying out the speed of sound in air experiment and calculation.

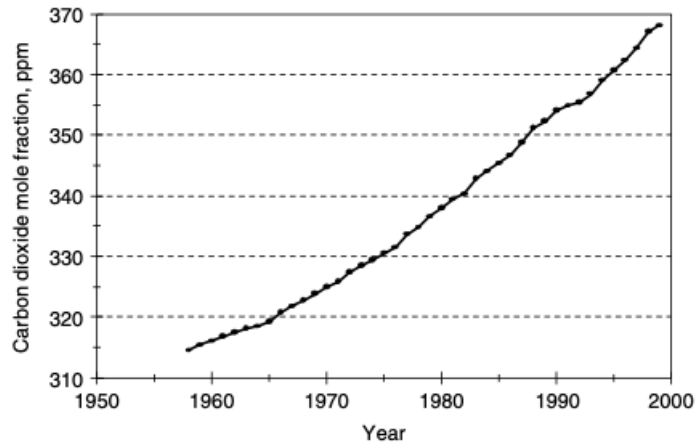


Figure 2-Mean annual mole fraction of carbon dioxide in dry air from 1958 to 1999[41]

When we discuss the dependence of speed of sound in air on carbon dioxide content, it becomes important to talk about various techniques handled by previous researchers in their work for the estimation of speed of sound in air. From the research review paper presented by George S.K. Wong [47] it can be observed that the carbon dioxide values are not considered during early stages of speed of sound in air estimation techniques. Later, they compensated for the carbon dioxide exclusion by subtracting the value of 0.018 m/s in order to compensate for lack of CO<sub>2</sub> from the calculated speed of sound in air [37]. In the papers [49], [50], the author followed the method of treating atmospheric air in order to dry out the moisture content and thereby obtain carbon dioxide free air. But, the efficiency of these treatment techniques was not discussed in detail by these authors and also its contribution to the uncertainties in speed of sound in air. The major constituents of air like nitrogen, oxygen and argon remain unchanged for a longer time and the changes were only minimal at  $\pm 0.004\%$ ,  $\pm 0.002\%$  and  $\pm 0.001\%$  respectively in its total volume for dry air [51]. But, the constituent's percentage with the carbon dioxide and water vapor content present in atmospheric air changed in large numbers during recent times [47], [48]. So, it becomes important to have clear knowledge about the values of CO<sub>2</sub> content and relative humidity while calculating the speed of sound in air with a well-known uncertainty.

## 2.8. Uncertainties in Speed of Sound

The technique employed by most researchers was to perform the experimental method to calculate the sound speed value and based on the prevailing conditions, they derived with required theoretical corrections. The uncertainties in the speed of sound are mainly caused because of the uncertainty in the values of absolute temperature, specific heat ratio, molar mass of air and universal gas constant. From the table it can be understood that most of the researchers did not consider the uncertainty that comes up with composition of air, length conversion, barometric pressure, absolute temperatures. In spite of ignoring all these uncertainty values, most investigators came close to a value of sound speed as 331.45 m/s with their theoretical corrections. The uncertainty budget was also presented in this based on the uncertainty values raised from the supporting parameters of the experiment in detail in the chapter of results and discussion. As the speed of sound values are also calculated based on the Cramer equation from the environmental parameters, the uncertainty related to the measurement of these environmental parameters is also presented for the comparison.

The speed of sound in air can be expressed as  $U$  after applying sufficient corrections related to the specific heat, virial co-efficient and relaxation correction as follows,

$$U^2 = U^2(1 + k_c)(1 + k_v)(1 + k_r) \quad (\text{eq 3.16})$$

Where  $k_c$ ,  $k_v$ ,  $k_r$  are the corrections of specific heat, virial co-efficient and relaxation co-efficient respectively and  $U_s$  is the simple speed of sound.

$$U_s^2 = \frac{\gamma_s RT}{M} \quad (\text{eq 3.16})$$

## 2.9. Cramer Equation for calculating Speed of sound in air based on Environmental Parameters

It is important to study the dependence of speed of sound in air on environmental parameters based on the previous experiments carried out by various researchers. The environmental parameters we are focusing on in this section are temperature, relative humidity, pressure and carbon dioxide content. The most common and popular equation used by various researchers was developed by Owen Cramer for studying about the environmental parameters influence on calculating the speed of sound in air. According to Owen Cramer, [59] this research results are valid for the temperature measurements at the range of 0 to 30 °C. With his research method, he proposed the following equations for speed of sound in air with an uncertainty of  $\pm 300$  ppm [52].

$$f(t, p, x_w, x_c) = a_0 + a_1 t + a_2 t^2 + (a_3 + a_4 t + a_5 t^2) x_w + (a_6 + a_7 t + a_8 t^2) p + (a_9 + a_{10} t + a_{11} t^2) x_c + a_{12} x_w^2 + a_{13} p^2 + a_{14} x_c^2 + a_{15} x_w p x_c \quad (\text{eq3.18})$$

The coefficients values are:

$$\begin{array}{ll}
 a_0 = 331.5024 & a_1 = 0.603055 \\
 a_2 = -0.000528 & a_3 = 51.471935 \\
 a_4 = 0.1495874 & a_5 = -0.000782 \\
 a_6 = -1.82 \cdot 10^{-7} & a_7 = 3.73 \cdot 10^{-8} \\
 a_8 = -2.93 \cdot 10^{-10} & a_9 = -85.20931 \\
 a_{10} = -0.228525 & a_{11} = 5.91 \cdot 10^{-5} \\
 a_{12} = -2.835149 & a_{13} = -2.15 \cdot 10^{-13} \\
 a_{14} = 29.179762 & a_{15} = 0.000486
 \end{array}$$

$$x_W = h f \frac{p_{sv}}{p} \quad (eq3.19)$$

where  $h$  is the relative humidity expressed as a fraction,  $f$  is the enhancement factor, and  $p_{sv}$  is the saturation vapor pressure of water vapor in air.

$$f = 1.00062 + 3.14 \cdot 10^{-8} + 5.6 \cdot 10^{-7} t^2 \quad (eq3.20)$$

$$p_{sv} = \exp\left(1.2811805 \cdot 10^{-5} t^2 - 1.9509874 \cdot 10^{-2} t + 34.04926034 - 6.3536311 \cdot \frac{10^3}{t}\right) \text{ Pa} \quad (eq3.21)$$

In this thesis, the speed of sound values is calculated from the experimental set-up build and along with Cramer equation for comparison. For the calculation of speed of sound values based on the Cramer equation, the environmental parameters like temperature, relative humidity, carbon-di-oxide content and pressure are measured simultaneously using various instruments.

## Chapter 3

# A review of calculating methods of Speed of Sound in air

### 3.1. Basic theory of Acoustic Thermometer

The technique of measuring the thermodynamic temperature present in a low density and monatomic gas cavity with an uncertainty level of up to  $3 \times 10^{-6}$  or lower has been established as a result of Acoustic Gas Thermometry. The speed of sound  $U$  and the thermodynamic temperature  $T$  for an ideal gas can be given by the equation as follows,

$$U = \left( \frac{\gamma RT}{M} \right)^{1/2} \quad (\text{eq2.1})$$

$\gamma$  is the adiabatic exponent and  $M$  is the molar mass of the gas. The temperature can be represented based on the following equation of speed of sound as follows, where  $l$  is the distance traveled by acoustic waves and  $t$  is the time taken.

$$T = \frac{Ml^2}{\gamma R t^2} \quad (\text{eq2.2})$$

It is important to note that the temperature values are accurate only when the temperature of the acoustic path remains uniform. The time taken by acoustic waves determines the change in temperature and gives an average temperature value along the path.

From the equation (1) it can be seen that speed of sound directly depends on the gas constant  $R$  and molar mass  $M$ . Any uncertainties in this can directly influence the uncertainty in measurement of temperature using the speed of sound.

The technique of using acoustic thermometers to measure temperature in an environmental condition has been studied for a few years now [24]. It makes use of the dependency of soundwaves on temperature during the transition period to measure precise temperature values. The transition period depends on the environmental parameters like temperature, pressure, relative humidity and  $\text{CO}_2$  content in an open environment. The ability of acoustic thermometer to utilise in the cases where physical sensors utilization is tougher makes it unique. This acoustic thermometer technique can also extend to various dimensional metrology applications like aerospace industry, precise manufacturing where high accurate values are needed. Acoustic thermometers can also be used in the much extreme situations like higher temperature and in nuclear reactors. Also, the conventional thermometers work based on the single point determination as opposed to the acoustic thermometer, where it gives the total temperature along its transmitted path.

### 3.2. Overview about acoustic thermometer

This paper [25] explains about the developed experimental set-up to measure temperature and humidity in the atmosphere with reduced sampling time. Also, with the integration of systems it operates as a stand-alone machine without the requirement of an external computer for data processing. The results from the research proves its ability of producing uncertainty less than  $0.1\text{ }^{\circ}\text{C}$ . The system proves to be suitable for temperature measurements along smaller distances in this case up to 1 m. The feasibility of measuring temperature along larger distances was not discussed in this research work. Many other researches have been carried out in the past and also in the present about employing acoustic measurements in order to compensate for the change in the air-refractive index in measurement of displacements. The research carried out in this field can be broadly classified based on the direction of ultrasonic pulses as (i) Uni-directional set-up, (ii) bi-directional set-up and (iii) two-way bi-directional measurements. Based on the source of the sound waves it can be classified into (i) measurement of the phase signal of a continuous wave and (ii) transmission of pulses in packets. It can also be classified into fixed and variable based on the changes in measuring distance.

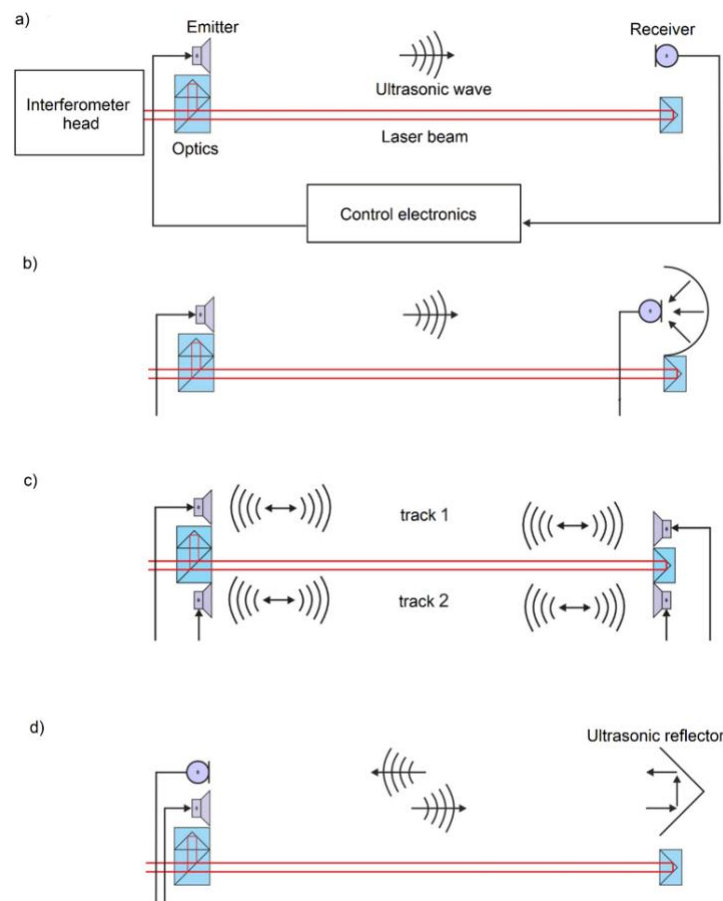


Figure 3-Variou techniques for acoustic measurement utilized (a)Unidirectional technique (b)unidirectional with mirror (c)bi-directional (d)bi-directional with reflector [26]

Some of the research that has been based on acoustic thermometers for precision dimensional measurements carried out in various metrology institutes are discussed briefly in this part. These researches were carried out in the distance measurement ranges from 2 m to 30 m and the temperature measurement uncertainty about 0.01 °C to 0.1 °C. The interference measurement axis is placed with a uni-directional acoustic path in parallel direction within a short distance. This uni-directional method is comparatively simple and mainly used in the applications with not much of significant air flow is present. The increased air flow can reduce the intensity of acoustic signals reaching the receiver. The synchronization of receiver and transmitter becomes primary and it is carried out by the transmission of pulses during the start and end of the ultrasonic transmission. The pulses can be sent through wires, the transmission of pulses through wireless makes the experimental set-up to measure larger distances more than few meters [27]. The speed of sound is calculated using the phase difference of the transmitted and received signal through a set of loudspeaker and microphone. The research [28] [29] carried out to compensate for air-refractive index through acoustic temperature is built with a two-way bi-directional measurement setup. With the transmission and receiving of signals in both directions, the measurements are made. The final results for thermal measurements are valued from average both directional values. This bi-direction measurement was useful in compensating for the errors that may arise due to the laminar air flow at windy conditions.

Based on [30], the phase delay error between transmitted and received signals at 10 ns for a distance of 1 m and the approximate speed of sound is 346 m/s (25 °C); it accounts for a relative uncertainty of  $3.5 \times 10^{-6} \text{ ms}^{-1}$  over 1 meter measuring range. Another important aspect to be considered for attaining such accurate metrological values is to concentrate on attenuation of signal received at the microphone [26]. Some of the acoustic thermometers setup was operated with the transmission of pulse pack to determine the speed of sound. The problem that has to be dealt with in this case is to establish the start and end of the pulse pack transmission. The research work involved in these kinds of transmission of signals, usually adding the sensor and time counter. This helps with the applied threshold to determine the phase delay between the start and end of the transmitted pulse pack [31][30]. This technique can prove to be efficient when there is a constant distance measurement [27]. With an increase in the distance, there occurs a delay related to the time taken by pulse to travel which can be lower than the set limit. With increase in distance, the amplitude of the received signal lowers based on the increment of occurred error. Some of the research carried out in [32] proposed an alternative method for detecting signals to overcome the possibility of higher errors which is based on Akaike Information Correction (AIC).

The authors of this paper [33] have carried out a research to accurately measure the temperature over a smaller distance up to 10 cm. Their experimental set-up is made of two transducer facing opposite to each other fixed at a constant distance. The results for phase delay are measured by the signals transmitted at the frequency of 40 kHz. The uncertainty of their smaller distance temperature measurement proves to be 0.05 °C based on their results. The research carried out by Korpeleinan [28] discusses about the utilization of acoustic waves for determining the effective temperature, there by calculating the accurate length in interferometric measurements through precise refractive index calculation. This research focusses on measuring speed of sound pulses of about 50 kHz in frequency along the

interferometer path for determination of refractive index. This research demonstrates about the accurate length interferometry up to distance of 5m. The temperature and refractive index of air uncertainties are estimated to be 25 mK and  $2.6 \times 10^{-8}$  over the distance measurement of 5 m.

The research paper [34] presents an acoustic method for measuring the temperature along the large distance measuring interferometer built in INRiM. They proposed this model by taking advantage of their setup capable enough to generate acoustic signal and amplitude modulation of laser to be in synchronous. To prove the traceability of experimental results obtained from acoustic model, the temperature values from 14 thermometer placed along the interferometer path is recorded. They proposed based on the initial results, this experimental setup is capable enough to get utilized in the larger distance interferometer measurements by its ability to act as an acoustic thermometer and estimating the air-refractive index with greater accuracy. Based on [34], at the resolution of 0.1 °C over larger distances with a corresponding uncertainty of  $10^{-7}$  in the interferometric measurements.

### **3.3. History related to Speed of Sound in air by various researchers**

During the 18<sup>th</sup> century, new methods started to develop for determining the speed of sound. The coincidence method was developed, which is done by creating sound waves at a periodical intervals and distance between source and reflector was adjusted. This is done until the interval between sound pulses gets multiples as exactly when compared with the reflected sound waves from the source. Lenihan developed an electronic version of this experiment to determine the speed of sound as 331.45m/s. Regnault tried performing a similar experiment inside tubes and resulted in much lower speed of sound than that in free space. Multiple pipes with different diameters are used by him and he made some assumptions to determine it for calculating the speed of sound in air. His final calculations lead to a speed of sound value in dry air around 330.7m/s [60].

More recently, many precise experimental methods are developed in order to determine accurate speed of sound and thermodynamic properties in free air conditions. The speed of sound is determined with the help of a resonator (a cavity with fixed path length). In order to receive maximum amplitude at the receiver end the oscillator fixed at the cavity source is adjusted accordingly. The speed of sound can be determined based on the accurate values of cavity dimensions, number of half lengths and resonance frequencies. Uncertainty in measurement for speed of sound is estimated around 200 ppm for a spherical resonator technique. But, with more accurate volume measurement of the resonator could close down the uncertainty level up to 5 ppm [60].

The sound speed measurement through direct methods can be broadly classified into three groups as follows:

1. Longer distance and open-air conditions
2. Controlled laboratory conditions within short distances
3. Measurement in cavity, tubes, pipes or spheres (resonators)

There are other indirect methods like determining the speed of sound specific heat ratio estimation and vital information regarding the composition of air.

### 3.4. Review on speed of sound in air calculating methods

Although many experiments have been carried out in the past, the paper [61] considered to hold historical appreciation. This is considered to be one of the first experiments carried out using interferometer technique to determine the speed of sound in air. The author stated the speed of sound in air as close to 331.4 m/s (at 0 °C), which is the standard value by also stating uncertainties within the range. This experiment was carried out using a sonic interferometer with a variable path method. One parabolic reflector is fixed and another one on a movable track in-line with the propagation of sound waves from the air whistle. The sound waves received from the stationary and moving reflectors provide an interference pattern through which the speed of sound in air is calculated. The authors carried out this experiment to avoid the wind effects on the speed of sound in air values. The authors also managed to measure temperature along the sound path using 11 thermometers and the relative humidity through the "Alurad" hygrometer. This technique of calculating speed of sound in air yields an uncertainty of about 0.12%.

The experiment carried out by W. G. Shilling and J. D. Partington [62] to calculate the speed of sound in air was also carried out using sonic interferometer as mentioned in previous method. They elaborated the last work over a wide range of temperatures around 273-1273 K in this experiment. Although atmospheric air is employed in the previous method, here the air intake is treated in order to remove the carbon-di-oxide content through which the authors tried to eliminate the effects of CO<sub>2</sub> on speed of sound measurement values. With the correction values applied for CO<sub>2</sub> removal and also for tube correction. The author claims uncertainty of about 0.067 % in the sound speed measurement.

The experiment presented in [38] was considered to be the first one to measure the speed of sound in air with an ultrasonic interferometer. With the help of X-cut quartz crystals, the ultrasonic frequency is in the range of 902 to 1081 kHz at room temperature at 20 °C. The ultrasonic frequency 551 to 610 kHz was carried out to measure the speed of sound in air at the standard conditions. The measurements are carried out in the CO<sub>2</sub> free content air by passing through the air intake taken from the atmosphere and passing it through phosphorous pentoxide. The researchers didn't take into account dewpoint temperatures values by making an assumption of it being close to zero as result of CO<sub>2</sub> removal process efficiency. The uncertainty contribution in values is summarized and valued to be around 0.021 % in the measured speed of sound in air valued by making adequate corrections.

The experimental method proposed in this article [63] briefs about the sound speed estimation through acoustic feedback technique for lower frequencies and pressure range. This experiment was carried out in the tube with dried air without CO<sub>2</sub> content and applying tube correction relative to the tube walls. In this method the sound waves propagated and received through a loudspeaker microphone are connected with an electrical tuned amplifier. Although authors carried out this experiment at room temperature, the reduction to standard conditions was carried out based on the methods presented in this article discussed earlier [38]. The authors also claim an uncertainty of  $\pm 0.22$  m/s in this method after taking measurement uncertainties of environmental parameters and tube measurements.

The experimental method carried out in acoustic laboratory of Harvard University presented a closed tube method for calculating speed of sound in air [64]. Like previously mentioned experiments, this is also carried out using a variable path interferometer. But, in contrast, inside a tube of length around 0.03 m enclosed with compressed and dried air. The author analyzed tube correction and also presented the uncertainties from various environmental parameters and frequency of sound waves. With this method of estimation, the author proposed an uncertainty of 0.05 m/s in speed of sound air at standard conditions. Although this uncertainty meets our requirements the experimental method was carried out along a small tube and with dry air. The author also cites the large contribution of its uncertainty as a result of the tube effect [65].

J.M.A. Lenihan carried out an experiment [66] in an indoor hall, but the experiment was not carried out in an anechoic chamber and the author cited avoiding errors due to deflection by employing a high frequency range about 13.5 kHz. The experiment was carried out at a variable length in the range of 0.15 to 1.65 m. a similar method presented in previous experiments was used to reduce the speed of sound to zero humidity level. The author predicted with an uncertainty of about 0.1 % their speed of sound in air at standard values.

### **3.5. Estimation of Speed of sound in air through time-of flight method**

It is important to discuss about the speed of sound in air experiment carried out in recent days using time-of flight method. The work of [67] was done in University of San Francisco by using a Polaroid Corporation camera to determine the time taken from emission and the arrival after echoing at the other end. This method's speed of sound in air at the temperature of 23.4 °C, relative humidity of 46.5 % proves to be 346.09 m/s and an uncertainty range of  $\pm 0.07$  m/s. This method didn't take into account errors from echoing, deflections and also the effect of carbon dioxide content by making an assumption of its negligible values.

The author in this paper [68] made an experiment to measure speed of sound in air by time-of flight method by using sound card and editing software. The authors carried out this in a tube where sound waves are transmitted for 1.6 m and reflected back for 1.076 m to the microphone with an uncertainty of 0.1 cm in the length measurement. With the help of sound cards and software, they conclude with the speed of sound in air at standard conditions to be 331.4 m/s and change of 0.61 m/s for every 1 °C temperature change and the uncertainty of 0.3 %.

This paper [69] demonstrates about estimating the speed of sound in air through time-of flight measurements from a new year celebration video recorded in New Zealand. The temperature values are reported from meteorological parameters and relative humidity assumption was made to be at 50%. As a result of this time-of flight method at macroscopic level, the author claims an uncertainty in speed of sound in air through video to be at 1 %. The technique of direct measurement of speed of sound in air presented in [70] by authors from Valencia University, Spain. They carried out a time-of flight direct measurement by using conventional microphone and loudspeaker. The sound speed values from this method were compared with literature values of speed of sound in air. The experiment was carried out in

variable lengths which were measured using metric tapes of resolution 0.001 m. The increment of distance variable is set at 5 cm for the range of 0 to 110 cm length. With the experimental result, the authors compared experimental values of speed of sound in air with [71] and resulted in a variation limit of 0.2 %. The authors although made a comparison with previous literature, the uncertainty budget of values contributed by environmental parameters are not presented.

In this part of thesis, the dependance of speed of sound in air on environmental parameters are presented briefly. The historical methods followed by researchers and the uncertainty calculating methods also presented. Finally, the latest related experiments carried out to determine speed of sound in air using time-off flight method is also discussed in detail.

To give an insight about the speed of sound in air values over the time calculated by various researchers using different techniques are presented below in table-4.

*Table 4-Speed of sound at 0 °C found by some investigators since 1919 [72]*

<b>Year</b>	<b>Investigator</b>	<b>Speed of sound value</b>	<b>Experiment distance</b>	<b>Source of frequency (kHz)</b>
1919	Esclangon	330.9	1.4 -14 km	Cannon
1919	Hebb	331.41	80-100 ft	1.3-3.1
1921	Dixon	331.8	0.16 m	Hammer pulse
1921	Gruneisen and Merkel	331.57	0.23-0.95 m	Up to 11
1921	Angrerer and Landenburg	330.78	Approx. 11 km	Explosion
1923	McAdie	331.79	Inclined direction	Steam Whistle
1925	Pierce	331.69	Approx.. 0.01m	206
1928	Shilling and Partington	331.4	Approx. 1 m	Approx.. 3
1928	Cornish and Eastman	331.41	1.68 m	Approx.. 0.1
1930	Reid	331.60	0.6 m	40-216
1933	Kaye and Sherratt	331.60	0.55 m	0.79-7.9
1933	Grabau	331.68	0.55 m	20-70
1935	Norton	331.78	10-40 $\lambda$	5-120
1937	Miller	331.36	7243-20312 ft	Cannon

1937	Warner	330.3 to 330.6	Approx 0.08 m	38.6-104.5
1938	Colwell	331.54	5-6 m	Pulses, 0.06
1938	Kukkamaki	330.8	1-1.3 km	Explosion
1939	Pielmeier	331.4 to 331.6	0.08 m estimated	Up to 1080
1942	Hardy	331.44	0.07-0.08 m	300-11--
1944	Itterbeck and Vandonick	331.9	0.1 m estimated	523.78
1946	Stewart	331.7	1 mm	3885
1948	Abbey and Barlow	331.4	1 m	1.0
1952	Lenihan	331.45	Approx. 1.5 m	13.5
1952	Ener	331.52	1 mm	Approx. 2000
1953	Smith	331.45	Approx. 0.17 m	1.0
1954	Harlow	331.45	1.85 m	1-1.5
1956	Bancroft	331.7 & 331.87	9-inch diameter sphere	2.12 and 3.65
1956	Itterbeek and Rop	330.92 to 331.65	0.1 m	Approx. 525
1957	Lee	331.46	Approx. 1.6 m	0.11-1.0
1959	Steel	331.49	Approx. 1.7 m	0.45-1.2
1959	Hovi	331.15 to 331.65	Approx. 2 m	1.25-2
1960	Smith and Wintle	331.45	1.75 m	0.08-1.5
1963	Lestz	331.49	<30 inches	2.5-4.3
1963	Smith and Harlow	331.45	1.85 m	0.09-1.5
1985	Wong	331.29	Indirect method	
1993	Cramer	331.46	Indirect method	

## Chapter-4

# Acoustic Thermometer: Experiment and Results

After studying about past works carried out related to acoustic thermometer and air-refractive index estimation, in this section the working principle of proposed acoustic thermometer is described in detail. The main aim of this experiment is to demonstrate a method capable of measuring the speed of sound in air using the phase delay detection with the help of a loudspeaker and microphone set-up. The experimental set-up is designed to be capable of measuring over several meter the average speed of sound. The speed of sound in air is also calculated using Cramer equation based on environmental parameters such as temperature, pressure, relative humidity and carbon-di-oxide content measured in the same environment. The speed of sound in air obtained using the experimental set-up is checked for its agreement with uncertainty limits of Cramer equation (300 ppm). The same uncertainty is attributed to the measurement of temperature obtained with the method.

Optical measurements are based on the knowledge of the speed of light i.e., of the refractive index of air. With Edlen formula, if the target is  $u(n)/n = 10^{-7}$  we need a knowledge of the parameters with  $u(T) = 0.1$  °C,  $u(P) = 40$  Pa,  $u(RH) = 12\%$ . While pressure and relative humidity are rather uniform in space, temperature can change substantially and the use of discrete thermometers is not sufficient. Moreover, thermometers can be slow and in order to have a measurement of the temperature averaged along the path a large number of thermometers should be used. To overcome this problem, we exploit the strong dependence of the speed of sound on the temperature of air to the purpose of air refractive index estimation.

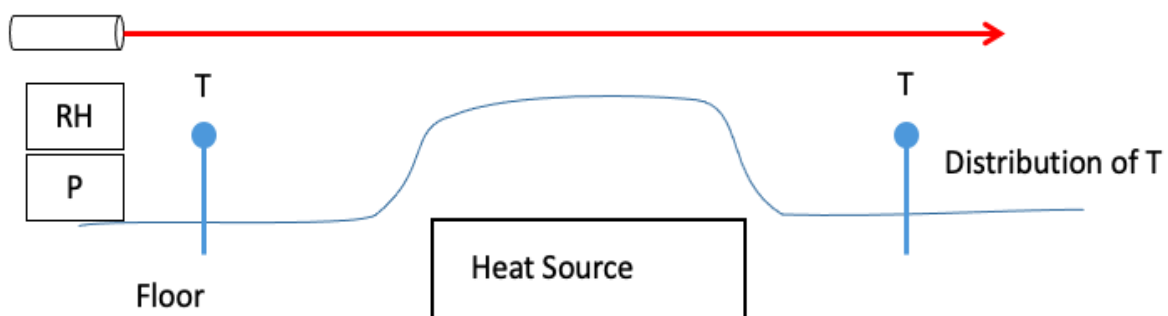


Figure 4-Along the optical path of an interferometric measurement the temperature can vary considerably, and for a correct estimation, a large number of thermometers should be used. On the other hand, humidity and pressure are quite uniform in space and can be sampled locally. The acoustic measurement allows to measure the average temperature along the same path travelled by light.

## 4.1. Working Principle of acoustic thermometer

This experiment is based on the principle of measuring the phase delay between the generation and recording of an acoustic wave at given frequency over a given distance. This measurement gives directly the speed of sound ( $u$ ) based on the following equation.

$$u(T) = \frac{d \cdot f}{\phi} \quad (\text{eq 4.1})$$

$d$  is the distance traveled by the acoustic wave

$T$  is the temperature

$f$  is the frequency

$\phi$  is the measured phase delay

The next step is to develop an experimental set-up to implement the working principle proposed in this part. As mentioned in the working principle, the experimental set-up should consist of a loudspeaker with capability of emitting continuous acoustic waves, a microphone for receiving the acoustic sound waves and phase meter for measuring the phase between signal sent to loudspeaker and the signal received by the microphone. Because of its cyclic nature, the phase signal has an ambiguity which derives from the lack of knowledge of the integer number of phase cycles (i.e., the number of acoustic wavelengths) due to delay between loudspeaker and microphone.

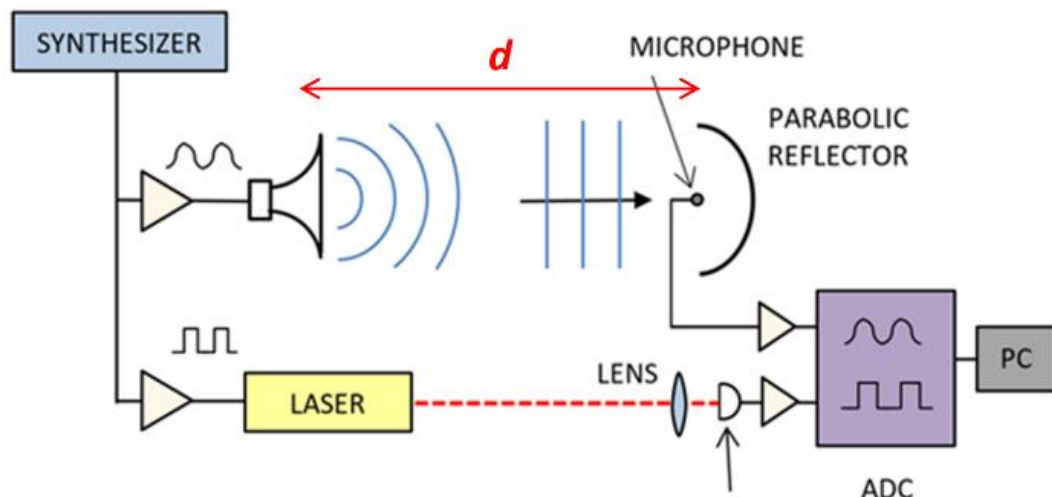


Figure 5-Working principle of acoustic thermometer experiment. A continuous acoustic wave is generated by the loudspeaker driven by a synthesizer at the left of the picture. After having run the distance  $d$ , the wave reaches the microphone at the right. A phase-meter is used to measure the phase delay between the generated wave and the received wave that is proportional to the distance and inversely proportional to the speed of sound.

Another important aspect to be addressed while making this experiment is to determine the distance travelled by acoustic signal waves. The starting point from the

loudspeaker and ending point at the microphone only represents the virtual position (visual start and end point of sound wave signals) and doesn't give measurement knowledge about precise acoustic distance of sound wave signals. So, it becomes important to formulate a technique for addressing this problem of measuring the effective acoustic distance. In order to eliminate both ambiguities (i.e., the integer number of wavelength and real value of distance) the following method has been proposed. The technique is based on sweeping the frequency in a given interval in the experimental set-up above, the phase changes continuously proportionally to the distance  $d$ . The equation relating the speed of sound ( $u$ ), frequency ( $f$ ), distance ( $d$ ) and phase ( $\varphi$ ) is expressed as follows,

$$d = u \frac{\delta\varphi}{\delta f} \quad (\text{eq 4.2})$$

The effective distance ( $d$ ) value can be obtained by measuring the slope of the function  $(\delta\varphi/\delta f)$  from equation (4.2). It is obvious that one can observe that the equation depends on the priori knowledge of the speed of sound ( $u$ ), so equation (4.1) and (4.2) apparently becomes recursive and no solution can be found in this case. After establishing a pair of microphone and speaker for the experimental set-up, by using this equation the distance ( $d$ ) is measured for a short distance between source and receiver (e.g., 1 m) and the speed of sound is estimated by making accurate temperature measurements with classical thermometers. Then the effective distance is measured by means of the frequency sweep method. The frequency sweep can be e.g. between 10 to 20 kHz. The next step is to measure the physical distance between loudspeaker and microphone with respect to physical fiducial point (standard of reference) and the relationship between physical distance and acoustic distance ( $d$ ) is established. Once this relationship for a pair of microphone and speaker is defined, the fiducial points are used to measure distance ( $d$ ). In the experiments performed, the distance is measured using an EDM (Bosch) having a resolution of 0.1 mm up to a distance of 10 m. The EDM used in this experiment has been calibrated at the INRiM, long range interferometry facility [74].

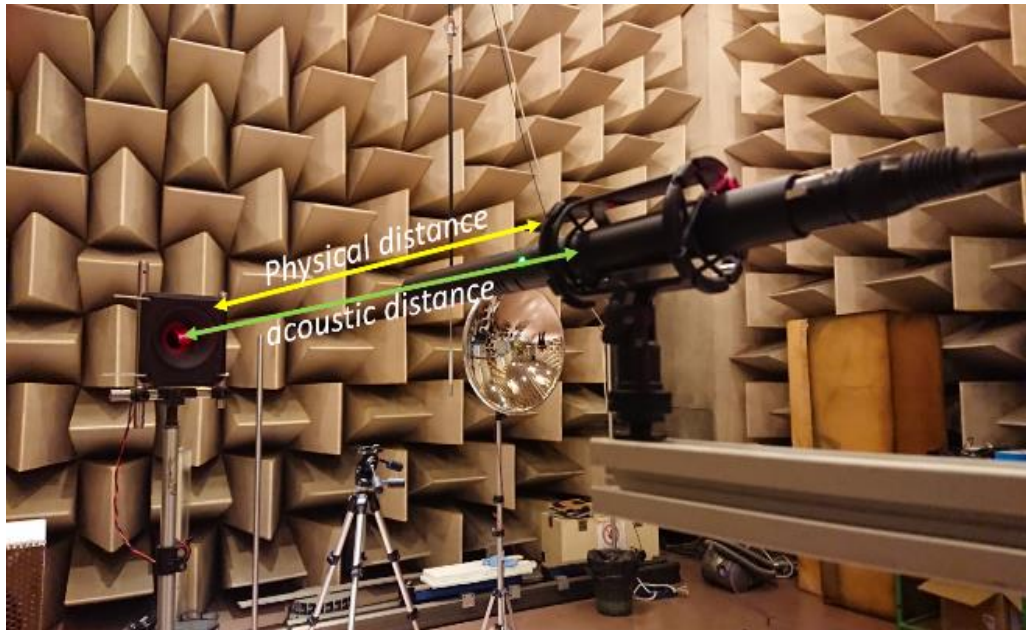


Figure 6- Effective distance measurement between loudspeaker and microphone. The effective distance is the value  $d$  in eq 4.1. This distance is not easily definable from the physical construction of the devices and must be found through eq. 4.2 by the seeping method.

## 4.2. Choice of Operating Frequency

Although in principle the operating frequency doesn't impact the experiment of speed of sound, it becomes important to choose optimum frequency range for this experiment considering many factors. Speed of sound in air experiment carried out in the past did not discuss frequency effects on the speed of sound in air. The Cramer equation doesn't take the frequency of sound waves into consideration, but Zuckerwar [54] stated a very small dependence of speed of sound in air on the frequency, although it is of only few parts per million.

An important factor to be considered while selecting the frequency of the sound waves operated through the experiment is the choice of loudspeaker and microphone combination. The choice of frequency also impacts other factors like directionality of the sound waves which can drastically improve the quality of the experiment with reduced loss in atmosphere. The attenuation and resolution of the experimental set-up is also largely dependent on the frequency of sound waves employed in the set-up. The table [5] presented below summarizes the various parameters mentioned and the effects based on the operating frequency of the experimental set-up. The first thing we have considered is the safety and comfort while carrying out experimental activities, thereby making a choice of ultrasound waves (>20 kHz) as the operating frequency considering this factor. As the low frequencies can be a little annoying and higher frequencies can be highly annoying and makes it mandatory to carry out all activities with ear protecting equipment. Working on ultrasonic regions also makes the resolution of the experimental set-up to push higher when compared with lower frequencies, furthermore, because of shorter wavelength, high frequencies allow to build a directional loudspeaker. The next important parameter to be taken for consideration is attenuation's effect on different frequencies. Attenuation of the energy of

the acoustic wave increases strongly with frequency. This phenomenon caused by dissipation can be clearly seen from the figure presented below. In contrast, the effect of higher directionality has a tendency to compensate for the effect of attenuation caused at higher frequencies. Other parameters like compactness of the experimental set-up, robustness of components and resolution is considered against different frequencies and frequency did not play a major role or impact in the experimental set-up.

From the below graph obtained from ISO/IEC 9613-2 1996 document that explains about the speed of sound in air and attenuation it can be clearly seen the effect of attenuation on higher frequencies. From second graph with better directionality as a result of higher frequencies the effect of attenuation can be minimised is presented.

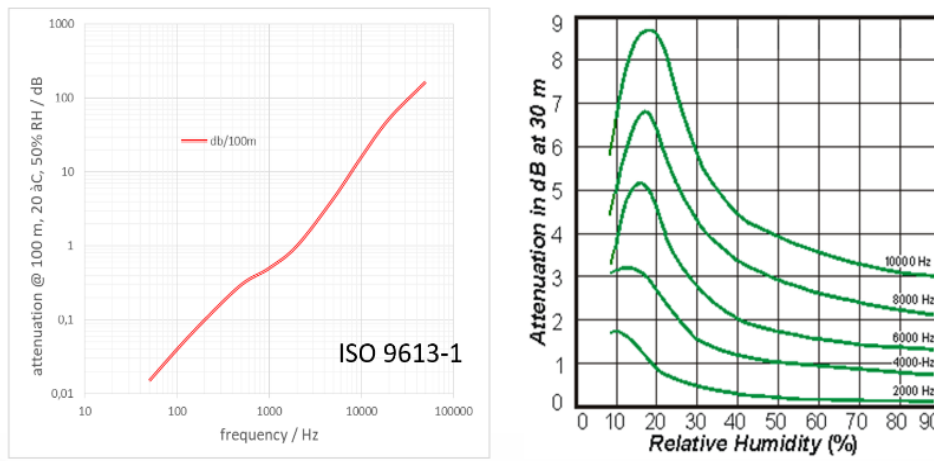


Figure 7-Attenuation of acoustic waves vs frequency and humidity [73]

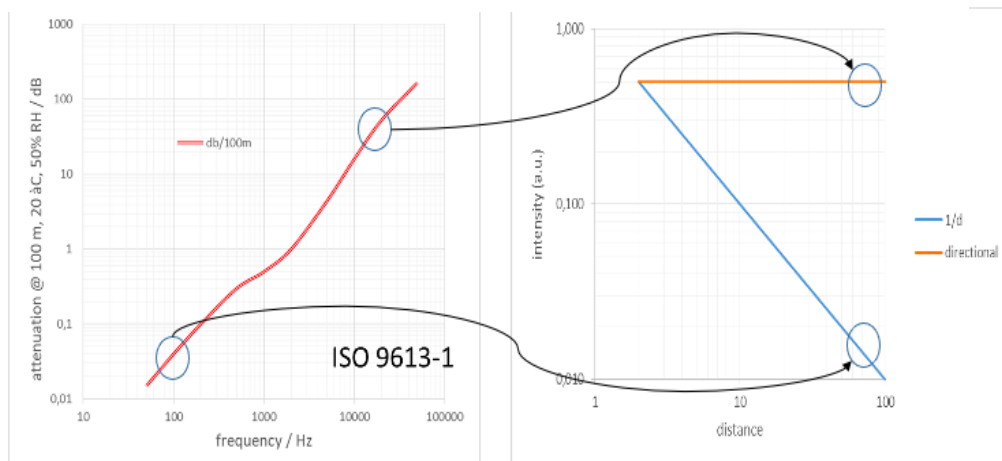


Figure 8-Attenuation of acoustic waves vs frequency and intensity: comparing the 100 Hz with the 20 kHz frequency, it can be seen that the much higher attenuation at high frequency can be partially compensated by the fact that the same can be made highly directional (orange curve) compared to the 1/d behavior of the low frequency (blue curve).

Table 5-Choice of operating frequency. Ultrasound frequencies has the high drawback of suffering from strong attenuation in atmosphere. On the other hand, the advantages of ultrasounds are evident. In red we have highlighted the disadvantages, in green the advantages with respect to other frequency ranges. At least over medium distances (tens of meters), the ultrasound range is the preferred one.

Frequency → Parameter ↓	Low Frequency (10-100 Hz)	High Frequency (1-10 KHz)	Ultrasound (>20 KHz)
<b>Safety/Comfort</b> (20Hz-20KHz is the audible range for human)	annoying	Highly annoying	Not audible (Constant exposure to ultrasound can be hazardous to human)
<b>Accuracy/resolution</b> (proportional to the inverse of the wavelength)	Low	Medium	High
<b>Directionality</b> (proportional to the ratio between the loudspeaker size and the wavelength)	impossible	moderate	good
<b>Attenuation</b> (strongly dependent on frequency)	Very low (0.01-1 db/100 m)	Medium (1-10 db/100 m)	very high (>10 db/100 m)
<b>Compactness</b>	moderate	good	good
<b>Robustness to phase slip due to turbulence</b>	good	good	moderate

### 4.3. Experimental Set-up

The whole experiment was carried out in the semi-anechoic chamber facility available at INRiM. The chosen combinations of loudspeaker and microphone are placed against each other on a stable tripod at a height of 1.3 m. During the initial experimental set-up various types of loudspeaker and microphones are employed and thereby producing very similar results with very little deviation. Some of the loudspeaker and microphones used are simple, capsule, focused, super-cardioid at various points in the preliminary phase of the experiment.

Although there are different types of microphones available in the market, super cardioid microphone type is employed in this experiment. The detailed specifications of these microphones are provided in the appendix section of this thesis. The dynamic-horn loudspeaker is chosen for its capability to transmit sound waves along an axis. Hertz ST 25A Neo is used in this experiment. The frequency response of this loudspeaker is in the range of 3000 Hz to 20,000 Hz. The data sheet of the loudspeaker is added in the appendix section of this thesis. The frequency generator used in this experiment is RIGOL DG 4162 (2 channel) which is capable of operating in the range of 1  $\mu$ Hz to 60 MHz and the resolution of used waveform generator is 1  $\mu$ Hz.



**MKH 416**  
P48 U3



*Figure 9- Some of the microphones and loudspeakers used in the preliminary study for the experiment. Above: a horn loudspeaker and a loudspeaker placed in the focus of a parabolic reflector. Below: an interference super-cardioid microphone and an omni-directional microphone placed in the focus of a parabola.*



*Figure 10- The loudspeaker and the microphone used in the final version of the experiments related to the results reported here. The loudspeaker (left) is a dynamic tweeter loaded with an expansion horn model Hertz S25 Neo. The microphone is a super cardioid interference condenser model BOYA-PVM1000.*

The comparison of experimental speed of sound in air with speed of sound in air calculated using Cramer equation is presented. In order to calculate speed of sound in air, respective environmental parameters have to be recorded simultaneously along with experiment. The environmental parameters to be recorded are temperature, relative humidity, pressure and carbon-di-oxide content. The temperature values along the transmission axis of sound waves have to be recorded in order to get more accurate values. The uncertainty related to Cramer equation to calculate speed of sound in air is about 300 ppm. So, it becomes important to use the instruments with higher accuracy and fast response, as uncertainty related to instrument could add up to uncertainty in speed of sound in air values. In order to obtain the temperature values at better accuracy, PT 100 probe (SE 012) sensor is used. The operating range of this sensor is about  $-50\text{ }^{\circ}\text{C}$  to  $250\text{ }^{\circ}\text{C}$  and an accuracy of about  $\pm 0.03\text{ }^{\circ}\text{C}$  @  $0\text{ }^{\circ}\text{C}$ . The series of temperature sensors (4 wires) are connected to the temperature acquisition board (Fluke 1586A Super-DAQ ) and the respective temperature are acquired using the LabVIEW software are recorded. The pressure values are determined using precision barometric indicator. In this case, Druck DPI 142 barometer is used in order to determine the pressure values. The accuracy of barometric pressure values is about 0.01 % in the temperature range of about  $10\text{ }^{\circ}\text{C}$  to  $40\text{ }^{\circ}\text{C}$ . The carbon-di-oxide content and relative humidity values are determined using Testo 440 digital probe. The digital probe is capable of measuring the carbon-di-oxide content in the range of 0 to 10,000 ppm and relative humidity in the range of 5 to 95%. The accuracy of carbon-di-oxide content values is about  $\pm 50\text{ ppm} + 3\%$  of measured value. The accuracy of relative humidity values is about  $\pm 3\%$  of measured values. The detailed technical specifications are presented in the section of appendix in this thesis.



Figure 11- The loudspeaker and the microphone used in the final version of the experiments related to the results reported here. The loudspeaker (left) is a dynamic tweeter loaded with an expansion horn model Hertz S25 Neo. The microphone is a super cardioid interference condenser model BOYA-PVM1000.

In this experiment, four PT100 temperature sensors are placed along the axis to measure the air temperature. The temperature sensors used in this experiment are calibrated in the thermal division of INRiM with an uncertainty of  $0.015^{\circ}\text{C}$ . Apart from the mentioned thermometers and loudspeaker-microphone combination, other hardware components include synthesizer with ability to generate 20 kHz tone and frequency sweep, a power amplifier to feed the loudspeaker, a National Instruments, 16 bit two channels digital to analog board to acquire signals coming from the synthesizer and microphone. A LabView software is in charge of measuring the phase delay between the transmitted and the received acoustic signals.

## 4.4. Results and Discussion

In the previous section, the working principle and experimental set-up of acoustic thermometer was presented and discussed in brief. Based on the preliminary experiments carried out, the components and instruments to be employed for obtaining data for analysis are also presented. The picture taken during the experiment process can be seen in fig-12 presented below. The experimental data presented here are taken during the period of January and February 2020. In the preliminary experiments, different loudspeakers and microphones are used. The experimental data presented in this section are carried out using a piezo-horn loudspeaker and a super-cardioid microphone. Because of its better directionality, this set of loudspeaker and microphone is used. The loudspeaker is connected with a frequency generator and the frequency was set to 20 kHz. In the previous section of operative frequency, the reason for utilizing ultrasonic range is explained in detail. The said microphone and loudspeaker are placed on top of stable tripods at fixed height and opposite to each other at a fixed distance.



*Figure 12-Preliminary experiments with different loudspeaker and microphones*

The four thermal sensors (PT 100) are fixed on tripods at the same height, closer to the axis of acoustic wave transmission. The thermal values of both thermal sensors are recorded simultaneously with time stamps using LabVIEW software. Also, an electric barometer is presented close to the experimental set-up in order to measure air pressure values. Similarly, a hygrometer is also introduced to measure the relative humidity values in the semi-anechoic chamber. The measurements taken in this experiment are several hours or several days long.

The distance between loudspeaker and microphone are measured using EDM during the start of every experiment and end of the experiment. As explained before, the acoustic distance is measured once with the frequency sweep method with the microphone and loudspeaker relatively close each other (see figure 17) and is related to the physical distance measured with the EDM (e.g. taken from the end of the microphone and the end of the loudspeaker). For larger distances, only the EDM measurement is used to estimate the acoustic distance  $d$  to be used in the formula. The initial and the final measurements yield a maximum difference in the order of 1 mm. The nominal distance value is determined for the whole record by averaging the two measurements.

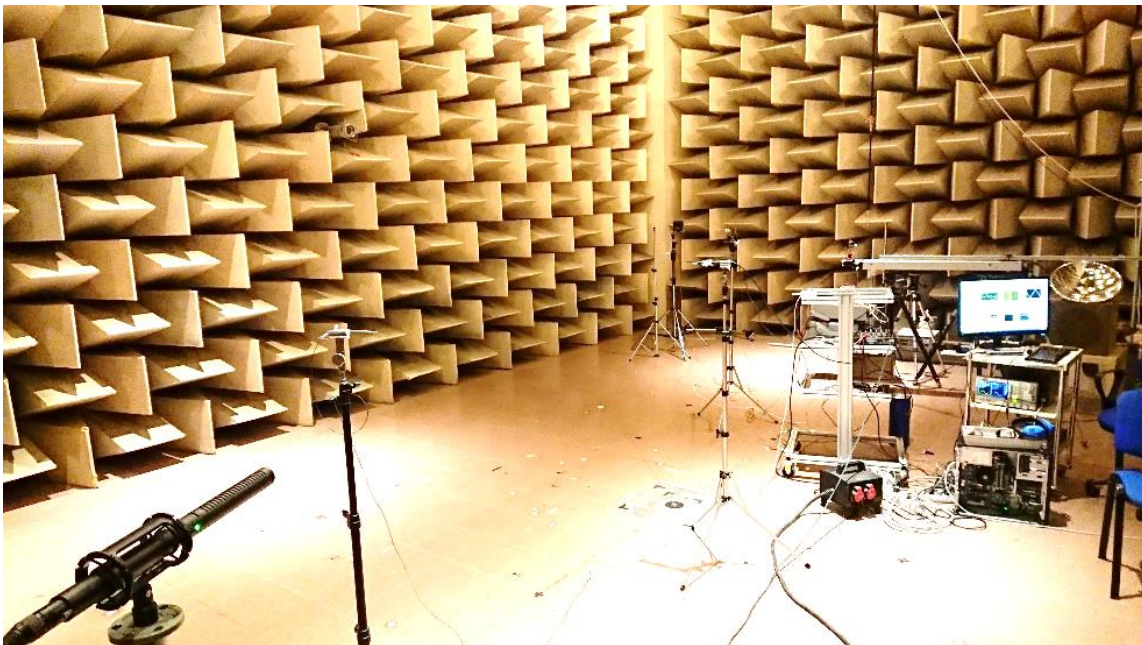


*Figure 13-Picture of the experiment carried out at 8.2 m*

#### **4.4.1. Speed of Sound comparison at 8.2 m**

In this part, two sets of experimental data obtained during the experiment are analysed and presented. In the first set of experiment the sampling time was 10 s and in the second experiment, the time sampling was reduced to 1 s, the efficiency of experimental set-up can be elaborated in detail.

In the working principle section, the method of determining the effective distance between microphone and loudspeaker is explained. The first experiment is carried out at a distance of 8.2 m between microphone and loudspeaker. At this distance, the first experiment is carried out at a sampling time of 10 s and the speed of sound is measured through the phase measurement. The speed of sound values is also calculated based on the environmental parameters with the help of Cramer equation.

The experiment is carried out in the anechoic chamber, in which the environmental parameters like temperature are controlled with the help of a temperature conditioning plant present in the chamber. In the first set of experiments, the temperature range was about 15-20 °C. The experimental set-up was allowed to run over 9 hours long and all parameters

required to determine speed of sound in air using acoustic thermometer and environmental parameters are recorded. During this period of time, the relative humidity range was about 17-33% and pressure values were about 99.5-99.8 kPa. A typical recording of speed of sound in air obtained using acoustic thermometer set-up and environmental parameters is presented in the form of a graph in figure 14.

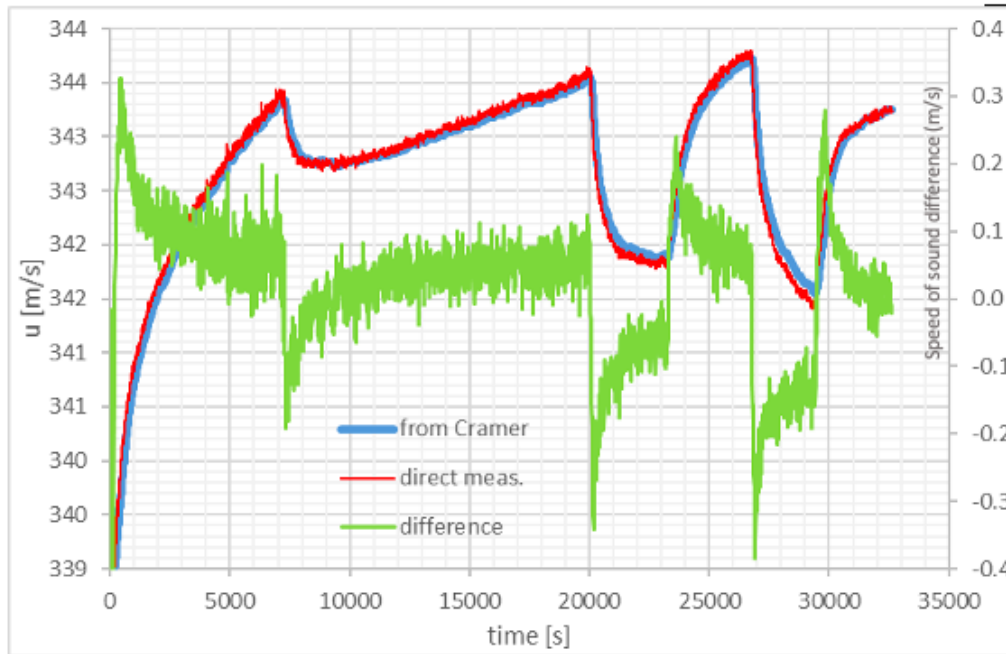


Figure 14-Speed of sound (exp & Cramer) vs time along with differences @8.2 m. red curve: speed of sound measured through the acoustic set-up. Blue curve: speed of sound estimated with the Cramer equation from the measured environmental parameters. Green curve: difference between measured and estimated speed of sound (right scale in m/s).

In the above graph, the time (s) values are represented in the x-axis. The speed of sound values is represented in the y-axis (primary axis). The blue curve represents speed of sound in air calculated from Cramer equation and the red curve represents the speed of sound values obtained using acoustic thermometer. The green curve represents the difference between two speeds of sound in air values and is presented in the secondary y-axis. From the graph, it can be seen that the difference between speed of sound values is about  $\pm 0.1$  m/s whenever the change of temperature occurs slowly. The speed of sound differences increases up to the range of  $\pm 0.3$  m/s, whenever the temperature changes at rapid pace. This phenomenon can be justified based on the thermal inertia of the temperature sensors utilised in the experimental set-up. But, the speed of sound values obtained based on the acoustic thermometer has zero inertia and leads to this difference whenever the change of temperature occurs rapidly.

#### 4.4.2. Speed of Sound comparison at 11 m

In the second experiment, the distance between loudspeaker and microphone was increased to a distance of 11 m. This is the maximum permissible distance possible in the anechoic room in which experiment is carried out and the feasibility of acoustic thermometers to act as a thermometer for refractive index estimation is presented. Based on the concept, this experiment is similar to the previous one except having higher noise due to the turbulence of air as the result of increased distance.

This experiment was carried out with 1 second of sampling time. Also, the experimental set-up was allowed to run for a period of about 3 days to obtain larger experimental data and environmental parameters to study in detail about the feasibility and efficiency of the acoustic thermometer set-up. This set of experiments is carried out by switching off the conditioning plant in the anechoic room to elaborate also about the thermal inertia studied during the previous experiment. By switching off the conditioning plant, the change of environmental parameters occurs in accordance with the external environment parameters, thereby the sharp increase or decrease of environmental parameters are not present. The temperature range over this experiment was about 12-18 °C. The relative humidity value ranges about 25-47% and pressure values are about 99.6-100.2 kPa.

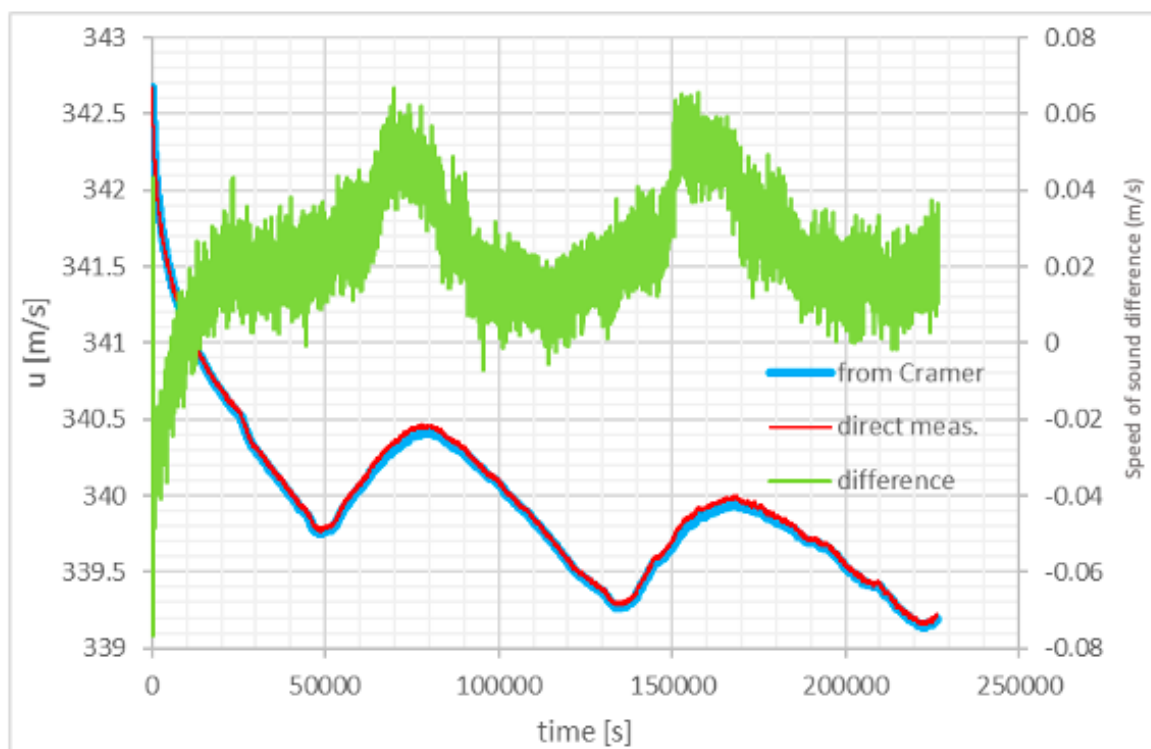


Figure 15-Speed of sound (experiment &Cramer) vs time along with differences @11m

The graph in figure 15 was plotted based on the speed of sound in air values obtained using acoustic thermometers set-up and environmental parameters using Cramer equation. The blue curve represents the speed of sound in air using Cramer equation and the red curve represents the speed of sound in air values using acoustic thermometer set-up. The x-axis values represent the time (s) and primary y-axis represents the speed of sound values. The secondary y-axis values represent the difference between speed of sound values in m/s. From the graph, it can be seen that the difference between two speed of sound measurements is within the range of  $\pm 0.06$  m/s. As said earlier, the difference value drops greatly when the environmental parameters changes are slow and justifies the larger difference in the first experiment as a result of thermal inertia.

#### **4.4.3. Comparison of temperature values: Acoustic Thermometer vs Classical Temperature Sensor**

After having verified the capability of the method in measuring the speed of sound with high accuracy, we have tried to use the device as a thermometer, basically inverting the approach adopted in the previous chapter. In the following the Acoustic Thermometer is used as a practical thermometer and compared with PT100 measurements. The average temperature values obtained using the PT100 sensors is compared with the temperature values calculated using the speed of sound from experiment, relative humidity and pressure values obtained using respective instruments and applying them in the inverted Cramer equation. The results of a typical measurement run are shown in fig 16. The difference between the temperature values is also presented in the same graph. This experiment was started after the temperature in the chamber cooled down in accordance with external temperature and then the conditioning plant was switched on with the heating resistors of the plant set to maximum power. This was done in order to study the complete feasibility of acoustic thermometer and its application for air-refractive index estimation over larger distances over a wide range of temperatures.

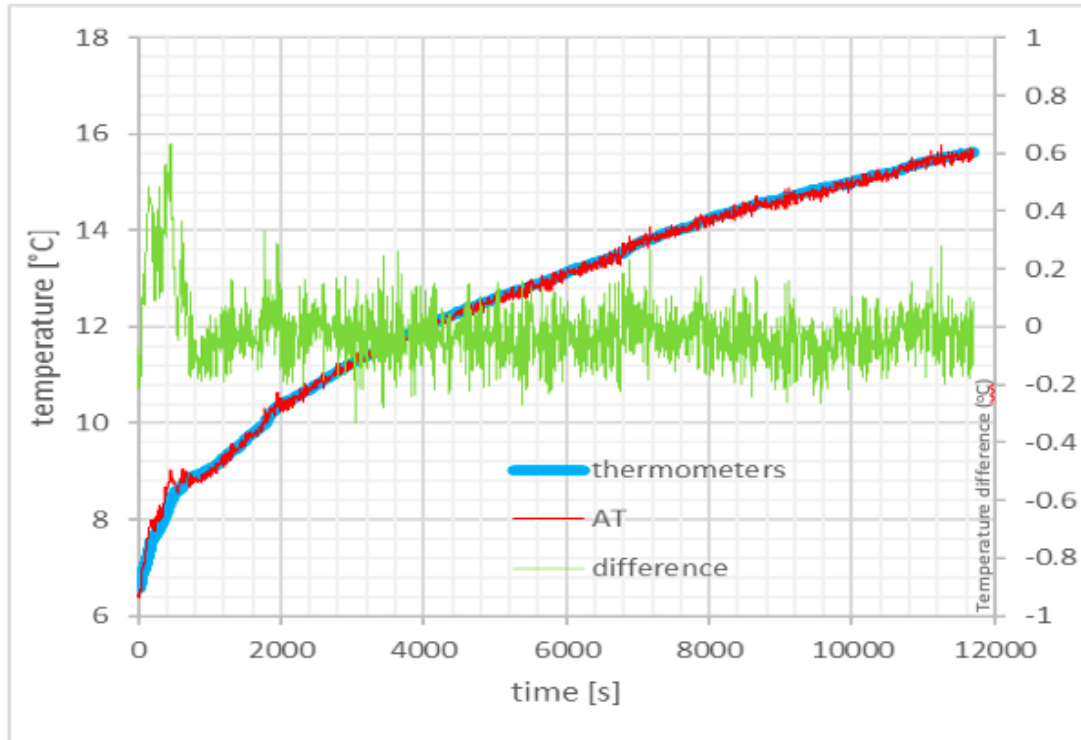


Figure 16-Temperature values (experiment and sensor) vs time along with difference

In the graph of figure 16, the x-axis values are represented by the time in seconds and the experiment was carried out for a duration of about 3 hours. The primary x-axis values are represented in temperature ( $^{\circ}\text{C}$ ) and secondary x-axis values are differences between temperature values obtained using acoustic thermometer and PT100 sensors. The blue curve is plotted using the temperature values obtained using acoustic thermometers set-up. The difference values are plotted using the green curve, from the comparison of temperature values obtained using PT 100 sensors and acoustic thermometers set-up over 11 m, it can be seen the difference was within  $\pm 0.2$   $^{\circ}\text{C}$  at most points of time in the experiment. The larger differences are again obtained as a result of rapid change in temperature as the result of a conditioning plant. These larger differences are accounted for as the results of thermal inertia of values obtained using thermometers because of slow reaction time when compared with acoustic thermometer set-up.

With these experiments we have demonstrated the feasibility of an absolute thermodynamic acoustic thermometer capable of measuring the average temperature over a distance  $d > 10$  m. Although the agreement between the acoustic thermometer and the classical platinum thermometer is within  $0.2$   $^{\circ}\text{C}$ , that can be easily attributed to the sub sampling of the thermometers along the path. If we wanted to give an uncertainty limit to the method, we must take into account the uncertainty associated to the Cramer formula. Being this uncertainty of 300 ppm on the speed of sound, this implies a minimum uncertainty of  $0.17$   $^{\circ}\text{C}$  on the temperature measurement. Having in mind our goal to reach  $0.1$   $^{\circ}\text{C}$  uncertainty, we need to reduce the uncertainty associated to the formula. This is the goal of the activity described in the next chapter.

## Chapter-5

# Speed of Sound in air: Experiment and Results

With the detailed literature review about past experiments carried out regarding speed of sound and speed of sound in air calculating methods, the following working principle and experimental method for determining speed of sound in air is proposed. The speed of sound in air estimation proposed by Owen Cramer [52], is estimated with an uncertainty of 300 ppm in reference to the temperature, relative humidity, carbon dioxide content and ambient pressure at which experiment is performed. The handbook authored by Zuckerwar also proposes a dependence of frequency on speed of sound in air. In addition, Zuckerwar claims an uncertainty of his equation's of 1000 ppm. So, it becomes important to develop a method and to implement an experiment to reduce the uncertainty of the estimation of the speed of sound from temperature and vice versa. We did not go into the theory of the speed of sound, rather we decided to measure in the most accurate way the speed of sound together with the environmental parameters in a given interval of practical use.

### 5.1. Working Principle

The experiment is based on the principle of measuring the phase delay between the generation and recording of acoustic waves at a given frequency over a distance. The study about this measurement gives directly the speed of sound ( $u$ ) based on the following equation.

$$u(T) = \frac{d * f}{\phi} \quad (\text{eq6.1})$$

$d$  is the distance traveled by the acoustic wave

$T$  is the temperature

$f$  is the frequency

$\phi$  is the measured phase delay

A challenging aspect to be addressed in this experimental set-up is to measure the accurate distance travelled by sound waves. To meet this requirement, the following technique is proposed. The unknown distance between loudspeaker and microphone is changed by a precisely known distance (1 m) in steps.

$$u = \frac{d}{t} \quad (\text{eq6.2})$$

where  $t$  is the time taken by sound waves to travel from loudspeaker to microphone.

$$t = \frac{\phi}{f} \quad (\text{eq6.3})$$

$$\begin{aligned} d_1 &= x \rightarrow t_1 \\ d_2 &= x + 1 \text{ m} \rightarrow t_2 \end{aligned}$$

Where  $d_1$  and  $d_2$  is the distance between loudspeaker at start end points respectively.  $d_1 = x$  is the unknown initial distance.  $t_1$  and  $t_2$  is the time taken by sound waves to travel from loudspeaker and microphone at start and end points respectively.

$$u = \frac{\Delta d}{\Delta t} \quad (\text{eq6.4})$$

Where  $\Delta d = 1 \text{ m}$  and  $\Delta t = t_2 - t_1$ , the above equation can be represented as follows,

$$u = \frac{1}{\Delta t} = \frac{f}{\Delta \phi} \quad (\text{eq6.5})$$

As mentioned in the working principle, the experimental set-up should consist of loudspeakers with capability of emitting continuous acoustic waves and a microphone for receiving the acoustic sound waves and phase meter for measuring the phase between signal sent to loudspeaker. The displacement method proposed for determining the speed of sound in air is performed by placing the loudspeaker on a carriage operated by an accurate stepping motor. The stepping motor is capable to displace at a fixed distance of 1 m to and fro with equally distributed 4000 steps. Each step corresponds to a nominal distance of 250  $\mu\text{m}$ . Although the stepping motor is capable to displace the carriage accurately, it becomes important to use an interferometer along with the proposed experimental set-up for measuring accurate displacement.

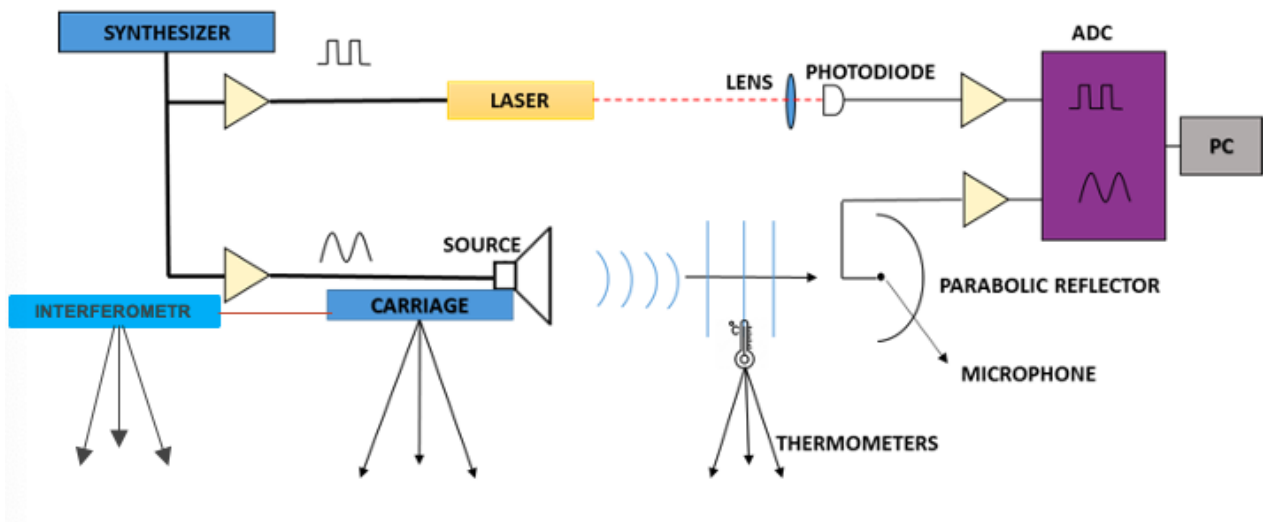


Figure 17-Experimental set-up for speed of sound in air. The key of the experiment is the accurate measurement of the change of the distance between loudspeaker and the microphone. The loudspeaker is mounted on a carriage having the capability of 1 m displacement while an interferometer accurately measures the same displacement.

The choice of frequency at which experimental set-up is operated is already explained in the Chapter 4.3 under Choice of Operating frequency for acoustic thermometer set-up and it applies to this experiment as well. Most of the following measurements have been carried out at 20 kHz.

## 5.2. Experimental Set-Up

The experiment was carried out in the semi-anechoic chamber facility available at INRiM. The microphone is placed on a stable tripod at a height of 1.3 m. the loudspeaker is placed opposite to the microphone, and placed on top of a moving rail. The moving rail is powered by a stepping motor, and controlled by computational software to move a distance of 1 m to and fro. Through this computational software, the directional movement, velocity of the carriage can be controlled. The set of loudspeaker and microphone is the same used for the previous experiment.

The displacement values obtained from interferometer (recording 10 measurements per second) and phase delay values obtained as result of sound wave transmission through loudspeaker is recorded and executed to be synchronous in sampling time with the help of a LabView software.

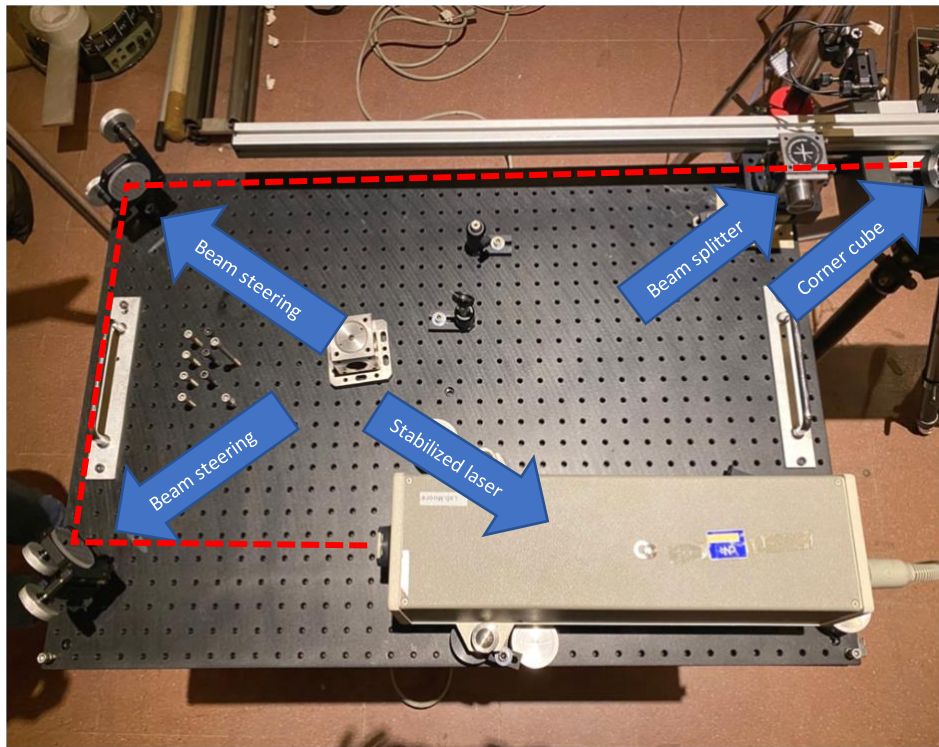


*Figure 18- Interferometer set-up used to measure the displacement of the carriage carrying the loudspeaker. It is based on a HP interferometer and on proprietary acquisition system.*

Before starting with the experiments, it is important to calibrate the carriage on which the loudspeaker is placed. With the interferometer facility available in INRiM, the carriage is calibrated with the linearity error being within the limit can be seen in the graph. In addition to the said components, other hardware components include a synthesizer with ability to generate 20 kHz tone and a power amplifier to feed the loudspeaker, a 16 bit two channels digital and analog board to acquire signals coming from the synthesizer and microphone. The LabVIEW program window presented below is the user interface of the management software. The software acquires the signals from the synthesizer and of the microphone, measures the phase change of the signals while the carriage is moving, performs the fit of the phase/displacement curve, saves this data, calculates the residuals of the linear fit. The latter is used as a check for the quality of the measurement. If the residuals exceed a given value, the data is considered corrupted (e.g. from a large turbulence) and is discarded.

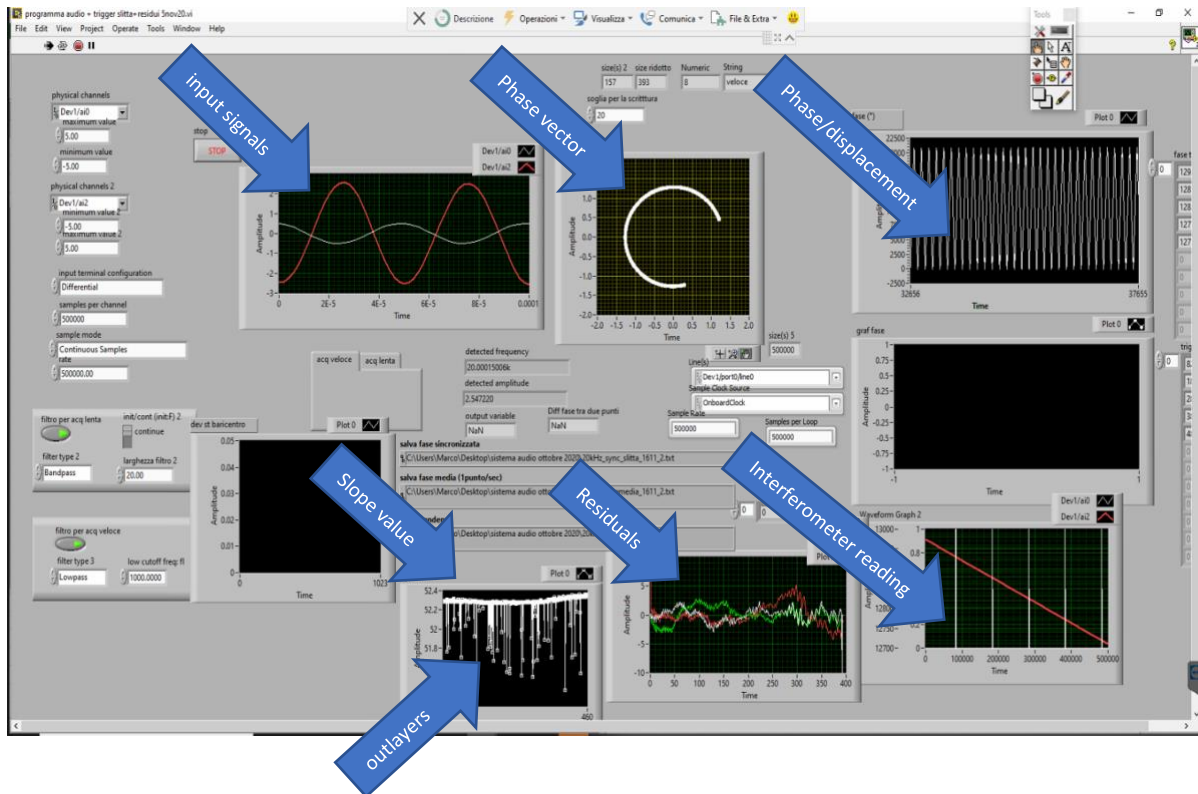


Figure 19- Data acquisition LabVIEW user interface

In order to make a comparison between speed of sound in air estimated through this experiment and make a comparison between the speed of sound in air through Cramer method, the environmental parameters have to be recorded at the same time when the experiment is carried out. The temperature values are obtained from the thermometers placed along the experiment. Small size PT 100 thermal sensors, which have high time when compared with other available sensors in the market, are employed in this experiment. In total, 6 PT100 thermal sensors are placed along the acoustic wave transmission and the temperature values are recorded using a LabView software, see fig. 20.

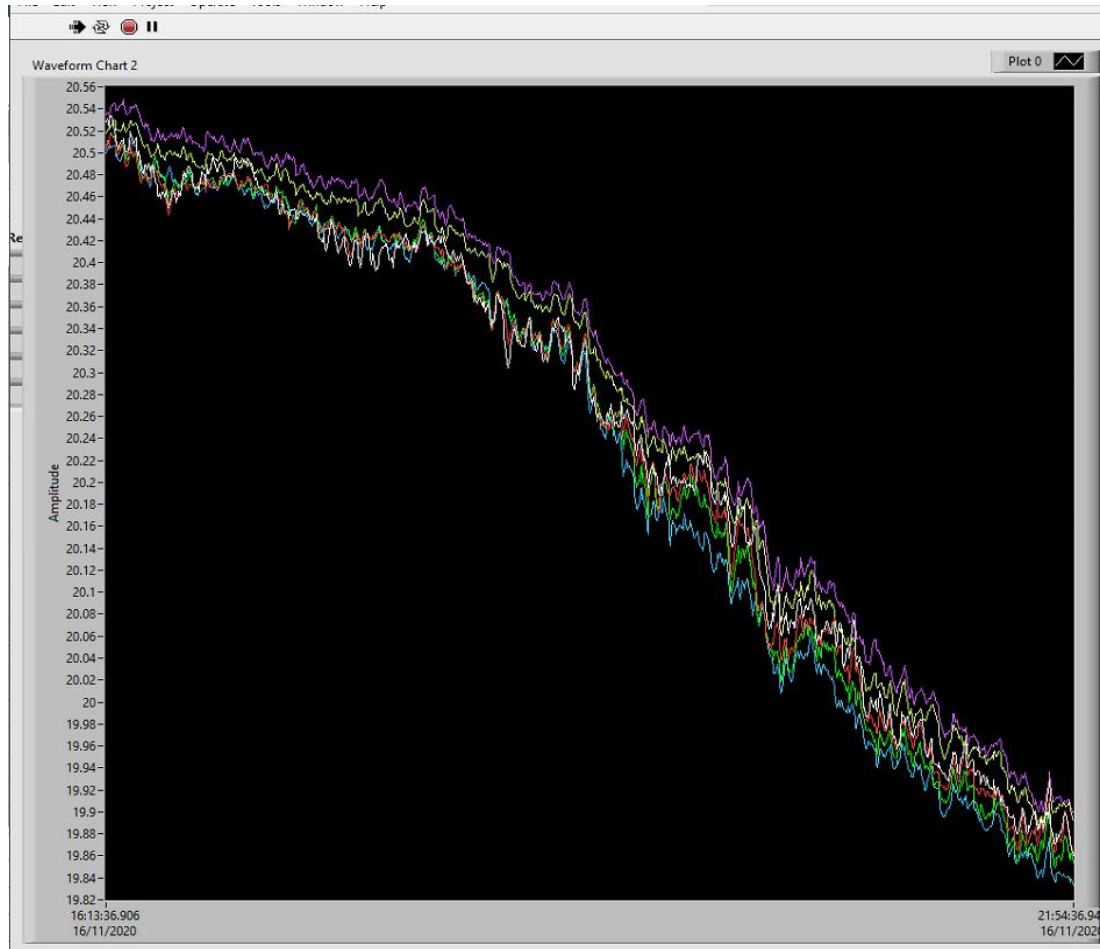
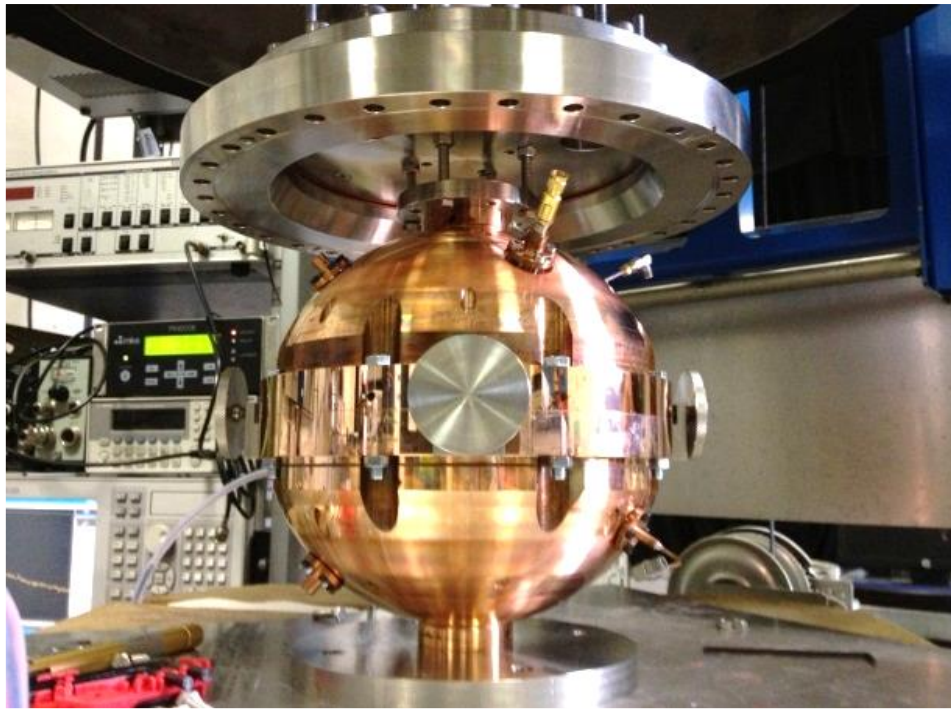


Figure 20--Typical data acquisition for the 6 temperature values. The temperature uniformity in the measurement volume can be appreciated.

The temperature sensors used in this experiment are calibrated in the thermal division of INRiM with an uncertainty of 0.015 °C. The relative humidity is measured with the help of a hygrometer and the barometer is added to the experiment in order to measure the pressure values of the semi-anechoic chamber. The digital barometer utilized in this experiment is also capable enough to record carbon-di-oxide values. All these values are recorded with help of a LabVIEW software capable to record at synchronized sampling stages.

Another research group from INRiM, also carried out their research of speed sound measurement with a quasi-spherical acoustic/microwave resonant cavity. A small stainless steel gold-plated quasi spherical (ellipsoidal resonator) was operated within the anechoic chamber side-by-side with the experiment. The experiment is carried out by maintaining a continuous flow air into the spherical resonator from the semi-anechoic chamber. The results obtained from this research group can be compared with the research, and to study about the expected frequency dependence of speed of sound in air at near ambient conditions.



*Figure 21-Spherical resonator used for the accurate measurement of the speed of sound with a complementary method. The spherical resonator method has an intrinsic uncertainty of few ppm.*

During the experimental set-up, it becomes important to study about the wind speed effect on the speed of sound in air estimation. The wind speed sums directly to the speed of sound. Since the semi-anechoic chamber can be controlled with the temperature control unit that generates unavoidable air flux, the effect of wind speed is studied with the control unit running. With the help of an anemometer, the wind speed is measured. The values of speed of wind have been included in the calculation of the speed of sound and the related uncertainty has been included in the uncertainty budget.

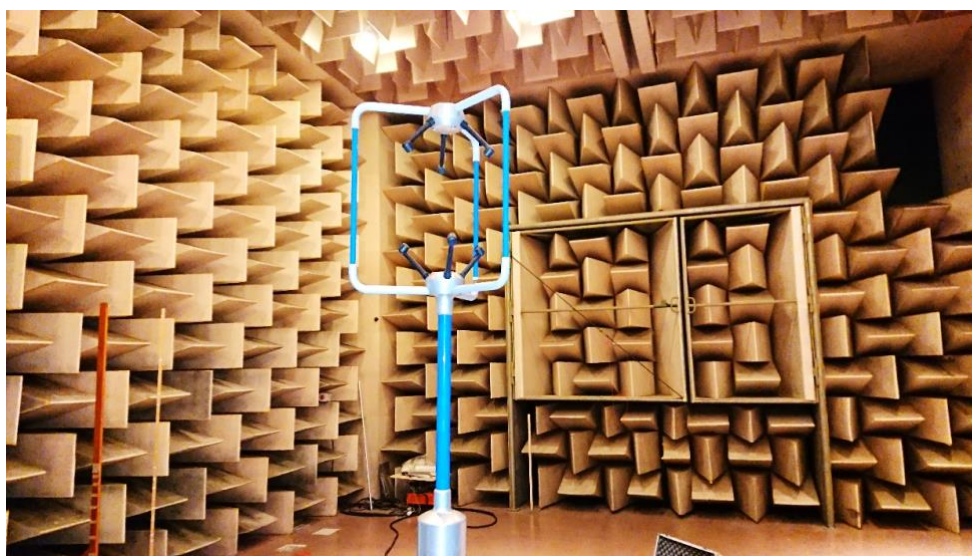


*Figure 22-Ultrasound anemometer set-up for wind speed measurement*



*Figure 23-Experimental set-up for the measurement of the speed of sound. At the background/left is visible the carriage carrying the loudspeaker. At the foreground on the right is visible the microphone on the tripod. At the left the array of resistance thermometers. Top right the experiment with the spherical resonator. On the floor foam absorbers for reducing acoustic reflections*

### 5.3. Results and Discussion

In the previous sections of the thesis, the working principle and experimental set-up for determining the speed of sound in air is explained. The preliminary experiments are carried out with the chosen components and presented in the figure [23]. The software for data acquisition and data analysis are also developed and presented. The experimental data presented here are taken during the period of October and November 2020. In the preliminary experiments, the wind speed is measured using an anemometer to determine the wind effect on the speed of the sound experiment carried out. Various sets of microphone and loudspeakers are utilised during the preliminary experimental set-ups in order to choose the better performing combination. At the end, the super cardioid microphone and piezo-horn loudspeaker are utilized in the process. The loudspeaker is connected with a frequency generator and the frequency was set to 20 kHz at most part of this experiment. The reason for carrying out this experiment in ultrasonic range is explained in the previous part.

The microphone is placed on top of a stable tripod. As mentioned in the experimental set-up, the loudspeaker is on a moving rail to support the proposed displacement method for determining the speed of sound in air. The moving rail is calibrated with the help of an interferometer facility during preliminary experimental set-ups and the linearity errors of displacement methods are recorded. Figure 25 shows the preliminary set-up carried out in the anechoic chamber with the help of an interferometer.

## 5.4. Calibration of moving rail and experimental set-up

As mentioned before, the loudspeaker is fixed on the moving rail for speed of sound measurement through displacement method. The rail is controlled by the interferometer, but we foresee to perform future measurements without the need of the interferometer that implies a rather complex set-up. Thus, for any measurement, we have recorded the difference between the nominal displacement of the carriage (1 m) and the displacement measured by the interferometer. The errors in displacement of moving rail were measured at different temperature values with the temperature ranging between about 10 to 28 °C. For any temperature, the nominal value of the carriage is compared with the interferometric reading. Based on these errors at different temperatures, a curve was plotted and presented in the graph of fig. 24. The dependence of the error from temperature turns out to be 10  $\mu\text{m}/^\circ\text{C}$ . This effect is compliant with the expected expansion of the screw of the actuator since the coefficient of linear thermal expansion of stainless steel is about 13.2  $\mu\text{m}/^\circ\text{C}$ . This calibration will be used for future experiments in which the moving rail will be used in the temperature range of 10 to 28 °C without the need of further calibration with the interferometer.

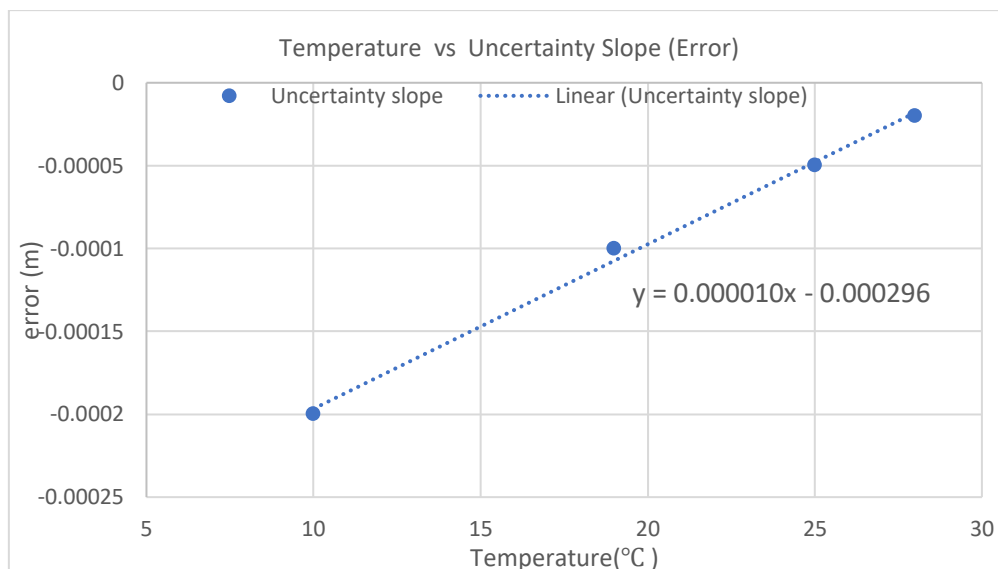
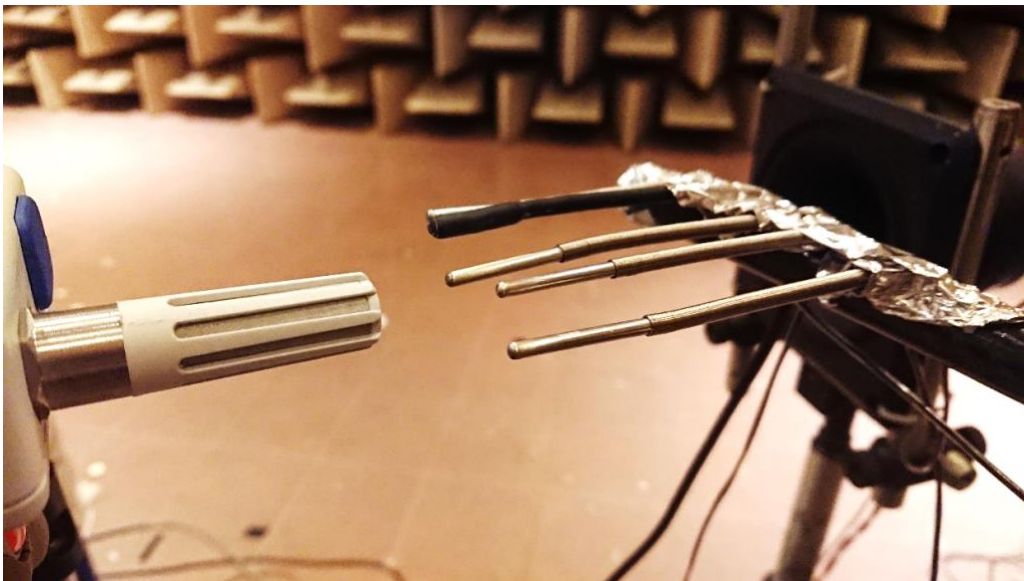


Figure 24- Errors of the moving rail vs temperature over 1 m stroke due to thermal expansion of the screw (Calibration of moving rail with interferometer set-up)



*Figure 25-Preliminary moving rail calibration*

In total six PT100 thermal sensors are connected with the PC through a data logger and the thermal values are acquired using the LabVIEW software. The hygrometer and the barometer, are also presented close to the experimental set-up to measure relative humidity, pressure values and CO<sub>2</sub> content which are acquired through a PC. The measurements taken with those experimental set-ups are several hours long. The phase delay acquired with the help of microphone and loudspeaker set-up is synchronous with the interferometer measurements obtained based on the displacement. The slope values based on the phase delay provides the speed of sound in air.



*Figure 26-On the left the Hygrometer head, on the right the PT100 thermal sensors*

Many sets of experimental data are obtained and presented in this section. The speed of sound in air obtained with the help of built experimental set-up and environmental parameters and the differences between these values are presented. The speed of sound values from the start to end of 1 m of displacement are measured based on the forward movement of the loudspeaker on the moving rail. Similarly, the speed of sound value is also calculated based on the displacement of the loudspeaker from end to start position backwards. In the presentation of data, both speed of sound values is averaged in every cycle to provide an average speed of sound in air calculated through the experimental set-up. The respective speed of sound in air calculated through environmental parameters is plotted against experimental value based on time stamps to elaborate the differences.

There are various factors that have capability to affect the experimental and calculated speed of sound in air such as the temperature gradient as the result of the position of thermometers in accordance with the acoustic path. Temperature distribution, as we employ 6 PT100 sensors and the average temperature values are used in determining the calculated speed of sound in air. There are also some factors that contribute to the uncertainty in experimental speed of sound in air. The factors like repeatability and resolution contributes to this set-up as similar to most experiments carried out. The Cramer equation doesn't explain frequency dependence speed of sound in air, but the Zuckerwar handbook does talk about small dependence on frequency and it is important to talk about the uncertainty contributed by it. Another important aspect to be considered is the position of the microphone and loudspeaker, as it can contribute to the uncertainty in accordance with its horizontal, vertical and angular alignments with each other. Another component that can contribute to the experimental speed of sound in air is the interferometric measurements obtained to determine the displacement positions on the moving rail. In order to reduce the effect of acoustic interference, the prism shaped foams are placed near the acoustic path and the positions are done randomly. It is important to study about the changes in acoustic interference in accordance with the position of the foams. These experiments are carried out in order to present the uncertainty budget related to the experimental set-up and presented in detail.

## **5.5. Results at different temperature ranges**

In this part the performance of experimental set-up on different temperature ranges is presented. The temperature of the anechoic room is controlled with the help of a conditioning plant and its thermal resistors and some of the data obtained in this part of results are several hour measurements. The overall range of the whole set of measurements covers the interval between 6 and 28 °C. Some subsets of measurements are presented in detail as an example of the analysis carried out. Then global data will be presented.

In this first example (figures 27 and 28), the temperature range was about 6 °C to 20 °C and carried out for about 24 hours. The relative humidity was about 26-38% and pressure at about 99.1 kPa to 99.6 kPa. The presented experimental and calculated results are obtained through the experiments carried out in the month of November 2020. The operating frequency was set to 20 kHz.

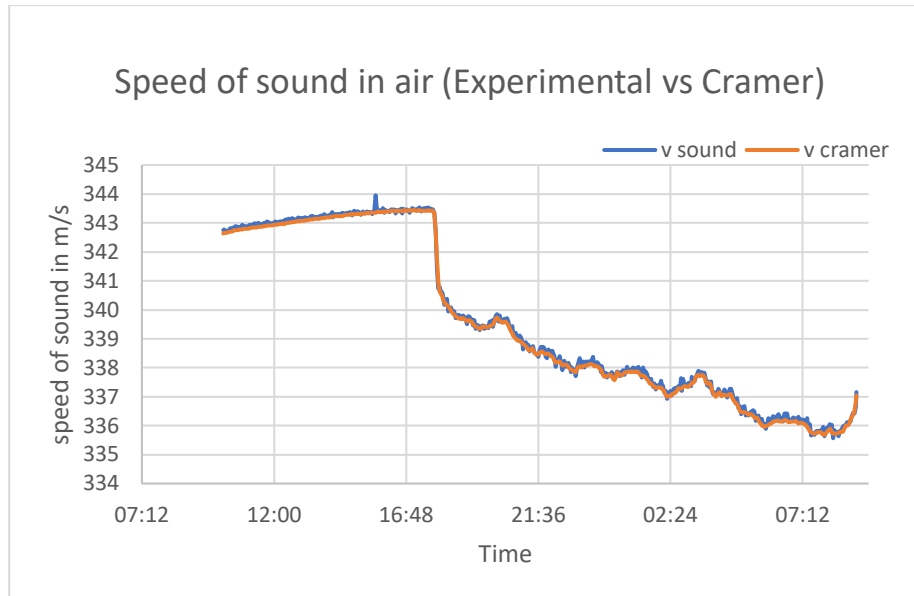


Figure 27-Speed of sound (Experiment vs Cramer) at 6°C to 20°C

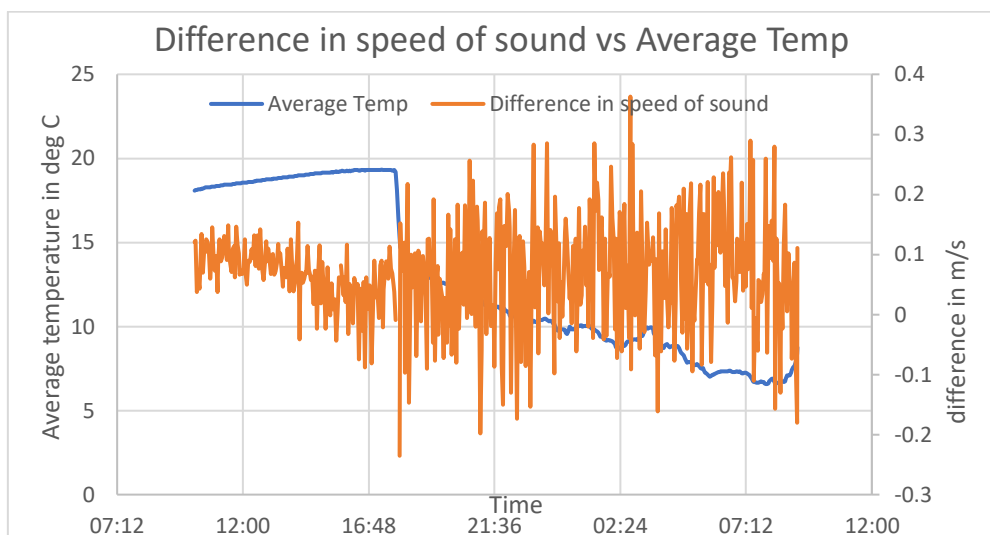


Figure 28-Temperature vs difference in speed of sound (Exp & Cramer) at 6°C to 20°C

From the above graph, it can be seen that the difference values are in the range of -0.2 m/s to +0.3 m/s. During the experiment, the blower in the semi-anechoic chamber was turned on (at about 18:00) for rapid cooling and resulting in a rapid drop in temperature. The effect of air turbulence induced by the blower is visible as an increased dispersion of the data. The slower response of thermal sensors is also another reason for higher differences.

The next set of results are presented in the temperature range of 18.9 °C to 19.3 °C and carried out for a duration of 6 hours long (figures 29 and 30). With this experiment, the performance of experimental set-up with a smaller change in temperatures are studied and presented in detail. In this experimental duration, the relative humidity range was about 43% to 49% and the pressure values in the range of 99.5 to 99.7 kPa.

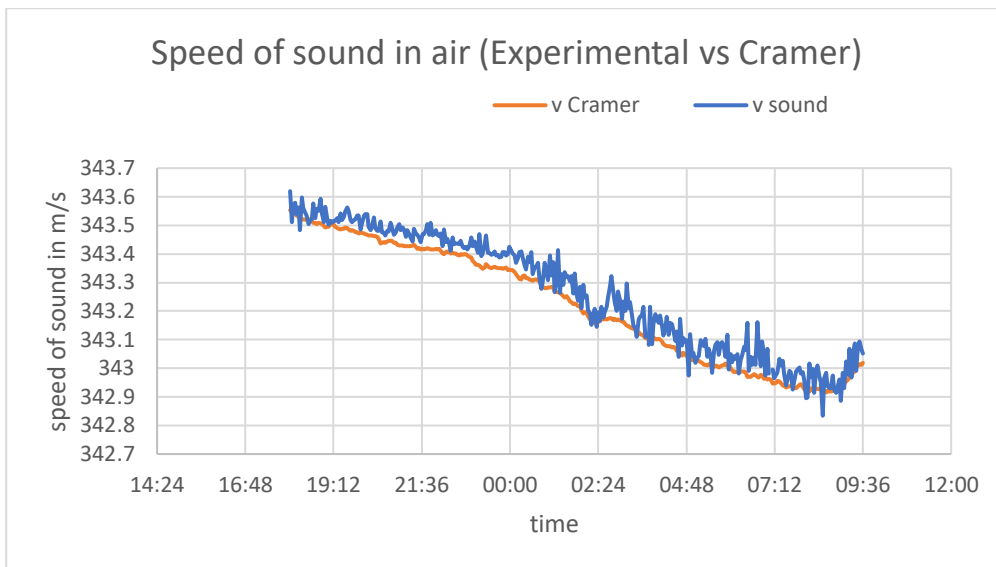


Figure 29-Speed of sound (Experiment vs Cramer) at 18.9°C to 19.3°C

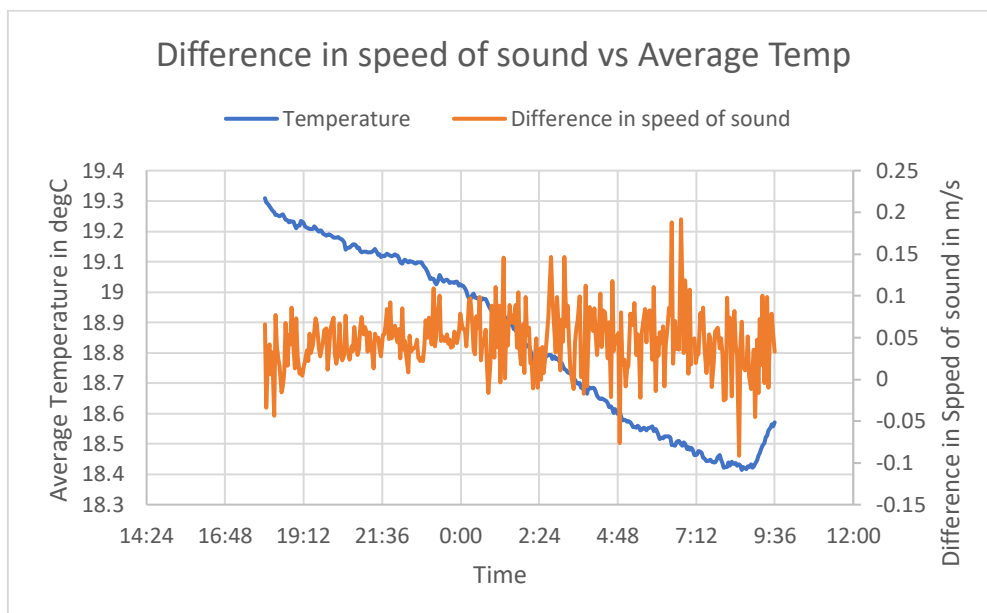


Figure 30-Temperature vs difference in speed of sound (Exp & Cramer) at 18.9°C to 19.3°C

In the next set of results (figures 31 and 32), the experiment was carried out in an increased temperature range at about 24 hours long and the speed of sound values based on the experiment and Cramer equation are recorded. The temperature changes can be noted from the curve plotted with average temperature value calculated with help of 6 PT100 thermal sensors presented below. The relative humidity values range about 29% to 37% and pressure values in the range of 99.5 kPa to 99.8 kPa.

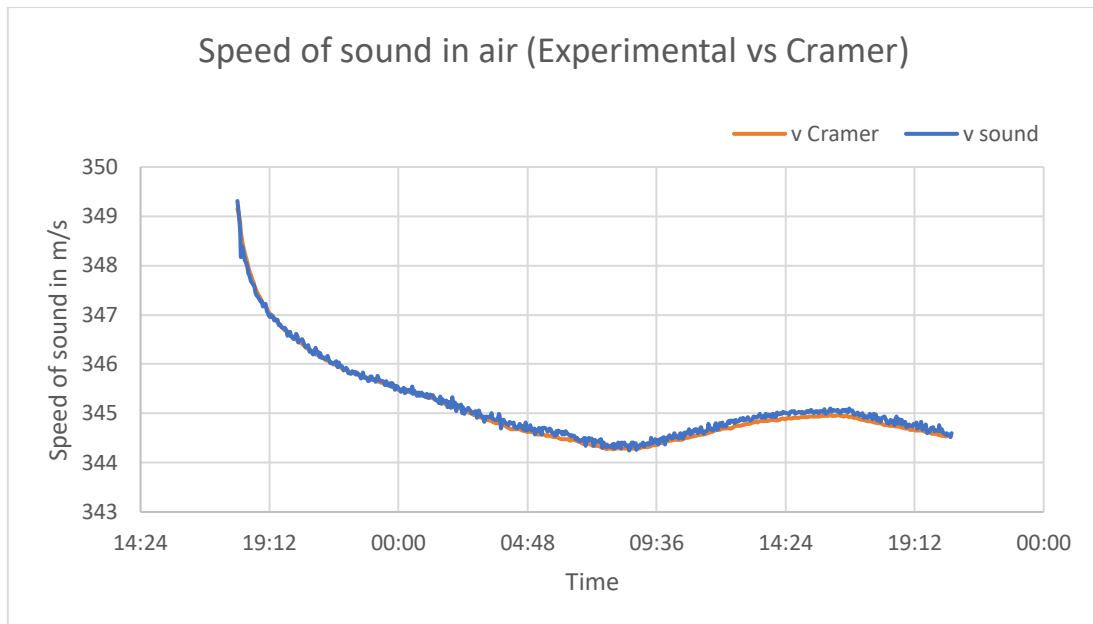


Figure 31-Speed of sound (Experiment vs Cramer) at 20°C to 28°C

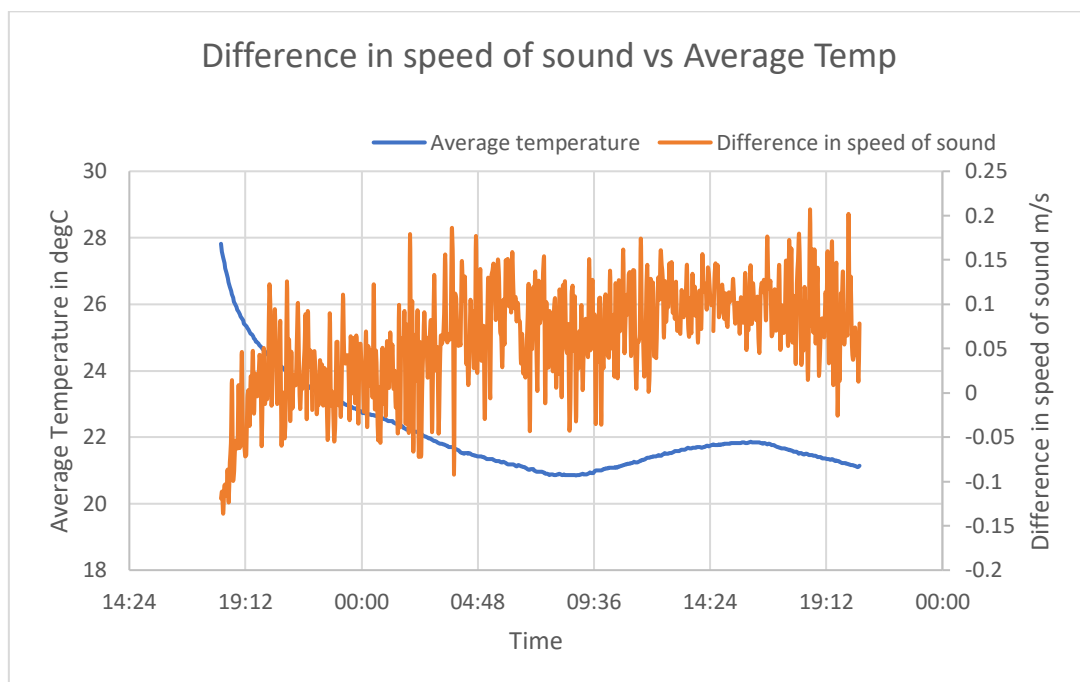


Figure 32-Temperature vs difference in speed of sound (Exp & Cramer) at 20°C to 28°C

The above curves represent the temperature changes and the relative speed of sound in air differences. Also, this experiment was allowed to run over the whole night in winter and sharp decrease in temperature at times could also account for the difference. The temperature sensor's slow response in picking up the sharp temperature changes would have been a possible reason for this.

In fig. 33 is shown a collection of measurements similar to the ones presented above. based on the results of speed of sound in air values and differences that are presented above. The differences in speed of sound in air calculated based on experiment and Cramer equation is plotted against the temperature ranges at which the experiment is carried out. Number of experiments are carried out with the frequency set at 20 kHz to study about the performance of experimental set-up at different temperatures. The speed of sound values obtained from experiments carried out at the temperature range of 7 °C to 28 °C is presented below in the graph.

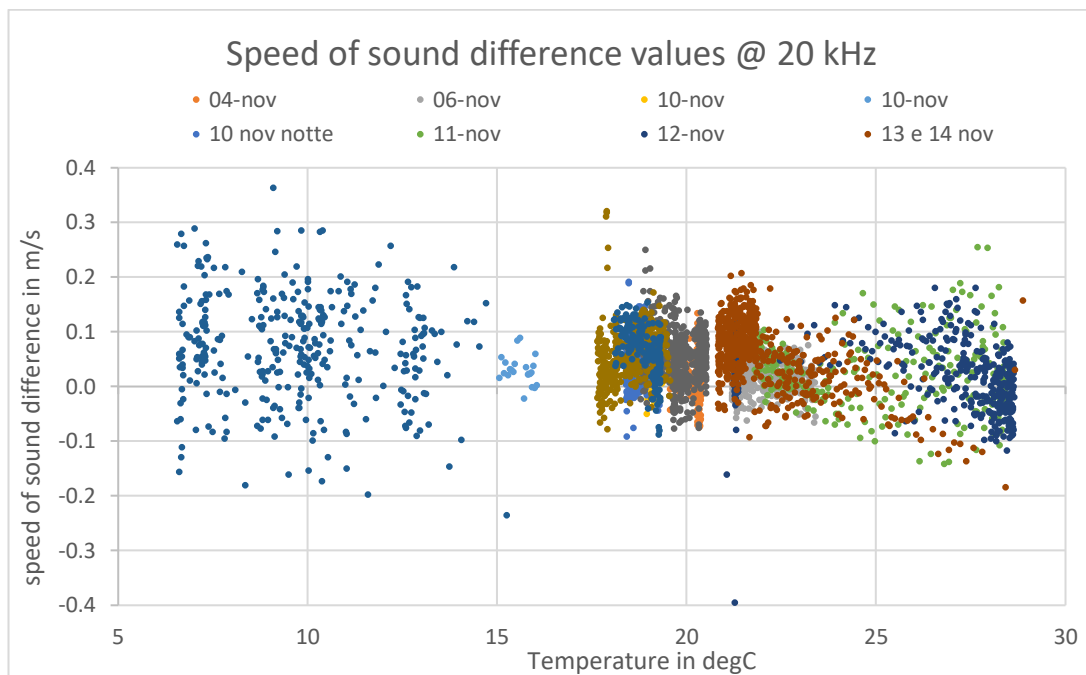


Figure 33- Scatter plot of speed of sound difference values at temperature range of 7 °C to 28 °C. The vertical axis is the difference between the speed of sound measured with the acoustic method and the speed of sound calculated from the environmental parameters through the Cramer formula. The different colors represent the different measurement runs.

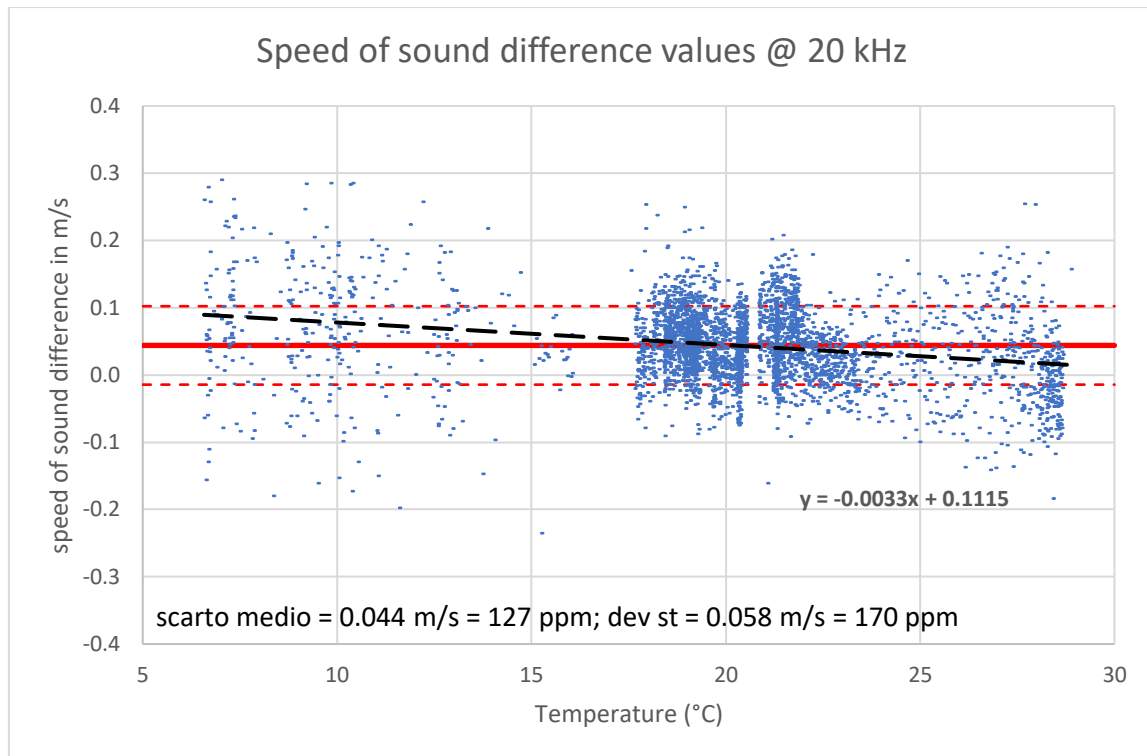


Figure 34- Scatter plot of speed of sound difference values at temperature range of 7 °C to 28 °C with average and standard deviation values (respectively solid and dashed red lines). The black dashed line is the linear tendency curve including all data.

In the graph of figure 34, the whole set of data is used to calculate the average difference with respect to Cramer estimation and the standard deviation of the data. The average difference represented with the solid red line is about 0.044 m/s and the standard deviation value based on the difference value is  $\pm 0.058$  m/s. The standard deviation limit is represented using the dotted red line. The slope of the dispersion is also represented in the curve to study the dependence of difference in sound values on different operating temperatures, but we decided not to use this for the moment.

The increase in data dispersion for higher and lower temperature is mainly due to the fact that both conditions were obtained with the conditioning plant on, whereas most of the measurements around 20 °C were taken with still air.

## 5.6. Temperature Gradients

The previous section explained about the dependency on temperature range, in this section the accuracy of the measurement of air temperature is analysed. The six PT100 sensors are placed close to the acoustic wave transmission to provide a good estimation of the temperature of the same volume of air where the acoustic wave travels. On the other hand, a too close position could also lead to possible acoustic interference; a compromise has been found. In order to evaluate a possible error in temperature estimation, we have measured the gradients around the measurement area by exploiting the same array of equally spaced thermometers used for the measurement.

The set of thermometers were placed orthogonally to the acoustic measurement direction across the acoustic beam. The temperature is measured for a given time and averaged. In figure 35 is shown the typical dispersion of the temperature on the thermometer's horizontal direction. The first PT100 sensor is to be considered in zero position and all other five sensors are placed respectively at a 31 cm distance from the first one, third sensor at 59 cm from first sensor, 94 cm between fourth and first sensor, 118 cm between fifth and first sensor and sixth sensor being 157 cm from the first sensor. The temperature values are recorded for every 20 seconds. The difference between the average temperature value and value from every sensor is calculated.

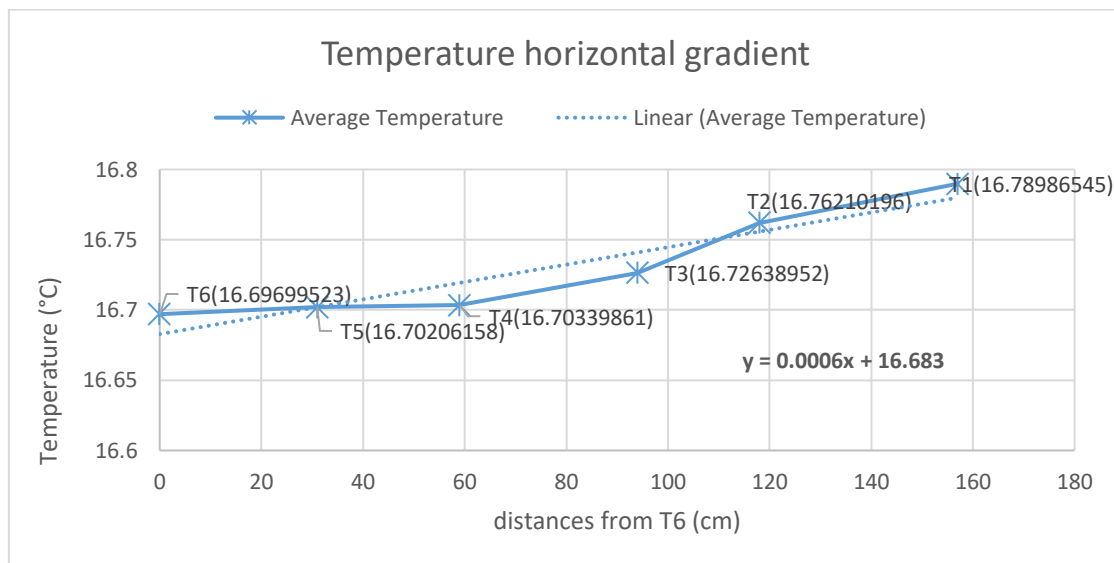


Figure 35-Typical temperature horizontal gradient of the measurement volume

The above graph is plotted based on the dispersion of temperature values from the average values obtained through PT100 sensors against the distance between every thermal sensor. The slope of the curve representing dispersion of thermal values is presented in the form of an equation on the graph. The thermal gradient will be used to calculate a possible error due to the estimation of the temperature in the measurement volume.

The next experiment was carried out to determine the vertical temperature gradient. In this experiment the PT100 sensors are placed vertically and the temperature values are recorded over 3 hours long. Based on these values, the average thermal values are calculated and recorded for every 20 seconds of sampling size. The graph of figure 36 represents the vertical gradient of thermal values in regard to its vertical position. As expected, the vertical gradient is much higher than the horizontal one. Furthermore, the gradient decreases when moving

away from the floor. For the evaluation of the uncertainty, we have considered the gradient in the interval between 100 and 150 cm from the floor where the experiment was carried out.

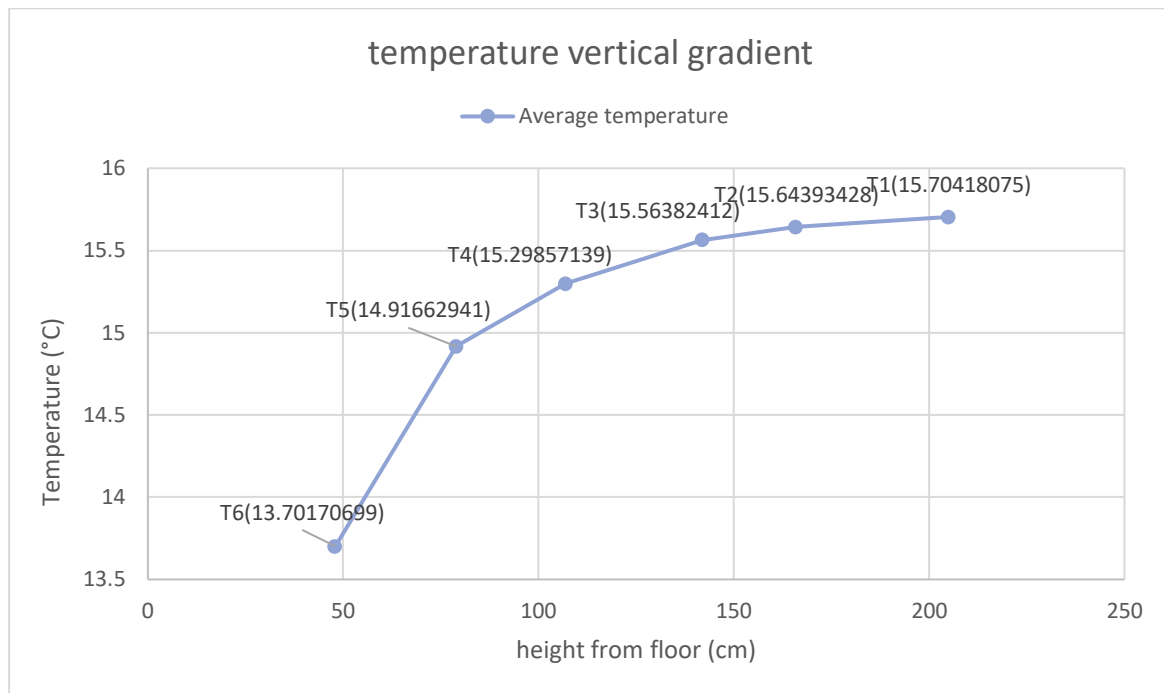


Figure 36-Temperature vertical gradient of 6 PT-100 sensors (T1-T6)

## 5.7. Temperature dispersion

The results are presented here to determine the temperature dispersion among all thermal sensors, due to natural errors of the thermometers, of the scanner, and of air fluctuations. The experiment is carried out along a temperature change of about 1 degree. The temperature change was between 23.3 °C to 24.3 °C during this data acquisition. The six sensor values are recorded and tabulated to determine the average temperature values. The graph plotted for dispersion thermal difference values of every sensor is plotted against temperature in °C.

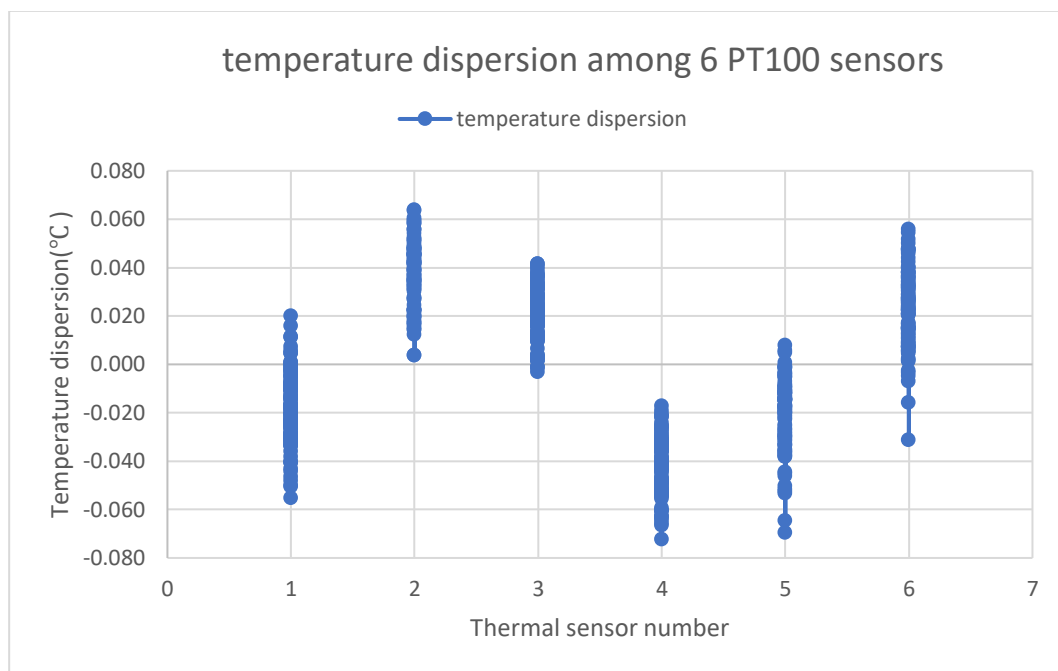


Figure 37-Thermal dispersion values among 6 PT-100 sensors(T1-T6)

From the experimental data, the first sensor yields an average difference of -0.019 °C from the total average obtained from all 6 PT100 sensors. Similarly, the second sensor yields an average difference of 0.037 °C from the median value, the third sensor yields an average difference of -0.042 °C, the fifth sensor yields an average -0.021 °C and the sixth sensor yields a difference of 0.023 °C. The first, fourth and fifth PT100 sensor yields a negative or undervalue from the average temperature values. The second, third and sixth PT100 sensors are distributed to provide overvalued thermal values than the average thermal values.

## 5.8. Effect of frequency

The Cramer equation doesn't deal with the dependence of speed of sound in air on the frequency of acoustic waves transmitted. On the other hand, the Zuckerwar handbook on speed of sound in air takes into consideration the frequency of waves transmitted. In figure 38, as an example, one of our experimental set of measurements (blue curve) is compared with the speed of sound calculated from the Cramer formula (brown curve) and with the Zuckerwar estimation for various frequencies from 3 kHz to 20 kHz.

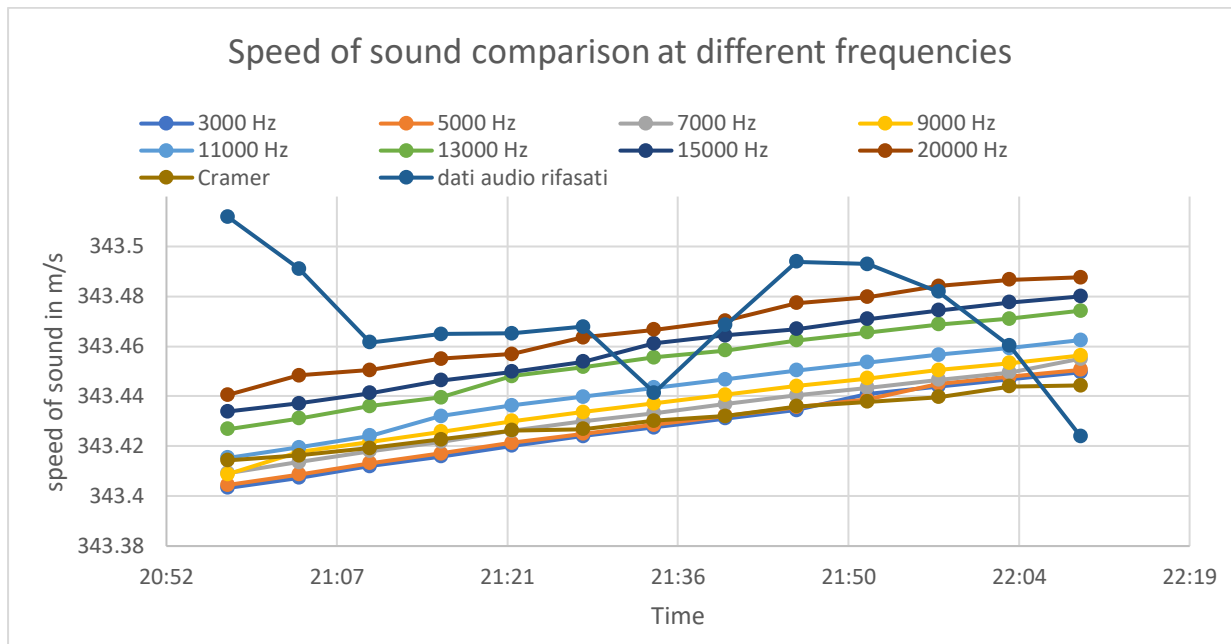
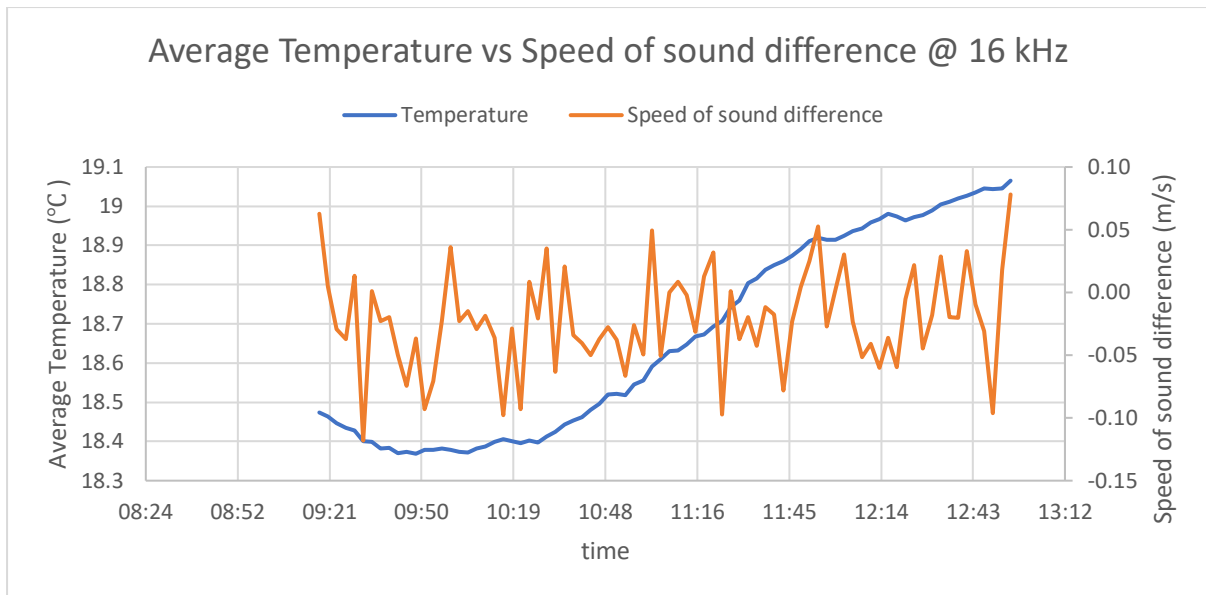


Figure 38-Speed of sound measurement at different frequencies based on Zuckerwar equation with speed of sound values based on experiment at 20 kHz

As explained, we made most of our measurements at 20 kHz, nevertheless we wanted to investigate the effect of frequency on our set-up.

To study the dependence, the experimental values are obtained at frequencies of 16 kHz, 18 kHz, 20 kHz and 22 kHz. The below graphs are presented to study about the speed of sound in air values based on Cramer equation and at different operating frequencies set for the experiment.



*Figure 39-Speed of sound difference values (Experiment & Cramer) @ 16 kHz*

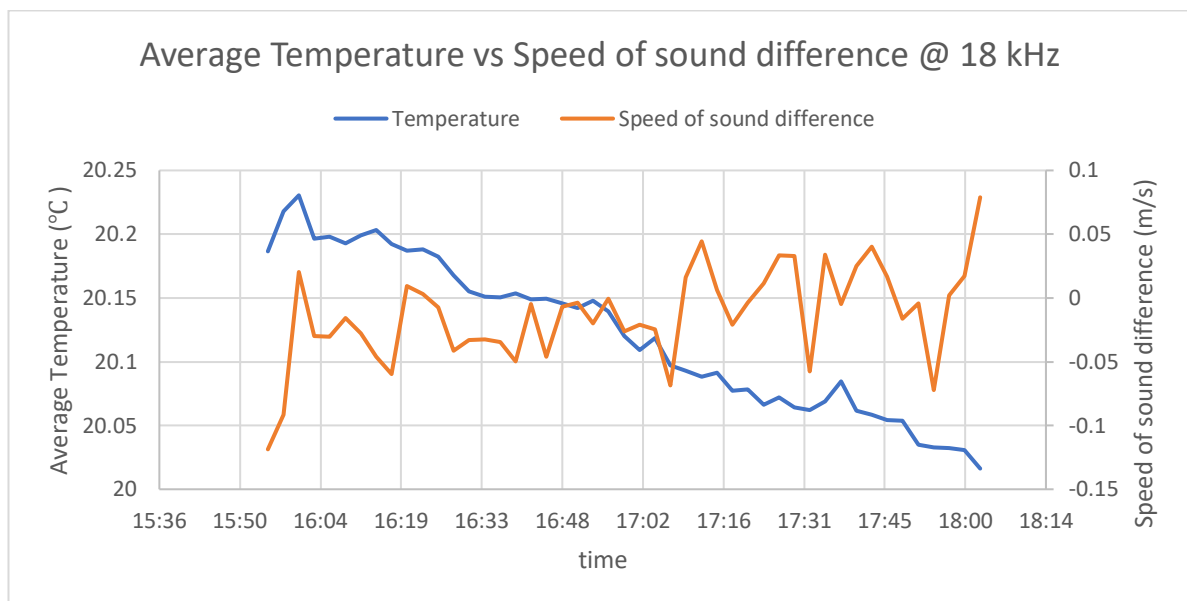


*Figure 40-Speed of sound difference values (Experiment & Cramer) @ 18 kHz*

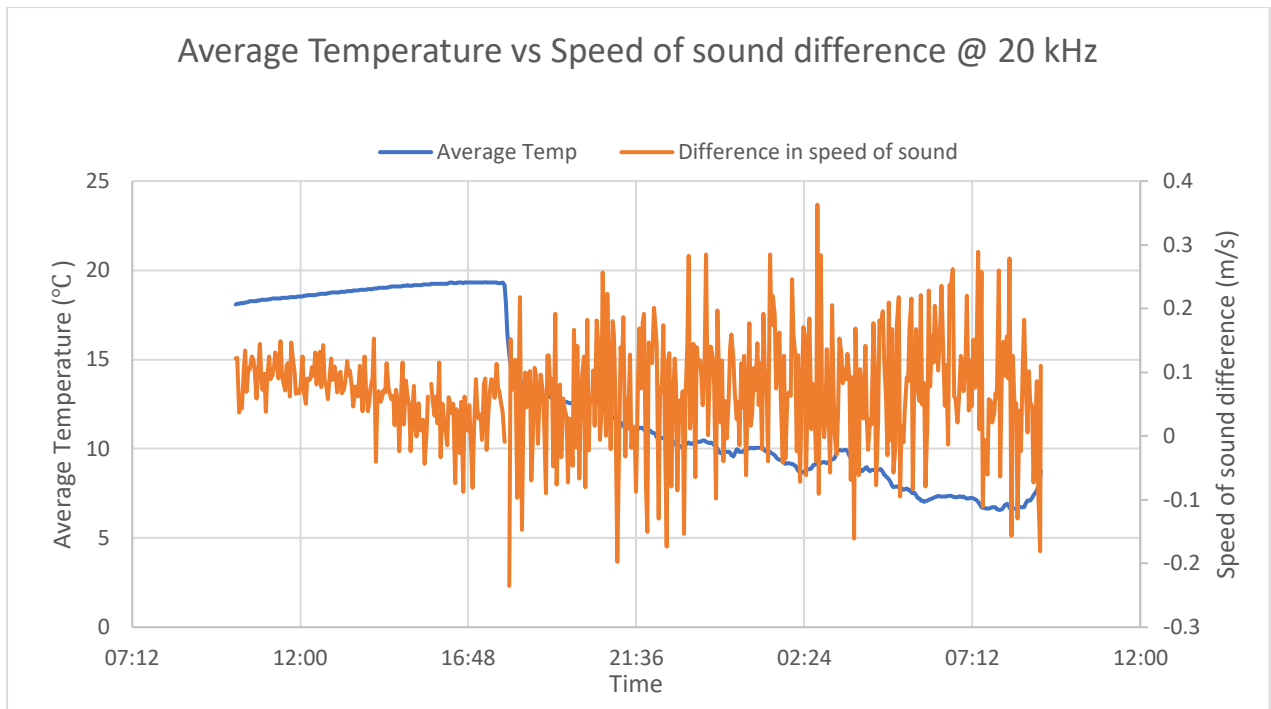


Figure 41-Speed of sound difference values(Experiment & Cramer) @ 20 kHz

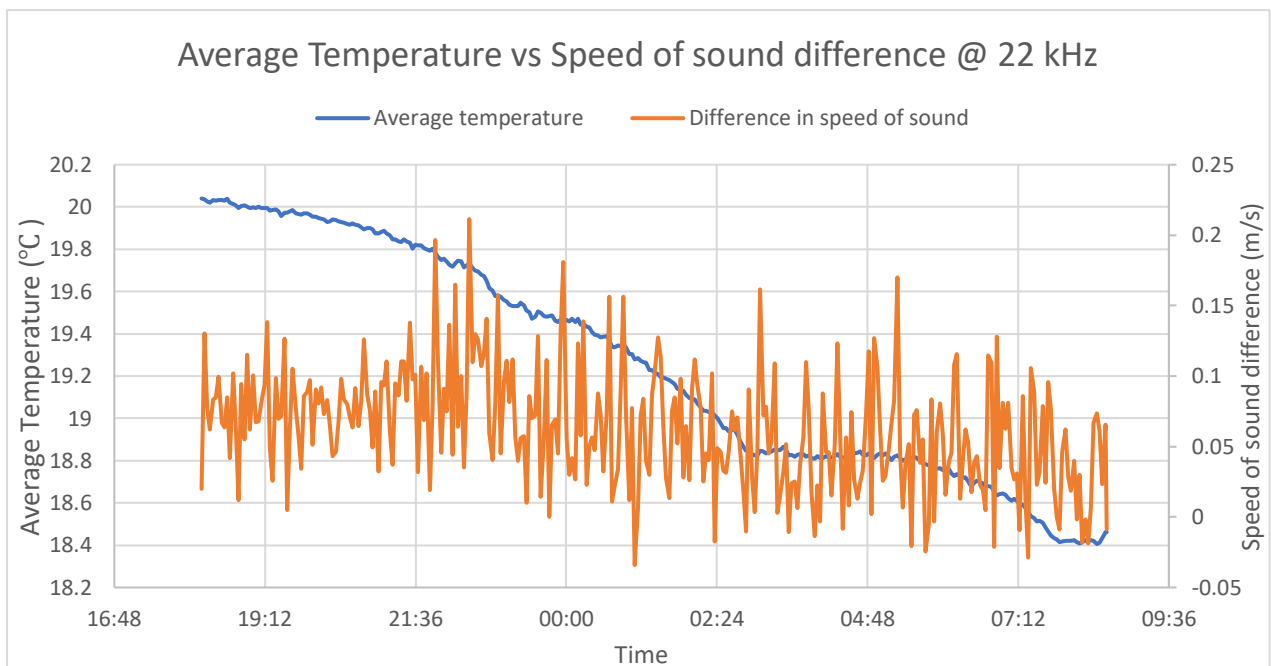


Figure 42-Speed of sound difference values (Experiment & Cramer) @ 22 kHz

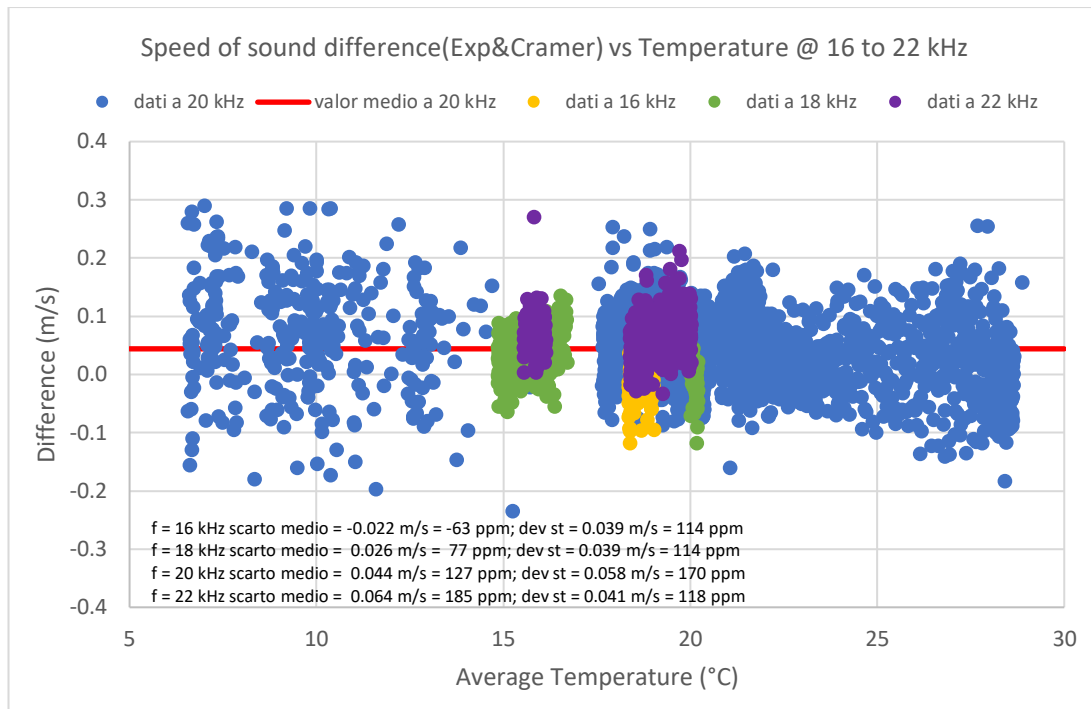


Figure 43-Scatter plot of speed of sound difference values at 16 to 22 kHz

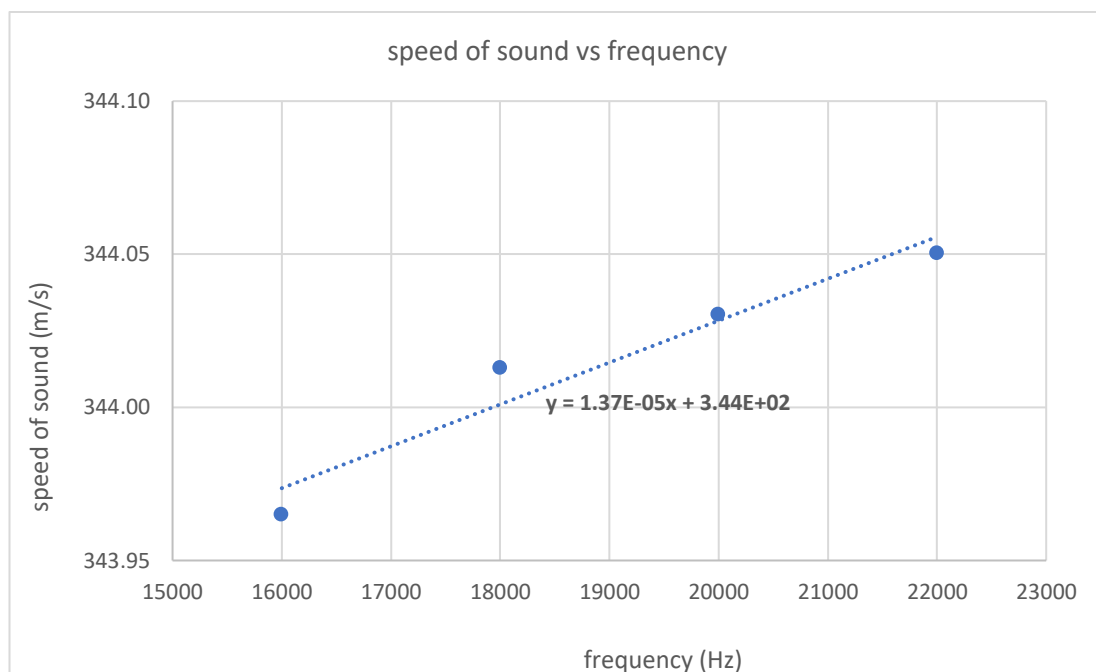


Figure 44-Speed of sound vs Frequency

The figure 43 represents various data points representing the speed of sound values obtained through experiment at different frequencies in various environmental conditions. The average and standard deviation of every frequency operating range was presented in the graph in comparison with the average speed of sound in air from 20 kHz. In the figure 44, the different speed of sound in air values taken in the same environmental conditions are presented in a slope to determine the dependence of experimental set-up on the operating frequency and slope values are presented in the graph. The increase of speed of sound with

frequency is not compliant with what foreseen by Zuckerwar since it is about one order of magnitude larger. We thus interpreted this effect as some spurious interference effect and did not consider it in the following analysis.

## 5.9. Relative alignment of Microphone and Loudspeaker

The relative position of loudspeaker and microphone has been checked by means of a laser beam. Maximum care was devoted to this operation, nevertheless some small misalignment errors can be present and their effect has to be evaluated. For this reason, we have estimated the effect of misalignment on the measurement of the speed of sound.

It becomes very important to study the relative position and alignment between microphone and loudspeaker. The lateral and angular alignment between the loudspeaker and microphone is studied and presented in this part.

Firstly, the horizontal alignment of the microphone is altered to -4 cm and +4 cm (to left and right) in relation to the original position and the experiment is carried out. The speed of sound values is determined in this case to present the dependence on horizontal alignment of the microphone in respect to the loudspeaker. Similarly, in the next step the vertical alignment is altered by adjusting the tripod height to +2.5 cm and -2.5 cm (below and above) in respect to the original position. In this altered condition, the experiment is carried out to determine experimental speed of sound in air values. In all these cases the speed of sound in air is measured at the original position as well. Based on these obtained experimental data, the following graph is presented to study the dependence on horizontal and vertical alignment of loudspeaker and microphone positions.

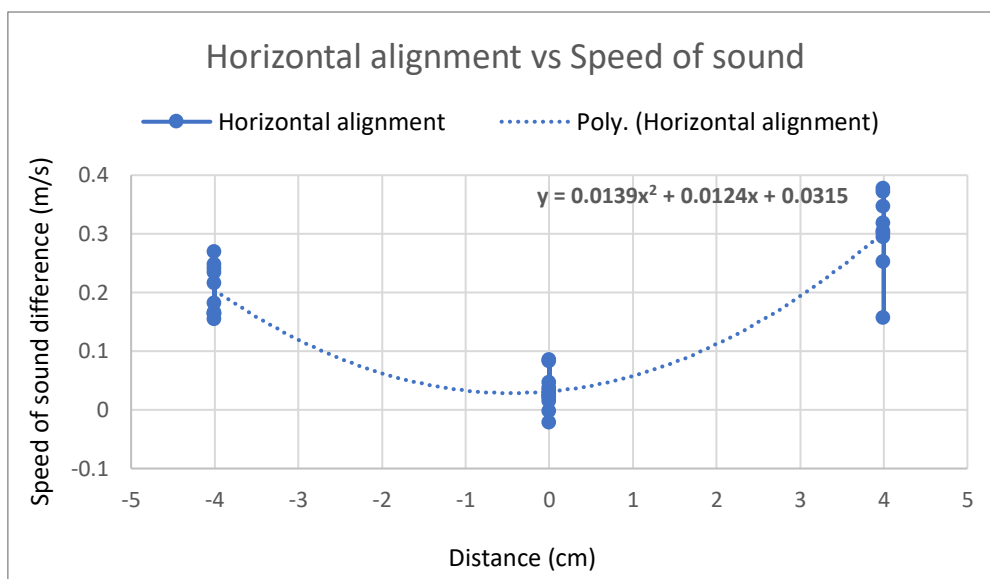


Figure 45-Horizontal alignment between loudspeaker and microphone vs speed of sound difference (Experiment)

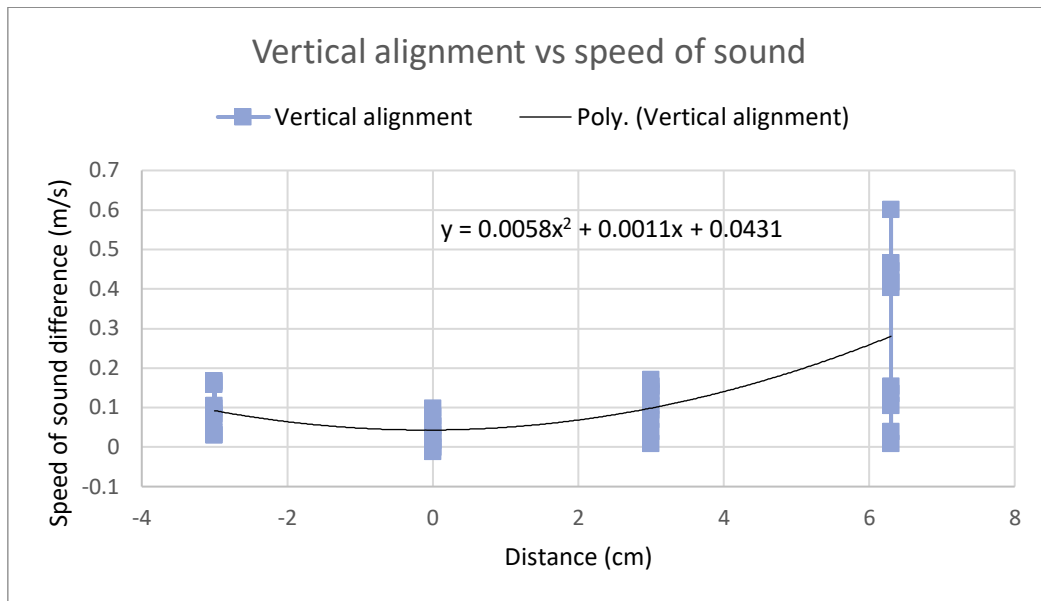


Figure 46-Vertical alignment between loudspeaker and microphone vs speed of sound difference (Experiment)

In the next step, the position of the microphone was altered angularly in relation to loudspeaker position and respective experimental speed of sound values were obtained. With the help of a standard angular measurement, position was altered to -3 and +3 degrees relative to original position. In all these cases, the speed of sound values in all three cases are presented in the following graph to study the dependence of speed of sound values on angular alignment. The graph demonstrates the dependence in the form of slope curve on speed of sound in air on angular alignment.

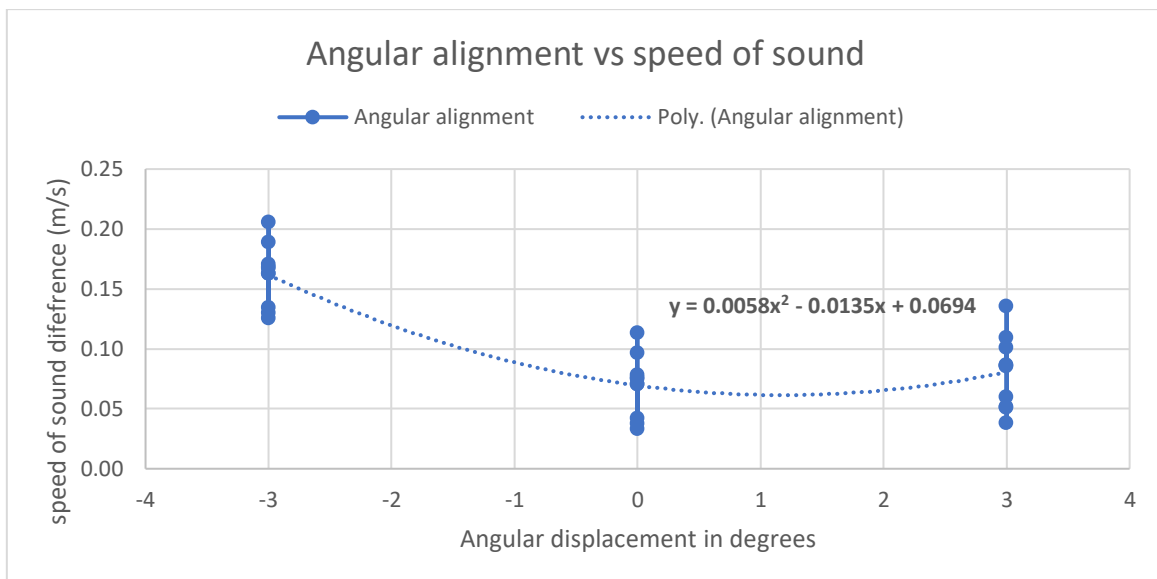


Figure 47-Angular alignment between loudspeaker and microphone vs speed of sound difference (Experiment)

## 5.10. Effect of reflections on the floor

In the experimental set-up, the prism shaped foams are presented below the acoustic path to reduce noise levels and in total 11 foams are introduced. It is important to study about the effect of these foam positions on the experimental speed of sound in air. In fact, we did not use a particular criterion on placing the prisms on the floor in the space between the loudspeaker and the microphone. The experiment is carried out to verify the hypothesis that the position has not systematic effect on the measurement. The prisms have been positioned in three different random arrangements and speed of sound values are recorded.



*Figure 48-Foams between loudspeaker and microphone at original position*



*Figure 49- Foams between loudspeaker and microphone at re-arranged position*

Based on these speed of sound values, the graph I figure 50 is presented to study and get a knowledge about the dependence of speed of sound in air foam positions and its arrangements.

We did not adopt a model for this effect, rather we considered a random possible change in the speed of sound measurement due to “unknown” spurious reflections and considered it in the uncertainty budget. As expected, no systematic effect is observed.

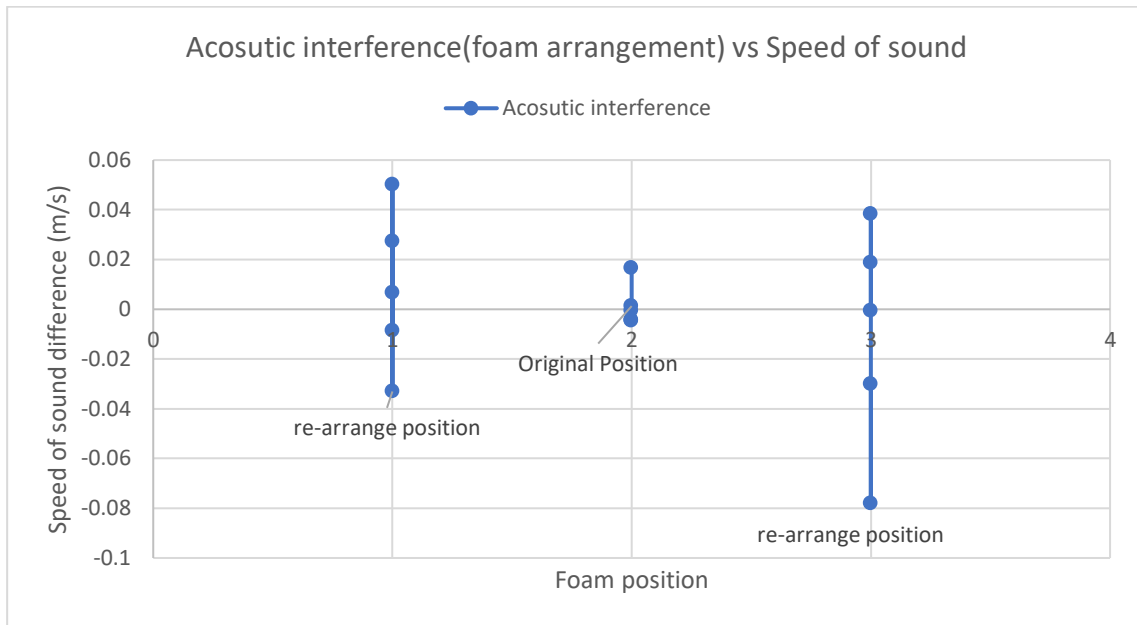


Figure 50-Speed of sound differences (Experiment & Cramer) vs Acoustic interferences at different positions of foams

## 5.11. Uncertainty Budget

In all these previous sections, all factors that could influence the error associated with the estimation of speed of sound in air through experiment and Cramer method. The main factors while determining the uncertainty budget for experimental speed of sound are repeatability, resolution, acoustic interference, frequency of sound waves. The vertical, horizontal and angular alignment of the microphone with respect to the loudspeaker is also studied. The effect of wind turbulence on the experimental speed of sound is determined with the help of an anemometer. With proper choosing of gaussian and rectangular distribution for respective values and the table representing uncertainty budget is presented below.

### 5.11.1. Uncertainty in Speed of Sound in air calculated from Experiment

The repeatability of the experimental set-up is determined based on the standard deviation obtained in the results over the small range of period, where the temperature remains uniform. The resolution is obtained based on the smallest unit readable from the experimental set-up. The frequency dependence of experimental set-up is determined by carrying out the experiment over a set of different frequencies at 20 °C and the slope representing the uncertainty was obtained. The interferometer performance at different temperatures is studied and the respective linear thermal coefficient of the carriage was measured and the respective uncertainty in speed of sound in air is presented. The acoustic interference effect on the experiment also remains as another contribution for uncertainty and it is determined based on various conditions of re-arranging the foams placed in between the loudspeaker and microphone. The combined uncertainty turns out to be around 0.0315 m/s which turns out to be 92 ppm in speed of sound in air at 20 °C.

*Table 6-Uncertainty budget for alignment between microphone and loudspeaker*

Sources of Uncertainty	Sensitivity Co-efficient	Unit	Error Value	Unit	Type	Distribution	Divisor	Std Uncertainty
Angular	1.83E-02	ms <sup>-1</sup> /deg	0.50	deg	A	Gaussian	1	0.0091
Lateral	1.245	ms <sup>-1</sup> /cm	0.02	cm	A	Gaussian	1	0.0249
Vertical	3.7E-01	ms <sup>-1</sup> /cm	0.02	cm	A	Gaussian	1	0.0074
							<b>Alignment Uncertainty</b>	0.0275

Table 7-Uncertainty budget for speed of sound (Experiment)

Sources of Uncertainty	Sensitivity Co-efficient	Unit	Error Value	Unit	Type	Distribution	Divisor	Std Uncertainty	Significance
Repeatability	1		0.024	m/s	A	Gaussian	1	0.0024	0.59%
Resolution	1		0.0001	m/s	A	Gaussian	1	0.0001	0.001%
Frequency	1.37E-05	ms <sup>-1</sup> /Hz	10	Hz	A	Gaussian	1	1.37E-04	0.002%
Interferometer Measurements	0.005	ms <sup>-1</sup> /μm	0.10	μm	A	Gaussian	1	5.00E-04	0.025%
Alignment								0.0275	76%
Acoustic Interference (reflections etc.)	1		0.005	m/s	A	Gaussian	1	0.005	2.5%
Speed of Wind	1		0.025	m/s	B	Rectangular	1.7321	0.0144	20.8%
							<b>Combined Uncertainty</b>	<b>0.0315 (92 ppm)</b>	

### 5.11.2. Uncertainty in speed of sound in air calculated from Cramer equation

In the next step, the uncertainty related to the environmental parameters acquisition for the calculation of speed of sound in air based on Cramer equation is presented in detail. The environmental parameters like temperature, pressure, relative humidity and CO<sub>2</sub> content are presented. In regards to the temperature measurement, the position of thermal sensors plays a major role in obtaining the temperature values closer to real values. Hence, the horizontal and vertical alignment of thermal sensors are done in order to determine the horizontal and vertical gradients of thermal measurements. Another factor considered is the temperature dispersion among all the thermal sensors utilized. Based on all these considerations, the uncertainty turns out to be 0.0315 m/s over the speed of sound values calculated at 20 °C with the help of Cramer equation in addition to the 300 ppm associated with Cramer equation estimation of speed of sound in air. The speed of sound in air calculated through Cramer equation yields an uncertainty contributed by environmental parameters acquisition turns out to be 304 ppm. The uncertainty value of speed of sound in air obtained through experiment, which is around 92 ppm lies well within the uncertainty determined through the Cramer equation associated with environmental parameters.

Table 8-Uncertainty budget related to Temperature (Cramer)

Sources of uncertainty	Sensitivity Co-efficient	unit	Error Value	Unit	Type	Distribution	Divisor	Std Uncertainty
Temperature sensor	1		0.015	°C	B	Gaussian	1	0.015
Temperature gradient (horizontal)	0.0006	°C/cm	0.5	cm	A	Gaussian	1	0.0003
Temperature gradient (vertical)	0.014	°C/cm	0.5	cm	A	Gaussian	1	0.0068
							<b>Temperature Uncertainty</b>	<b>0.0164</b>

Table 9- Uncertainty budget for speed of sound (Cramer)

Sources of uncertainty	Sensitivity Co-efficient	Unit	Value	Unit	Type	Distribution	Divisor	Std Uncertainty	Significance
Temperature measurement	0.62	ms <sup>-1</sup> /°C	0.0164	°C	A	Gaussian	1	0.0102	0.96%
Pressure	7.00E-06	ms <sup>-1</sup> /Pa	10	Pa	B	Rectangular	1.7321	4.041E-05	0.00001%
CO <sub>2</sub> content	1.06E-04	ms <sup>-1</sup> /ppm	5	ppm	B	Rectangular	1.7321	0.000305	0.0008%
Relative Humidity	0.012	ms <sup>-1</sup> /%	1	%	B	Rectangular	1.7321	0.006928	0.44%
Cramer Eqn								0.1032 (300 ppm)	98.58%
							<b>Combined Uncertainty</b>	<b>0.1039 (302 ppm)</b>	

The below graph is presented to represent the speed of sound in air obtained through experimental set-up and Cramer equation at 20 °C. The uncertainty limits of speed of sound in air through experiment is defined by the values obtained from uncertainty budget, which is 0.0315 m/s over the two sides of average speed of sound in air obtained through experiment at 20 °C. The average speed of sound in air obtained through acoustic experiment at 20 °C turns out to be 343.986 m/s in air obtained through calculation with the help of Cramer equation is also presented along with uncertainty values of 0.0364 m/s.

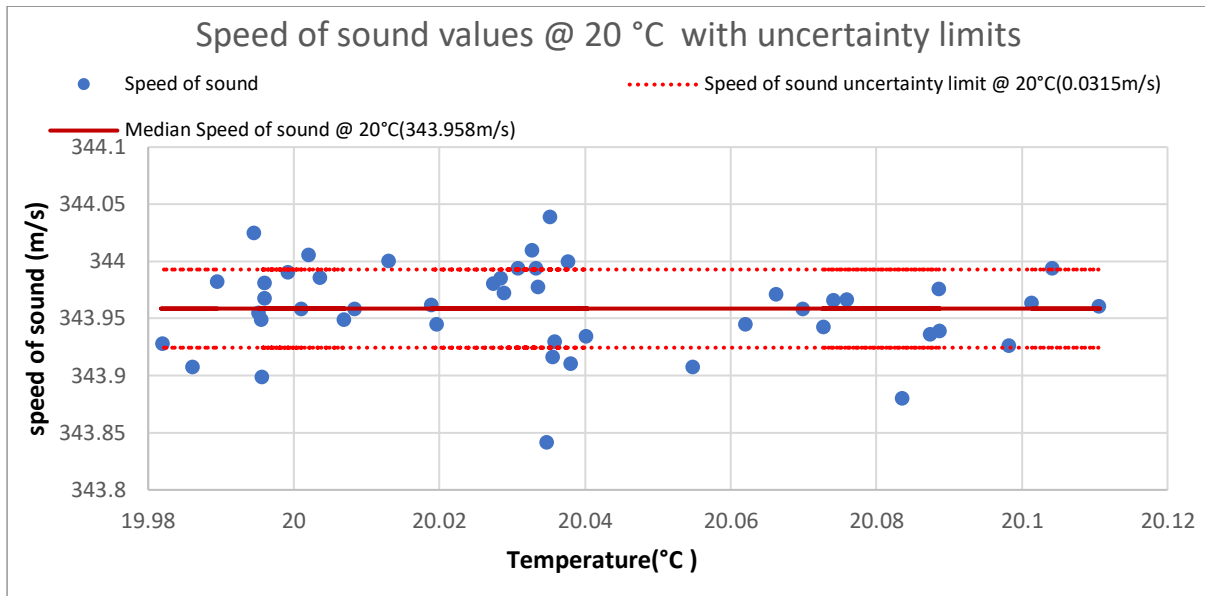


Figure 51-Graph of speed of sound from experiment at 20 °C with respective uncertainty limits

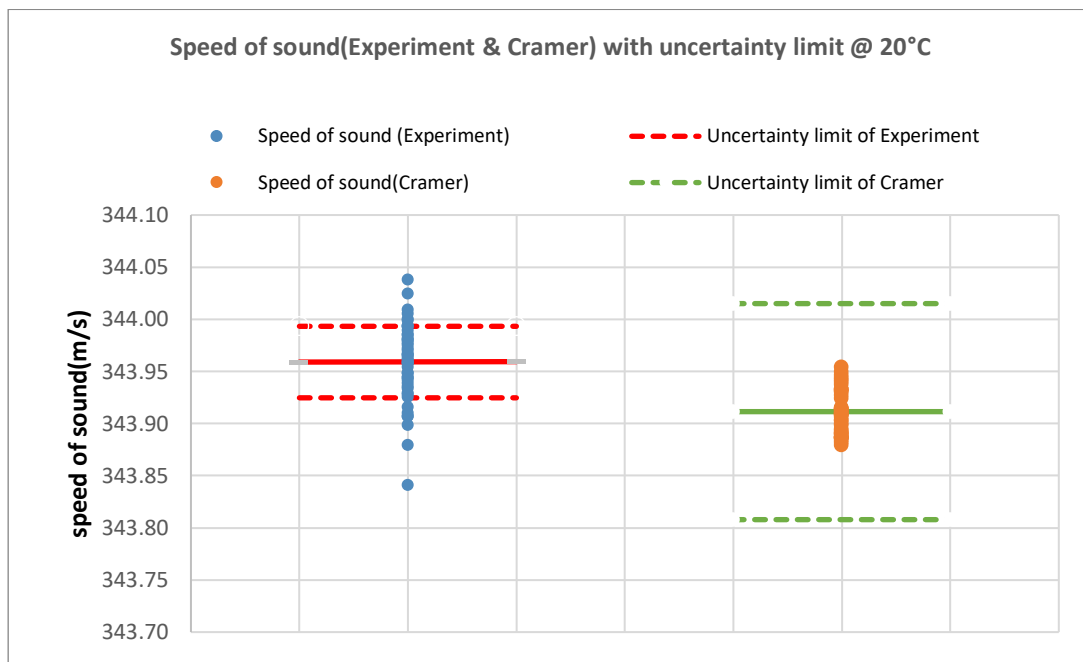


Figure 52-Speed of sound values at 20°C (Experiment & Cramer) with uncertainty limits

## 5.12. Comparison of Speed of Sound in air measurements from Acoustic Thermometer Experiment & Spherical Resonator

As mentioned in the experimental set-up section, the spherical resonator was also placed closer to the experiment by another research group from INRiM. The comparison of environmental speed of sound in air measurements with an acoustic interferometer and a spherical resonator is presented in the below graph. The spherical resonator operates at different radial modes  $(0,n)$  with a frequency range between 2 kHz and 20 kHz and speed of sound values are recorded. Similarly, the speed of sound values based on the Zuckerwar equation at 3 kHz and 20 kHz is also presented in the graph below. The experiment carried out the environmental conditions of temperature ranging from 20.29 °C to 20.33 °C, pressure values at 99.95 kPa, relative humidity of 55% and CO<sub>2</sub> content at 540 ppm. It can be seen from the graph, the speed of sound values obtained based on the experiment lies well within its uncertainty limit of 100 ppm regardless of whether the values obtained from experiment have noise.

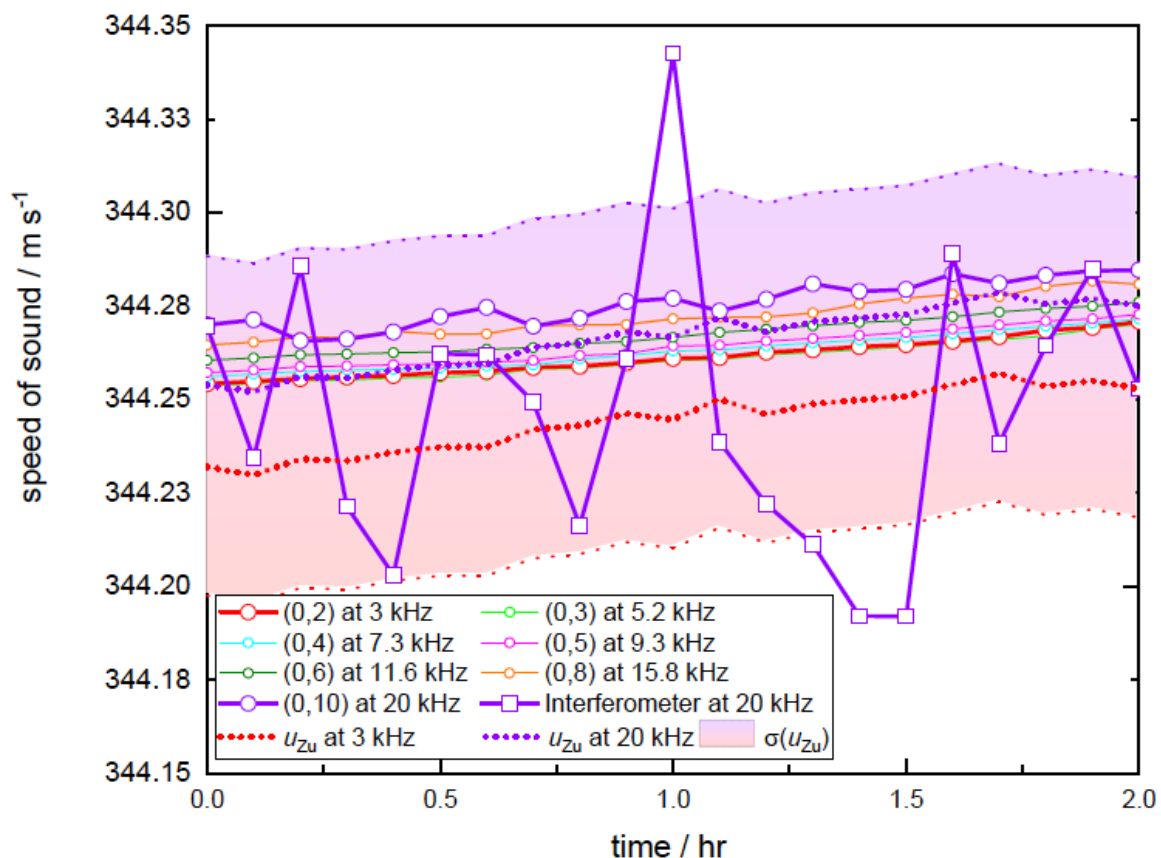


Figure 53-comparison of experimental speed of sound in air measurements with an acoustic interferometer and a spherical resonator the interferometer operates at 20 kHz; several radial  $(0, n)$  resonator modes span the frequency range between 2 kHz and 20 kHz experimental results are compared to the theoretical prediction of Zuckerwar at 3 kHz and 20 kHz the temperature of air rises in two hours from 293.44 K to 293.48 K, at 99.95 kPa, HR = 55 %,  $x_{CO_2}$  = 540 ppm

The below graph is presented to compare the speed of sound values at 20 °C, at zero frequency with help of the Zuckerwar equation and Cramer equation. The speed of sound values presented here are recorded at the following environmental conditions with temperature range of 20.29°C to 20.33 °C, pressure values at 99.95 kPa, relative humidity of 55% and CO<sub>2</sub> content at 540 ppm. The Zuckerwar presented an uncertainty of 1000 ppm, but with the selected temperature range and environmental conditions, the uncertainty limit turns out to be around 100 ppm. The uncertainty related to Cramer equation in determining the speed of sound values is around 300 ppm.

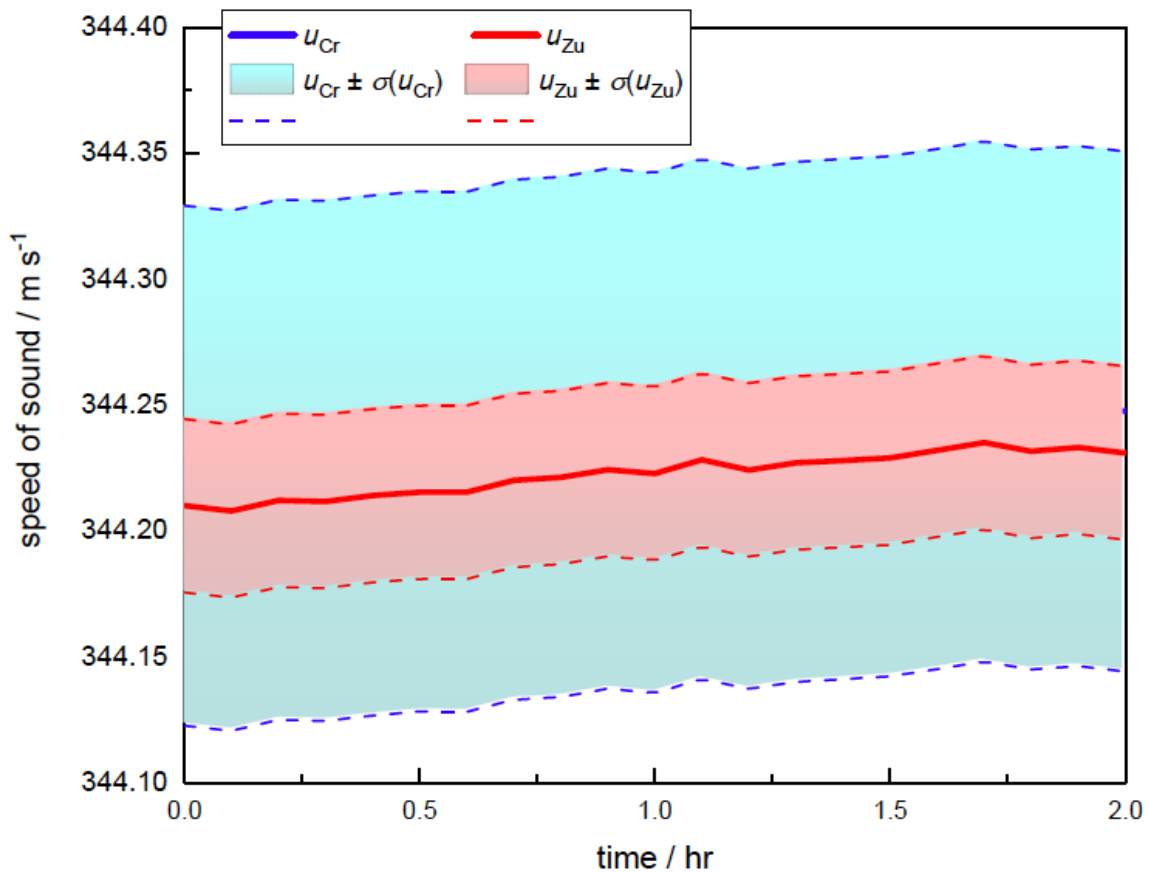


Figure 54-comparison of theoretical speed of sound in humid air at zero frequency as predicted by Cramer (Cr) and Zuckerwar (Zu) for a sample of air undergoing a temperature rise between 293.44 K and 293.48 K, at 99.95kPa, HR=55%, xCO<sub>2</sub> = 540 ppm

# Chapter-6

## Conclusions

We have realized a method capable of measuring the speed of sound in air at the scale of 10 m or more. The method allows us to estimate the average temperature of air along the acoustic path. The efficiency of the method has been demonstrated by comparing the acoustic temperature measurement with the same temperature measured by classical calibrated platinum thermometers. The agreement between the two measurements is of the order of 0.1 °C on a distance of 10 m. The accuracy of the comparison is likely limited by the limited sampling of the thermometers (only four along the 10 m path) and to the different time constant of the two methods. This result should allow us to estimate the refractive index of air and hence to perform interferometric measurements with a relative accuracy of  $10^{-7}$ .

The advantage of the acoustic thermometer is twofold: first it is possible to measure the average temperature over long distances; second it is based on the thermodynamic temperature of air.

The first advantage means that it is not needed to use physical thermometers distributed along the measurement path. Indeed, for an accurate measurement a large number of measurement units are required, otherwise under-sampling could cause large errors. On the other hand, only the average temperature is measured, but this is exactly what is needed to correct the measurements based on the speed of light (interferometers or EDMs).

The second advantage means that we do not need to take care of the classical errors of resistance thermometers, such as self-heating, sensitivity to direct radiation from the Sun and sensitivity to wind. The thermodynamic measurement takes care only of the average speed of the air molecules and is not affected by such problems.

Next research efforts will be devoted to:

- Realize a transportable device to perform measurements outdoors or in a larger environment (see the schematic in figure 55).
- Duplicate the device in order to demonstrate the capability of measuring temperature gradients in large environments and to cancel the effect of the wind speed in outdoor applications

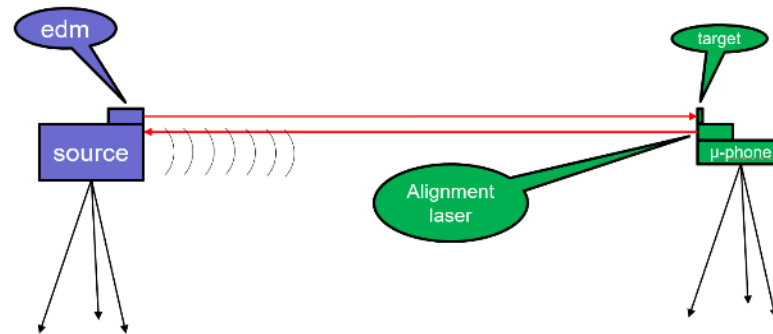


Figure 55-Proposed portable acoustic thermometer set-up for outdoor measurement

The measurement of the temperature from the speed of sound comes by the inversion of the Cramer or the Zuckerwar formula; both formulas have an intrinsic uncertainty larger than 300 ppm, that is too large for some dimensional applications where  $10^{-7}$  uncertainty is required (i.e., an uncertainty on the speed of sound of about 100 ppm is needed). In the second part of the work, we have performed absolute measurements of the speed of sound in a practical range of temperatures with an uncertainty that we have estimated 98 ppm. The measurements are confirmed by an independent measurement, made with an acoustic resonator by another research group, in the same environment. Eventually, we can state that, for a given interval of temperature and humidity, the Cramer and the Zuckerwar formulas can be considered valid with an uncertainty on the speed of sound of the order of 100 ppm. This will allow us to use the acoustic thermometer with an uncertainty of  $0.06\text{ }^{\circ}\text{C}$  at  $1\sigma$ .

Further developments of the acoustic thermometer, will be to duplicate the units with the twofold purpose of reducing the effect of wind, and of measuring the vertical gradient of temperature.

In outdoor measurements, in the presence of wind, the speed of sound is directly affected by the speed of wind, that can be only partially corrected. By realizing a double measurement in two opposite directions, the effect of wind along the measurement axis is cancelled.

In interferometric measurements at long distances, also in closed environments, the vertical thermal gradient is a cause of error because of the bending of the laser beam. With the use of two parallel acoustic thermometers, it is possible to measure and correct for the thermal gradient.

Finally, we plan to perform further measurements of the speed of sound on a wider range of temperatures in order to extend the operative interval where the acoustic thermometer can be used with low uncertainty.

# Bibliography

- [1] M. Astrua, M. Pisani, and M. Zucco, "Air temperature measurements based on the speed of sound to compensate long distance interferometric measurements," 2014. doi: 10.1051/C.
- [2] P. E. Ciddor, "Refractive index of air: new equations for the visible and near infrared," *Applied Optics*, vol. 35, no. 9, pp. 1566–1573, 1996.
- [3] P. E. Ciddor, "Refractive index of air: 3. The roles of CO<sub>2</sub>, H<sub>2</sub>O, and refractivity virials," *Optical Society of America*, vol. 41, no. 12, 2002.
- [4] P. E. Ciddor and R. J. Hill, "Refractive index of air. 2. Group index," *Applied Optics*, vol. 38, no. 9, pp. 1663–1667, 1999.
- [5] K. Meiners-Hagen, A. Abou-Zeid, G. Bönsch, and E. Potulski, "Measurement of the refractive index of air and comparison with modified Edlén's formulae," *Metrologia*, vol. 35, pp. 133–139, 1998.
- [6] K. P. Birch and M. J. Downs, "Correction to the Updated Edlén Equation for the Refractive Index of Air Related content An Updated Edlén Equation for the Refractive Index of Air," *Metrologia*, vol. 31, 1994.
- [7] K. P. Birch and M. J. Downs, "An Updated Edlén Equation for the Refractive Index of Air," *Metrologia*, 1993.
- [8] H. Matsumoto and T. Honda, "High-accuracy length-measuring interferometer using the two-colour method of compensating for the refractive index of air," *Measurement Science and Technology*, vol. 3, pp. 1084–1086, 1992.
- [9] T. B. Quoc, M. Ishige, Y. Ohkubo, and M. Aketagawa, "Measurement of air-refractive-index fluctuation from laser frequency shift with uncertainty of order 10<sup>-9</sup>," *Measurement Science and Technology*, vol. 20, no. 12, 2009, doi: 10.1088/0957-0233/20/12/125302.
- [10] V. Korpelainen, "Acoustic method for determination of the effective temperature and refractive index of air in accurate length interferometry," *Optical Engineering*, vol. 43, no. 10, p. 2400, Oct. 2004, doi: 10.1117/1.1787834.
- [11] N. Khé Lifa, H. Fang, J. Xu, P. Juncar, and M. Himbert, "Refractometer for tracking changes in the refractive index of air near 780 nm," *Optical Society of America*, vol. 37, no. 1, 1998.
- [12] K. Meiners-Hagen and A. Abou-Zeid, "Refractive index determination in length measurement by two-colour interferometry," *Measurement Science and Technology*, vol. 19, no. 8, Aug. 2008, doi: 10.1088/0957-0233/19/8/084004.
- [13] J. Zhang, Z. H. Lu, and L. J. Wang, "Precision measurement of the refractive index of air with frequency combs," *Optics letters*, 2005.
- [14] K. P. Birch *et al.*, "Measurements of the Refractive Index of Air Using Interference Refractometers," 1986.
- [15] W. Hou and R. Thalmann, "Accurate measurement of the refractive index of air," *Elsevier*, 1994.
- [16] M. Pisani, M. Astrua, and M. Zucco, "An acoustic thermometer for air refractive index estimation in long distance interferometric measurements," *Metrologia*, vol. 55, no. 1, pp. 67–74, Dec. 2017, doi: 10.1088/1681-7575/aa9a7a.
- [17] B. Edlén, "The Dispersion of Standard Air," *J. Opt. Soc. Am.*, vol. 43, no. 5, pp. 339–344, May 1953, doi: 10.1364/JOSA.43.000339.

- [18] M. Dobosz and M. Ściuba, "Ultrasonic measurement of air temperature along the axis of a laser beam during interferometric measurement of length," *Measurement Science and Technology*, vol. 31, no. 4, p. 45202, Jan. 2020, doi: 10.1088/1361-6501/ab491b.
- [19] H. Matsumoto and T. Honda, "High-accuracy length-measuring interferometer using the two-colour method of compensating for the refractive index of air," *Measurement Science and Technology*, vol. 3, pp. 1084–1086, 1992.
- [20] Y.-S. Jang and S.-W. Kim, "Compensation of the refractive index of air in laser interferometer for distance measurement: A review," *International Journal of Precision Engineering and Manufacturing*, vol. 18, no. 12, pp. 1881–1890, 2017, doi: 10.1007/s12541-017-0217-y.
- [21] J. Fischer and B. Fellmuth, "Temperature metrology," *Reports on Progress in Physics*, vol. 68, no. 5, pp. 1043–1094, 2005, doi: 10.1088/0034-4885/68/5/r02.
- [22] M. de Podesta, R. Underwood, L. Bevilacqua, and S. Bell, "Air temperature measurement challenges in precision metrology," in *Journal of Physics: Conference Series*, Nov. 2018, vol. 1065, no. 12. doi: 10.1088/1742-6596/1065/12/122027.
- [23] R. Underwood, T. Gardiner, A. Finlayson, S. Bell, and M. de Podesta, "An improved non-contact thermometer and hygrometer with rapid response," *Metrologia*, vol. 54, no. 1, pp. S9–S15, Feb. 2017, doi: 10.1088/1681-7575/aa54c6.
- [24] H. Plumb and G. Cataland, "Acoustical Thermometer and the National Bureau of Standards Provisional Temperature Scale 220 (1965)," *Metrologia*, vol. 2, no. 4, pp. 127–139, Oct. 1966, doi: 10.1088/0026-1394/2/4/001.
- [25] M. de Podesta, G. Sutton, R. Underwood, S. Legg, and A. Steinitz, "Practical acoustic thermometry with acoustic waveguides," in *International Journal of Thermophysics*, Sep. 2010, vol. 31, no. 8–9, pp. 1554–1566. doi: 10.1007/s10765-010-0793-x.
- [26] M. Dobosz and M. Ściuba, "Ultrasonic measurement of air temperature along the axis of a laser beam during interferometric measurement of length," *Measurement Science and Technology*, vol. 31, no. 4, 2020, doi: 10.1088/1361-6501/ab491b.
- [27] Jaroslav Obraz, *Ultradźwięki\_w\_tech\_nice\_pomiarowej*. Wydawnictwa Naukowo-Techniczne, 1983.
- [28] V. Korpelainen, "Acoustic method for determination of the effective temperature and refractive index of air in accurate length interferometry," *Optical Engineering*, vol. 43, no. 10, p. 2400, Oct. 2004, doi: 10.1117/1.1787834.
- [29] V. Korpelainen and A. Lassila, "Online determination of the refractive index of air by ultrasonic speed of sound measurement for interferometric displacement measurements DynaMITE View project DynaMITE-Dynamic applications of large volume metrology in industry of tomorrow environments View project Antti Lassila VTT MIKES metrology Online determination of the refractive index of air by ultrasonic speed of sound measurement for interferometric displacement measurements," 2004. [Online]. Available: <https://www.researchgate.net/publication/228510431>
- [30] G. Cadet, J. L. Valdes, and J. W. Mitchell, "Ultrasonic time-of-flight method for on-line quantitation of semiconductor gases," in *IEEE 1991 Ultrasonics Symposium*, 1991, pp. 295–300 vol.1. doi: 10.1109/ULTSYM.1991.234173.
- [31] G. D. Hallewell and L. C. Lynnworth, "A simplified formula for the analysis of binary gas containing a low concentration of a heavy vapor in a lighter carrier," in *1994 Proceedings of IEEE Ultrasonics Symposium*, 1994, vol. 3, pp. 1311–1316 vol.3. doi: 10.1109/ULTSYM.1994.401834.

- [32] A. Ebrahimkhanlou and S. Salamone, "Probabilistic location estimation of acoustic emission sources in isotropic plates with one sensor," in *Proc.SPIE*, Apr. 2017, vol. 10170. doi: 10.1117/12.2258618.
- [33] K. N. Huang, C. F. Huang, Y. C. Li, and M. S. Young, "High precision, fast ultrasonic thermometer based on measurement of the speed of sound in air," *Review of Scientific Instruments*, vol. 73, no. 11, p. 4022, Nov. 2002, doi: 10.1063/1.1510576.
- [34] M. Astrua, M. Pisani, and M. Zucco, "Air temperature measurements based on the speed of sound to compensate long distance interferometric measurements," 2014. doi: 10.1051/C.
- [35] M. Trusler, *Physical Acoustics and Metrology of Fluids*. CRC Press, 1991. doi: 10.1201/9781003062851.
- [36] G. S. K. Wong and T. F. W. Embleton, "Ratio of specific heat  $\gamma$  of humid air," *The Journal of the Acoustical Society of America*, vol. 75, no. S1, pp. S17–S17, May 1984, doi: 10.1121/1.2021302.
- [37] DAYTON CLARENCE MILLER, *Sound Waves Their Shape And Speed*. New York: The Macmillan Co, 1923.
- [38] H. C. Hardy, D. Telfair, and W. H. Pielemeier, "The Velocity of Sound in Air," *Journal of the Acoustical Society of America*, vol. 13, no. 3, pp. 226–233, 1942, doi: 10.1121/1.1916169.
- [39] A. van Itterbeek and W. de Rop, "MEASUREMENTS ON THE VELOCITY OF SOUND IN AIR UNDER PRESSURES UP TO 20 ATM COMBINED WITH THERMAL DIFFUSION," 1955.
- [40] A. H. Hodge, "An Experimental Determination of Ultrasonic Velocity in Several Gases at Pressures Between One and One Hundred Atmospheres," *Journal of Chemical Physics*, vol. 5, no. 12, pp. 974–977, 1937, doi: 10.1063/1.1749973.
- [41] Allan J. Zuckerwar, *Handbook of the speed of sound in real gases*, vol. 3. Elsevier, 2002.
- [42] D. H. Smith and R. G. Harlow, "The velocity of sound in air, nitrogen and argon Related content The Propagation of Sound through Gases contained in Narrow Tubes L E Lawley-Systematic Errors in Primary Acoustic Thermometry in the Range 2-20 K A R Colclough-The Velocity of Sound in Air at Low Pressures D E Caro and L H Martin-Recent citations The velocity of sound in air, nitrogen and argon," 1963.
- [43] G. S. K. Wong, "Speed of sound in standard air," *The Journal of the Acoustical Society of America*, vol. 79, no. 5, May 1986, doi: 10.1121/1.393664.
- [44] H. C. Hardy, D. Telfair, and W. H. Pielemeier, "The Velocity of Sound in Air," *Journal of the Acoustical Society of America*, vol. 13, no. 3, pp. 226–233, 1942, doi: 10.1121/1.1916169.
- [45] Partington, "The Specific Heats of Gases," *Nature*, vol. 114, no. 2878, p. 927, 1924, doi: 10.1038/114927b0.
- [46] Dayton Clarence Miller, "Sound Waves," *Nature*, vol. 2582, 1938.
- [47] G. S. K. Wong and T. F. Embleton, "Variation of the speed of sound in air with humidity and temperature," *Journal of the Acoustical Society of America*, vol. 77, no. 5, pp. 1710–1712, 1985, doi: 10.1121/1.391918.
- [48] G. S. Wong and T. F. Embleton, "Variation of specific heats and of specific heat ratio in air with humidity," *Journal of the Acoustical Society of America*, vol. 76, no. 2, pp. 555–559, 1984, doi: 10.1121/1.391597.
- [49] D. H. Smith and H. J. Wintle, "The propagation of sound in relaxing gases in tubes at low frequencies," 1960.

- [50] S. S. Lestz, "A Method for Measuring the Sound Wavelength in Gases," *American Journal of Physics*, vol. 31, no. 2, pp. 96–98, Feb. 1963, doi: 10.1119/1.1969332.
- [51] D. Bancroft, "Measurement of Velocity of Sound in Gases," *American Journal of Physics*, vol. 24, no. 5, pp. 355–358, May 1956, doi: 10.1119/1.1934227.
- [52] O. Cramer, "The variation of the specific heat ratio and the speed of sound in air with temperature, pressure, humidity, and CO. concentration," *Journal Society America*, vol. 93, no. 5, 1993, [Online]. Available: <http://asadl.org/terms>
- [53] R. S. Worland and D. D. Wilson, "The speed of sound in air as a function of temperature," *The Physics Teacher*, vol. 37, no. 1, pp. 53–57, Jan. 1999, doi: 10.1119/1.880153.
- [54] A. J. Zuckerwar, *Handbook of the Speed of Sound in Real Gases*, first., vol. 3. San Diego, CA : Academic Press, 2002.
- [55] C. M. Harris, "Effects of Humidity on the Velocity of Sound in Air," *The Journal of the Acoustical Society of America*, vol. 49, no. 3B, pp. 890–893, Mar. 1971, doi: 10.1121/1.1912429.
- [56] G. S. K. Wong and T. F. Embleton, "Variation of the speed of sound in air with humidity and temperature," *Journal of the Acoustical Society of America*, vol. 77, no. 5, pp. 1710–1712, 1985, doi: 10.1121/1.391918.
- [57] C. L. Morfey and G. P. Howell, "Speed of sound in air as a function of frequency and humidity," *Journal of the Acoustical Society of America*, vol. 68, no. 5. pp. 1525–1527, 1980. doi: 10.1121/1.385080.
- [58] P. J. Ouseph and J. J. Link, "Variation of speed of sound in air with temperature," *American Journal of Physics*, vol. 52, no. 7, pp. 661–661, Jul. 1984, doi: 10.1119/1.13872.
- [59] O. Cramer, "The variation of the specific heat ratio and the speed of sound in air with temperature, pressure, humidity, and CO2 concentration," *Journal of the Acoustical Society of America*, vol. 93, no. 5, pp. 2510–2516, 1993, doi: 10.1121/1.405827.
- [60] George S. K. Wong, "Air Sound Speed Measurements and Computation: A Historical Review," *National Research Council of Canada*, 1986.
- [61] T. C. Hebb B. C. Vancouver, "The Velocity of Sound and the Ratio of the Specific Heats for Air," *Phys. Rev.*, vol. 14, no. 1, pp. 74–84, 1919.
- [62] J.R.Partington and W.G.Shilling, "THE SPECIFIC HEATS OF GASES," *Ernest Benn, Ltd*, vol. 43, no. 32, pp. 813-undefined, 1924.
- [63] R. L. Abbey and G. E. Barlow, "THE VELOCITY O F SOUND I N GASES," 1947.
- [64] F. v Hunt and A. E. Benfield, "Precision Measurement of the Velocity of Sound in Air," 1953. [Online]. Available: <http://acousticalsociety.org/content/terms>.
- [65] D. H. Smith and R. G. Harlow, "The velocity of sound in air, nitrogen and argon," *British Journal of Applied Physics*, vol. 14, no. 2, pp. 102–106, 1963, doi: 10.1088/0508-3443/14/2/316.
- [66] J. M. A. Lenihan, "The velocity of sound in air," *Acta Acustica united with Acustica*, vol. 2, no. 5, pp. 205–212, 1952.
- [67] J. C. Albergotti, "Speed of sound by a time-of-flight method," *American Journal of Physics*, vol. 49, no. 6, pp. 595–596, Jun. 1981, doi: 10.1119/1.12466.
- [68] A. Aljalal, "Time of flight measurement of speed of sound in air with a computer sound card," *European Journal of Physics*, vol. 35, no. 6, Nov. 2014, doi: 10.1088/0143-0807/35/6/065008.

- [69] M Vollmer, "Direct speed of sound measurement within theatmosphere during a national holiday in NewZealand," 2018.
- [70] J. A. Gómez-Tejedor, J. C. Castro-Palacio, and J. A. Monsoriu, "Direct measurement of the speed of sound using a microphone and a speaker," 2014.
- [71] S. Velasco, F. L. Román, A. González, and J. A. White, "A computer-assisted experiment for the measurement of the temperature dependence of the speed of sound in air," *American Journal of Physics*, vol. 72, no. 2, pp. 276–279, Feb. 2004, doi: 10.1119/1.1611479.
- [72] G. S. K. Wong, "Speed of sound in standard air," *Journal Acoustic Society America*, vol. 79, no. 5, 1986, [Online]. Available: <http://acousticalsociety.org/content/terms>.
- [73] "ISO/IEC 9613-2 1996 Attenuation of Sound During Propagation Outdoors," Geneva, 1996.
- [74] M. Astrua, M. Pisani and M. Zucco, "Traceable 28 m-long metrological bench for accurate and fast calibration of distance measurement devices" *Measurement Science and Technology* 26(8) (2015) DOI: 10.1088/0957-0233/26/8/084008

# Appendix

Key instruments used in the experiments are:

- Loudspeaker (HERTZ-ST25ANeo)
- Microphone (BOYA-BM6060, BOYA-PVM1000, SENNHEISER MKH 416-P48U3)
- Temperature sensor (Fluke 1586A Super-DAQ with PT 100)
- Humidity sensor (Testo 605i)
- Pressure sensor (DRUCK DPI 142)
- Synthesizer:(RIGOL DG-4162 Frequency Generator)
- Mixer (SAMSON MIX PAD 9)
- Anemometer (GILL 1590-PK-020)
- EDM (BOSCH GLM 250 VF)
- ADC Board (Agilent 34970A)
- Software (LabVIEW)

## TECHNICAL SPECIFICATIONS

<b>Component</b>		High Efficiency Compression Driver
<b>Size</b>	mm (in.)	44 (1.8)
<b>Power Handling</b>	W peak	100 Hi-pass filtered @ 5 kHz - 12 dB Oct.
<b>Impedance</b>	$\Omega$	4
<b>Frequency Response</b>	Hz	3k ÷ 20k
<b>Sensitivity</b>	dB/SPL	107
<b>Voice Coil <math>\phi</math></b>	mm (in.)	25 (1)
<b>Magnet</b>		Neodymium
<b>Dome/Cone</b>		Aluminium
<b>Weight of one component</b>	kg (lb.)	0,39 (0.86)

Figure A1-Technical specifications of HERTZ-ST25ANeo loudspeaker

Type:	Condenser
Polar Pattern:	Super-cardioid
Frequency Response:	60Hz-20000Hz
Sensitivity:	-36±3dB(0dB=1V/Pa@1KHz)
Signal-to-Noise Ratio:	80dB
Output Impedance:	200Ω
Power Requirements:	24-48V phantom power or 1.5V AA battery
Output:	3-pin XLR
High Pass Filter:	150Hz
Weight:	129g(4.6oz)

Figure A2-Technical specifications of BOYA-BM6060 microphone

Acoustic Principle	Line plug gradient
Polar pattern	Super-Cardioid
Frequency Response	25-20,000Hz
Sensitivity	-33dB +/- 1dB / 0dB=1V/Pa, 1kHz
Signal to Noise Ratio	80dB or more
Output Impedance	300 Ohm or more---phantom 600 Ohm or more ---battery
Power	1.5V battery or 48V phantom
Plug	mini-pin plug (3-pin XLR)
Filter	Controlled by low-cut filter switch
Length	27.8cm
Net Weight	110g

Figure A3- Technical specifications of BOYA-PVM1000 microphone

**Technical Data**

Pick-up pattern .....	super-cardioid/lobar
Frequency response .....	40 – 20,000 Hz
Sensitivity (free field, no load, 1 kHz) .....	25 mV/Pa ± 1 dB
Nominal impedance .....	25 Ω
Min. terminating impedance .....	800 Ω
Equivalent noise level	
A-weighted (DIN IEC 651) .....	appx. 13 dB
CCIR-weighted (CCIR 468-3) .....	appx. 24 dB
Max. sound pressure level .....	130 dB at 1 kHz
Power supply .....	phantom 48 ± 12 V
Supply current .....	2 mA
Dimensions .....	∅ 19 x 250 mm (∅ 0.75" x 9.84")
Weight .....	appx. 165 g (5.82 oz)

Figure A4- Technical specifications of SENNHEISER MKH 416-P48U3 microphone

SE012 PT100 probe specifications	
Temperature range	-50 to +250 °C
Accuracy	±0.03 °C @ 0 °C Tenth-DIN
Dimensions	
Length	150 mm
Diameter	4 mm
Cable	2 m
Material	Stainless steel probe, PTFE cable
Handle	No
Connector	4-pin mini-DIN
Number of wires	4

Figure A5- Technical specifications of SE012 PT100 temperature sensor

<b>Sensor type</b>	<b>Humidity – capacitive</b>
Measuring range	0 to 100% RH
Accuracy	±3.0 %RH (10 to 35 %RH) ±2.0 %RH (35 to 65 %RH) ±3.0 %RH (65 to 90 %RH) ±5 %RH (< 10 %RH or > 90 %RH) (at 77 °F)
Resolution	0.1% RH
<b>Sensor type</b>	<b>NTC</b>
Measuring range	-4 to 140 °F
Accuracy	±1.4 °F (-4 to 32 °F) ±0.9 °F (32 to 140 °F)
Resolution	0.1 °F
<b>General technical data</b>	
Compatibility	requires iOS 8.3 (or later) / Android 4.3 (or later) requires mobile device with Bluetooth 4.0
Storage temperature	-4 to 140 °F
Operating temperature	-4 to 122 °F
Battery type	3 AAA Batteries (incl.)
Battery life	150 hrs
Dimensions	8.6 x 1.2 x 1.0 in Probe shaft: 2.9 in (L), 0.5 (dia.)
Warranty	2 years
Measuring Units	°F, °C, %rF / %RH, °Ftd, °Ctd, wetbulb °F, wetbulb °C

Figure A6-Technical specifications of Testo 605i hygrometer

**Standard Specification**

**Standard Pressure Ranges**

10.9 - 16.7 psia (750 - 1150mbar absolute) (barometric only).  
 0.5 - 19 psia (35 - 1310mbar absolute).  
 0.5 - 38 psia (35 - 2620mbar absolute).  
 0.5 - 50 psia (35 - 3500mbar absolute).

**Over Range**

1.1 x FS pressure range.

**Maximum Working Pressure**

58 psia absolute.

**Pressure Media**

Non-corrosive dry gases only.

**Display**

**Panel**

High contrast, back-lit LCD.

**Readout**

±9999999 maximum, updated 2 times per second.

**Pressure Units**

24 units plus two user-defined and altitude in feet (ft) or meters (m).

**Languages**

English, Chinese, French, German, Italian, Japanese, Portuguese, Spanish.

**Process Features**

Hold, Maximum/minimum value, Tare and programmable filter.

**Performance**

**Precision**

Precision 0.01% FS includes non-linearity, hysteresis, repeatability and temperature effects over 10° to 40°C.

**Measurement Stability**

Better than 100 ppm (0.01% FS) per year.

**Electrical**

**Communications**

RS232 serial interface supplied as standard (SCPI Protocol). IEEE-488 optional.

**Power Supply**

11V to 26V AC or DC, 10VA, via 0.083 inch (2.1mm) Jack, supplied with AC/DC power adaptor 90 to 264 VAC, 45 to 65 Hz.

**Environmental**

**Temperature**

Operating: 5° to 50°C  
 Calibrated: 23°C  
 Storage: -20° to 60°C

**Humidity**

Compliant with Def Stan. 66-31 8.6 cat. 3

**Vibration**

Compliant with Def Stan. 66-31 8.4 cat. 3

**Shock**

Mechanical shock conforms to EN61010

**Conformity**

Electrical and mechanical safety: EN61010  
 EMC Emission: EN61326-1  
 EMC Immunity: EN61326-1  
 Certification: CE marked

**Physical**

**Weight**

2.2 pounds (1kg) nominal.

**Dimensions**

7.3" W x 7.7" D x 3" H (185mm W x 195mm D x 75mm H)

**Pressure Connection**

1/8 NPT female

**Options**

**(A) Analog Output**

0 - 10V, 0 - 5V, -5V to 5V, 0/4 - 20mA outputs selectable. Accuracy 0.05% FS, update rate 2 readings per second. Programmable between minimum and full scale pressure for proportional output against pressure.

**(B) IEEE 488 digital communications**

Full computer control is available via a databus using the SCPI protocol. IEEE parallel D connector is provided on the rear panel.

**(C) Panel mounting kit**

Two sided plates and front panel cutout enable easy mounting to racks and panels.

**Supplied as Standard**

User handbook, calibration certificate and AC/DC power adaptor.

Figure A7- Specifications of Pressure sensor (DRUCK DPI142)

Model	DG4202	DG4162	DG4102	DG4062
Number of Channels	2	2	2	2
Maximum Frequency	200MHz	160MHz	100MHz	60MHz
Sample Rate	500MSa/s			

Waveforms	
Standard Waveform	Sine, Square, Ramp, Pulse, Noise, Harmonics
Arbitrary Waveform	150 kinds, including Sinc, Exponential Rise, Exponential Fall, ECG, Gauss, HaverSine, Lorentz, Dual-Tone, DC, etc.

Frequency Characteristics				
Sine	1µHz to 200MHz	1µHz to 160MHz	1µHz to 100MHz	1µHz to 60MHz
Square	1µHz to 60MHz	1µHz to 50MHz	1µHz to 40MHz	1µHz to 25MHz
Ramp	1µHz to 5MHz	1µHz to 4MHz	1µHz to 3MHz	1µHz to 1MHz
Pulse	1µHz to 50MHz	1µHz to 40MHz	1µHz to 25MHz	1µHz to 15MHz
Harmonic	1µHz to 100MHz	1µHz to 80MHz	1µHz to 50MHz	1µHz to 30MHz
Noise (-3dB)	120MHz bandwidth	120MHz bandwidth	80MHz bandwidth	60MHz bandwidth
Arbitrary Waveform	1µHz to 50MHz	1µHz to 40MHz	1µHz to 25MHz	1µHz to 15MHz
Resolution	1µHz			
Accuracy	±2ppm, 18°C to 28°C			

Sine Wave Spectrum Purity	
Harmonic Distortion	Typical (0dBm) DC to 1MHz: <-60dBc 1MHz to 10MHz: <-55dBc 10MHz to 100MHz: <-50dBc 100MHz to 200MHz: <-40dBc
Total Harmonic Distortion	<0.1% (10Hz to 20kHz, 0dBm)
Spurious (non-harmonic)	Typical (0dBm) ≤10MHz: <-65dBc >10MHz: <-65dBc + 6dB/octave
Phase Noise	Typical (0dBm, 10kHz deviation) 10MHz: ≤-115dBc/Hz

Figure A8-Specifications of RIGOL DG-4162 Frequency Generator

	Normal	Limit
<b>Frequency Response (Trim @ Min, unity gain <math>\pm</math> 3 dB)</b>		
Mic to Main	5 Hz - 65 kHz	10 Hz - 50 kHz
Line to Main	5 Hz - 65 kHz	
Aux Return to Main	5 Hz - 75 kHz	
Line to Aux Send 1/2	5 Hz - 75 kHz	
<b>T.H.D. (Trim @ Min, +4dBu output, unity gain, 1 kHz w/30 Hz LPF)</b>		
Mic/Line to Main (Mono Ch)	0.002%	0.01%
Line to Main (Stereo Ch)	0.002%	0.01%
Line to Aux Send	0.002%	0.01%
<b>Equivalent Input Noise ("A" filter on, input shorted)</b>		
Mic	-128 dB	-128 dB
Line	-111 dB	-111 dB
<b>Maximum Voltage Gain</b>		
Mic to Main	74 dB	
Line to Main (Mono Ch)	54 dB	
Line/Tape to Main (Stereo Ch)	34 dB	
Aux Return to Main	20 dB	
Mic to Aux Send 1 (Mono Ch)	64 dB	
Mic to Aux Send 2 (Mono Ch)	74 dB	
Line to Aux Send 1 (Stereo Ch)	24 dB	
Line to Aux Send 2 (Stereo Ch)	34 dB	
<b>Residual Noise (30 kHz LPF, all control Min)</b>		
L/R Main	100 dB	95 dB
Aux Send 1/2	92 dB/91 dB	85 dB
<b>Crosstalk (@ 1 kHz w/ 30 kHz LPF)</b>		
Ch vs. Ch	77 dB	70 dB
Input vs. Output	82 dB	75 dB
<b>Peak LED Sensitivity (before clipping)</b>		
	3 dB	3 $\pm$ 2dB
<b>Headphone output (600 ohm load)</b>		
	112 mW	100 mW
<b>Maximum Input Level (1 kHz, <math>\pm</math> 3dB)</b>		
Mic Input (Mono Ch)	+22 dBu	
Line Input (Stereo Ch)	+7 dBu	
<b>Input Channel Equalizer (<math>\pm</math> 2dB)</b>		
High (shelving)	10 kHz $\pm$ 15 dB	
Low (shelving)	100 Hz $\pm$ 15 dB	
<b>Dimensions (W x D x H)</b>		
	MIXPAD 9: 239 x 228 x 58 mm (9.4 x 9 x 2.3 in.)	
	MIXPAD 12: 324 x 228 x 58 mm (12.75 x 9 x 2.3 in.)	
<b>Weight</b>		
	MIXPAD 9: 2.5 kg • 5.5 lbs	
	MIXPAD 12: 2.9 kg • 6.5 lbs	

Figure A9-Specifications of MIXER (MIX PAD 9)

Parameter	WindMaster
<b>Outputs</b>	
Output rate	0.25, 0.5, 1, 2, 4, 8, 10, 16, 20, (32 option) Hz
Sample rate (automatically selected)	20 or 32 Hz
Units of measure	m/s, mph, KPH, knots, ft/min
Format	UVW or Polar
Averaging	Flexible 0 - 3600 s
<b>Wind Speed</b>	
Range	0 - 50 m/s
Resolution	0.01 or 0.001 m/s
Accuracy (12 m/s) (to special order) #	< 1.0 % RMS
Accuracy (12 m/s)(Standard)*	< 1.5% RMS
'w' improvement multiplication factor applied as table, allows comparison to data previously collected with older WindMaster units with firmware 2329-601 or lower without multiplication factor.	w component only: +w = 1.166, -w = 1.289
<b>Direction</b>	
Range	0 - 359.9°
Resolution	1° or 0.1°
Accuracy (12 m/s) (Standard)*	2°
Accuracy (12 m/s) (to special order)* #	0.5°
<b>Speed of Sound</b>	
Range	300 -370 m/s
Resolution	0.01 m/s
Accuracy	< ± 0.5% @ 20°C
<b>Power requirement</b>	
	9 -30 V dc, (55 mA @ 12 V dc) (excluding analogue outputs)
<b>Digital output</b>	
Protocol (ASCII and Binary)	RS232, RS422, (RS485 WindMaster Networking)
Baud rates	2400 - 57600
<b>Analogue outputs (optional)</b>	
4 channels	Resolution 12 or 14 bit
Selectable range	User selectable full scale wind speed
Output type	0-20 mA, 4-20 mA, 0-5V, ±5V, ±2.5V
<b>Analogue inputs (optional)</b>	
Up to 4 single-ended or 2 differential	Resolution 12 or 14 bit
Input range	±5 V
<b>Sonic temperature</b>	
Range	-40 °C to +70 °C
T <sub>s</sub> Accuracy (≥ 1 Hz) (All models, unchanged)	Eddy Covariance Quality
T <sub>s</sub> Accuracy (slow response, used as ambient thermometer, unit firmware 2329-706 or higher)	± 2°C between -20° C to +30° C

Figure A10-Specification of anemometer (GILL 1590-PK-020)

### LASER BEAM CHARACTERISTICS

**Type:** Helium-Neon, Continuous, Two-Frequency

**Maximum Beam Power Output:** 1 milliwatt

**Minimum Beam Power Output:** 180 microwatts

**Beam Diameter:** 6 millimeters (0.24 inch) typical

**Vacuum Wavelength Accuracy (3 sigma, lifetime):** ±0.1 ppm

**Vacuum Wavelength Stability (typical 1 hour):** ±0.002 ppm

**Vacuum Wavelength Stability (typical lifetime):** ±0.02 ppm

**Nominal Vacuum Wavelength:** 632.9913540 nanometers

**Safety Classification:**

Class II Laser Product conforming to U.S.

National Center for Devices and Radiological

Health Regulations 21 CFR 1040.10 and 1040.11.

### OUTPUTS

**Reference Frequency (5519A):** 2.4 - 3.0 MHz

**Reference Frequency (5519B):** 3.4 to 4.0 MHz

Figure A11-Specifications of interferometer laser head(5518A)

Laser diode	635 nm, < 1 mW
Measurement range	0.05 – 250.00 m
Weight, approx.	0.24 kg
Measurement time, typical	< 0.5 s
Laser class	2
Measurement accuracy, typical	± 1.0 mm* (*plus use-dependent deviation)
Measurement time, max.	4 s
Power supply	4 x 1.5 V LR03 (AAA)
Automatic deactivation	5 min
Units of measurement	m/cm/mm
Memory capacity (values)	30
Dust and splash protection	IP 54
Tripod thread	1/4"
Viewfinder	integrated
Laser colour	Red
Measuring range, up to	250 m

*Figure A12-Specifications of EDM (BOSCH GLM 250 VF)*